IIW Collection

A.F. Hobbacher

Recommendations for Fatigue Design of Welded Joints and Components

Second Edition

INTERNATIONAL INSTITUTE OF WELDING
A world of joining experience

Springer

IIW Collection

Series editor

Cécile Mayer, Villepinte, France

About the Series

The IIW Collection of Books is authored by experts from the 59 countries participating in the work of the 23 Technical Working Units of the International Institute of Welding, recognized as the largest worldwide network for welding and allied joining technologies.

The IIW's Mission is to operate as the global body for the science and application of joining technology, providing a forum for networking and knowledge exchange among scientists, researchers and industry.

Published books, Best Practices, Recommendations or Guidelines are the outcome of collaborative work and technical discussions-they are truly validated by the IIW groups of experts in joining, cutting and surface treatment of metallic and non-metallic materials by such processes as welding, brazing, soldering, thermal cutting, thermal spraying, adhesive bonding and microjoining. IIW work also embraces allied fields including quality assurance, non-destructive testing, standardization, inspection, health and safety, education, training, qualification, design and fabrication.

More information about this series at http://www.springer.com/series/13906

A.F. Hobbacher

Recommendations for Fatigue Design of Welded Joints and Components

Second Edition

IIW document IIW-2259-15
ex XIII-2460-13/XV-1440-13

This document is a revision of
XIII-2151r4-07/XV-1254r4-07

INTERNATIONAL INSTITUTE OF WELDING
A world of joining experience

Springer

A.F. Hobbacher
University of Applied Sciences
Wilhelmshaven
Germany

1st edition: "Fatigue Design of Welded Joints and Components: Recommendations of IIW Joint Working Group XIII–XV", Crc Press, 1996, ISBN: 978-1855733152

ISSN 2365-435X ISSN 2365-4368 (electronic)
IIW Collection
ISBN 978-3-319-23756-5 ISBN 978-3-319-23757-2 (eBook)
DOI 10.1007/978-3-319-23757-2

Library of Congress Control Number: 2015950054

Springer Cham Heidelberg New York Dordrecht London

This Springer imprint is published by the registered company Springer Nature Switzerland AG
The registered company address is: Gewerbestrasse 11, 6330 Cham, Switzerland

The original version of this book was revised.
An erratum to this chapter can be found at
DOI 10.1007/978-3-319-23757-2_7
An erratum to this chapter can be found at
DOI 10.1007/978-3-319-23757-2_8

The International Institute of Welding

Mission
"To act as the worldwide network for knowledge exchange of joining technologies to improve the global quality of life"

The International Institute of Welding (IIW) was founded in 1948 by the welding institutes/societies of 13 countries who considered it crucial to make more rapid scientific and technical progress possible on a global level. Their vision was for the IIW to be the international vehicle by which innovation and best joining practices could be promoted, while providing an international platform for the exchange and dissemination of evolving welding technologies and applications.

From its humble beginnings, the IIW is today a universal reference, recognized as the largest worldwide network for welding and allied joining technologies, boasting a current membership of 59 countries from the five continents. The IIW's Mission is to operate as the global body for the science and application of joining technology, providing a forum for networking and knowledge exchange among scientists, researchers and industry. Through the work of its 23 Technical Commissions and Working Units, the organization's technical focus encompasses the joining, cutting and surface treatment of metallic and non-metallic materials by such processes as welding, brazing, soldering, thermal cutting, thermal spraying, adhesive bonding and microjoining. IIW work also embraces allied fields including quality assurance, non-destructive testing, standardization, inspection, health and safety, education, training, qualification, design and fabrication.

Preface

This document has been prepared as a result of an initiative by Commissions XIII and XV of the International Institute of Welding (IIW). The task was transferred to the Joint Working Group XIII–XV, where it was discussed and drafted in the years 1990–1996 and updated in the years 2002–2007. The recent version was updated in 2013–2014. The main points of that update were: Revision of the chapter on structural hot spot stress, consideration of aluminium at the effective notch stress method, a chapter on improvement techniques and a revision of the chapter on multi-axial loading. The update from 2014 contains, besides a continuous refinement and adjustment to the most recent developments and completely revised chapters on fracture mechanics.

Contents

Contributors List

The document contains contributions from:

Prof. Dr. A.F. Hobbacher, Jade University of Applied Sciences Wilhelmshaven, Germany, as Chairman
Prof. Dr. W. Fricke, Hamburg University of Technology (TUHH), Germany
Prof. P.J. Haagensen, Institute of Technology, Trondheim, Norway
Prof. Dr. A.F. Hobbacher, University of Applied Sciences, Wilhelmshaven, Germany
Dr. M. Huther, Bureau Veritas, Paris France
Prof. Dr. K. Iida, Institute of Technology, Shibaura, Japan
Dr. H.P. Lieurade, CETIM, Senlis, France
Dr. I. Lotsberg, DNV, Oslo, Norway
Prof. S.J. Maddox, The Welding Institute, Cambridge, UK
Prof. Dr. G. Marquis, Lappeenranta University of Technology, Finland
Prof. Dr. Ch. Miki, Institute of Technology, Tokyo, Japan
Prof. Erkki Niemi, Lappeenranta University of Technology, Finland
Dr. A. Ohta, NRIM, Tokyo, Japan
Mr. O. Ørjasæter, SINTEF, Trondheim, Norway
Prof. Dr. H.J. Petershagen, Hamburg University of Technology (TUHH), Germany
Prof. Dr. C.M. Sonsino, LBF Darmstadt, Germany

Suggestions for a future refinement of the document are welcome and should be addressed to the chairman:

Prof. Dr. A.F. Hobbacher, Jade University of Applied Sciences, Friedrich-Paffrath-Str. 101, D-26389 Wilhelmshaven, Germany, e-mail: hobbacher@t-online.de

Chapter 1
General

The IIW, and every other body or person involved in the preparation and publication of this document, hereby expressly disclaim any liability or responsibility for loss or damage resulting from its use, for any violation of any mandatory regulation with which the document may conflict, or for the infringement of any patent resulting from the use of this document.

It is the user's responsibility to ensure that the recommendations given here are suitable for his/her intended purposes.

1.1 Introduction

The aim of these recommendations is to provide a basis for the design and analysis of welded components loaded by fluctuating forces, to avoid failure by fatigue. In addition they may assist other bodies who are establishing fatigue design codes. It is assumed that the user has a working knowledge of the basics of fatigue and fracture mechanics [3–8].

The purpose of designing a structure against the limit state due to fatigue damage is to ensure that the performance is satisfactory during the design life with an adequate survival probability. The required survival probability is obtained by the use of appropriate partial safety factors.

1.2 Scope and Limitations

The recommendations present general methods for the assessment of fatigue damage in welded components, which may affect the limit states of a structure, such as the ultimate and serviceability limit states [1].

The original version of this chapter was revised. An erratum to this chapter can be found at DOI 10.1007/978-3-319-23757-2_7

A.F. Hobbacher, *Recommendations for Fatigue Design of Welded Joints and Components*, IIW Collection, DOI 10.1007/978-3-319-23757-2_1

The recommendations give fatigue resistance data for welded components made of wrought or extruded products of ferritic/pearlitic or bainitic structural steels up to $\mathbf{f_y = 960}$ MPa, of austenitic stainless steels and of aluminium alloys commonly used for welded structures.

The recommendations are **not** applicable to low cycle fatigue, where $\boldsymbol{\Delta\sigma_{nom} > 1.5 \cdot f_y}$ or $\boldsymbol{max\sigma_{nom} > f_y}$, for corrosive conditions or for elevated temperature operation in the creep range.

1.3 Definitions

Characteristic value	Loads, forces or stresses, which vary statistically, at a specified fractile, here: 95 % survival probability referred to a two-sided confidence level of the mean of 75 %, for details see Sect. 3.7
Classified or standard structural detail	A structural detail containing a structural discontinuity including a weld or welds, for which the nominal stress approach is applicable, and which appear in the tables of these fatigue design recommendations. Also referred to as standard structural detail
Concentrated load effect	(i) A local stress field in the vicinity of a point load or reaction force, (ii) membrane and shell bending stresses due to loads causing distortion of a cross section not sufficiently stiffened by a diaphragm
Constant amplitude loading	A type of loading causing a regular stress fluctuation between constant maximum and minimum stress limits
Crack propagation rate	Amount of crack extension per stress cycle
Crack propagation threshold	Limiting value of stress intensity factor range below which crack propagation can be considered as negligible
Cut off limit	Fatigue strength under variable amplitude loading, below which the stress cycles are considered to be non-damaging
Cycle counting	Procedure of converting the history of variable amplitude loading into an equivalent spectrum or transition matrix (e.g. 'Rainflow' or 'Reservior' methods)
Design value	Characteristic value factored by a partial safety factor
Effective notch stress	Notch stress calculated for a notch with a certain assumed notch radius
Equivalent stress range	Constant amplitude stress range which is equivalent in terms of fatigue damage to a variable stress history for the same number of applied stress cycles

Fatigue	Deterioration of a component caused by the crack initiation and/or by the growth of a crack
Fatigue action	Load effect causing fatigue, i.e. fluctuating load
Fatigue damage ratio	Ratio of fatigue damage sustained to fatigue damage required to cause failure, defined as the ratio of the number of applied stress cycles and the corresponding fatigue life at constant amplitude loading
Fatigue life	Number of stress cycles of a particular magnitude required to cause fatigue failure of the component
Fatigue limit	Fatigue strength under constant amplitude loading corresponding to a high number of cycles large enough to be considered as infinite
Fatigue resistance	Structural detail's resistance to fatigue actions expressed in terms of a S-N curve or crack propagation properties
Fatigue strength	Magnitude of stress range leading to a particular fatigue life
Fracture mechanics	A branch of mechanics dealing with the behaviour and strength of components containing cracks
Hot spot	A point in a structure where a fatigue crack may initiate due to the combined effect of structural stress fluctuation and the weld geometry or a similar notch
Local or modified nominal stress	Nominal stress including macro-geometric effects, concentrated load effects and misalignments, disregarding the stress raising effects of the welded joint itself
Local notch	A localised geometric feature, such as the toe of a weld, that causes stress concentration. The local notch does not alter the structural stress but generates a nonlinear stress peak
Macro-geometric discontinuity	A global discontinuity, the effect of which is usually not taken into account in the collection of standard structural details, such as a large opening, a curved part in a beam, a bend in a flange not supported by diaphragms or stiffeners, discontinuities in pressure containing shells, eccentricity in a lap joint (see Fig. 2.3)
Macro-geometric effect	A stress raising effect due to macro-geometry in the vicinity of the welded joint, but not due to the welded joint itself
Membrane stress	Average normal stress across the thickness of a plate or shell
Miner sum	Summation of individual fatigue damage ratios caused by each stress cycle or stress range block above a certain cut-off limit according to the Palmgren-Miner rule
Misalignment	Axial and angular misalignments caused either by detail design or by poor fabrication or welding distortion

Modified nominal stress	See 'Local nominal stress'
Nominal stress	A stress in a component, resolved using general theories, e.g. beam theory. See also local nominal stress
Nonlinear stress peak	The stress component of a notch stress which exceeds the linearly distributed structural stress at a local notch
Notch stress	Total stress at the root of a notch taking into account the stress concentration caused by the local notch, consisting of the sum of structural stress and nonlinear stress peak
Notch stress concentration factor	The ratio of notch stress to structural stress
Paris-Erdogan law	An experimentally determined relation between fatigue crack growth rate and stress intensity factor range
Palmgren-Miner rule	Method for estimating fatigue life under variable amplitude loading from the constant amplitude S-N curve (see Sect. 4.3.1). Often referred to as Miner's rule
Range counting	A procedure of determining various stress cycles and their ranges from a stress history, preferably by rainflow counting method
Shell bending stress	Bending stress in a shell or plate-like part of a component, linearly distributed across the thickness as assumed in the theory of shells
S-N curve	Graph of the dependence of fatigue life **N** on applied stress range **S** ($\Delta\sigma_R$ or $\Delta\tau_R$), also known as Wöhler curve
Stress cycle	A part of a stress history containing a stress maximum and a stress minimum, usually determined by cycle counting
Stress history	A time-based presentation of a fluctuating stress, defined by sequential stress peaks and troughs (valleys), either for the total life or for a certain period of time
Stress intensity factor	The fracture mechanics parameter, which is a function of applied stress, crack size and geometry
Stress range	The difference between the maximum and minimum stresses in a cycle
Stress range block	A part of the total spectrum of stress ranges which is discretized in a certain number of blocks
Stress spectrum	A tabular or graphical presentation of the cumulative frequency of stress range exceedence (e.g. the number of stress ranges exceeding a particular magnitude of stress range in a stress history, where frequency is the number of occurrences)
Stress ratio	Ratio of minimum to maximum algebraic value of the stress in a particular stress cycle
Stress intensity factor ratio	Ratio of minimum to maximum algebraic value of the stress intensity factor of a particular load cycle

Structural discontinuity	A geometric discontinuity due to the type of welded joint, usually to be found in the tables of classified structural details. The effects of a structural discontinuity are (i) concentration of the membrane stress and (ii) formation of secondary shell bending stresses (see Fig. 2.6)
Structural or geometric stress	A stress in a component, resolved to take into account the effects of a structural discontinuity, and consisting of membrane and shell bending stress components
Structural stress concentration factor	The ratio of structural stress to local or modified nominal stress
Structural hot spot stress	The value of structural stress on the surface at a hot spot
Variable amplitude loading	A type of loading causing irregular stress fluctuation with stress ranges (and amplitudes) of variable magnitude

1.4 Symbols

A	Cross sectional area of loaded plate (a suffix may be added) or weld throat size
B	Plate width
C	Constant in equation of S-N curve with exponent m
CV	Comparison value used in verification procedure for assessing combined loading
D	Fatigue damage sum according to the Palmgren-Miner rule or mean diameter
$\mathbf{D_{max}}$	Maximum diameter
$\mathbf{D_{min}}$	Minimum diameter
E	Elastic modulus
F	Force or statistical safety factor
FATx	Classification reference to S-N curve, in which x is the stress range in MPa at 2×10^6 cycles
H	Fillet weld leg length
K	Stress intensity factor
$\mathbf{K_{max}}$	Stress intensity factor caused by $\boldsymbol{\sigma_{max}}$
$\mathbf{K_{min}}$	Stress intensity factor caused by $\boldsymbol{\sigma_{min}}$
L	Attachment length in direction of loading considered
M	Bending moment
$\mathbf{M_k}$	Magnification function for **K** due to nonlinear stress peak
$\mathbf{M_{k,m}}$	Magnification function for **K**, concerning membrane stresses
$\mathbf{M_{k,b}}$	Magnification function for **K**, concerning shell bending stresses
N	Fatigue life in cycles

$\mathbf{N_i}$	Constant amplitude fatigue life at the i-th stress range
R	Stress ratio
Stdv	Standard deviation of logN
W	Fillet weld leg length (see Table 6.4)
Y	Correction function for **K**, taking into account crack form, aspect ratio, relative crack size etc.
$\mathbf{Y_m}$	Correction function for **K**, concerning membrane stress
$\mathbf{Y_b}$	Correction function for **K**, concerning shell bending stress
a	Weld throat size or depth of a surface crack or semi length of an embedded crack
$\mathbf{a_o}$	Initial depth of a surface crack
$\mathbf{a_f}$	Value of **a** at fatigue failure
b	Distance between crack centre and nearest plate edge
c	Half length of surface or embedded elliptical crack
d	Deviation from the true circle due to angular misalignment
e	Eccentricity, amount of offset misalignment
$\mathbf{f_y}$	Actual or specified yield strength of the material
$\mathbf{k_m}$	Stress magnification factor due to misalignment
$\mathbf{k_s}$	Stress concentration factor due to structural discontinuity
$\mathbf{k_t}$	Stress concentration factor due to local notch
m	Exponent of S-N curve or Paris power law
n	Exponent in thickness correction or number of data pairs
$\mathbf{n_i}$	Number of applied stress cycles at the i-th stress range
t	Plate thickness, thickness parameter (crack centre to nearest surface)
$\mathbf{\Delta K}$	Stress intensity factor range
$\mathbf{\Delta K_{S,d}}$	Design value of stress intensity factor range caused by actions
$\mathbf{\Delta K_{th}}$	Threshold stress intensity factor range
$\boldsymbol{\Delta\sigma}$	Stress range
$\boldsymbol{\Delta\sigma_{S,d}}$	Design value of stress range caused by actions
$\boldsymbol{\Delta\sigma_{R,L}}$	Characteristic value of stress range at knee point of S-N curve
$\boldsymbol{\Delta\tau}$	Shear stress range
$\boldsymbol{\gamma_M}$	Partial safety factor for fatigue resistance in terms of stress
$\boldsymbol{\Gamma_M}$	Partial safety factor for fatigue resistance in terms of cycles
$\boldsymbol{\sigma}$	Normal stress
$\boldsymbol{\sigma_b}$	Shell bending stress
$\boldsymbol{\sigma_{en}}$	Effective notch stress
$\boldsymbol{\sigma_{ln}}$	(Local) notch stress
$\boldsymbol{\sigma_{max}}$	Stress maximum in stress history
$\boldsymbol{\sigma_m}$	Membrane stress
$\boldsymbol{\sigma_{min}}$	Stress minimum in stress history
$\boldsymbol{\sigma_{nl}}$	Nonlinear stress peak
$\boldsymbol{\sigma_{nom}}$	(Modified) nominal stress
$\boldsymbol{\sigma_{hs}}$	Structural hot spot stress

Subscripts:

S Fatigue actions
R Fatigue resistance
d Design value
k Characteristic value
τ Shear stress

1.5 Basic Principles

According to the ISO format for verification of structures [1], fatigue action and fatigue resistance are clearly separated. The main fatigue resistance data provided in this document are in the form of S-N or fatigue crack growth curves, based on constant amplitude test results. No specific recommendations are given for the fatigue load (action) side, or for the partial safety factors on fatigue resistance $\boldsymbol{\gamma_M}$ or actions $\boldsymbol{\gamma_F}$.

The different approaches for the fatigue assessment of welded joints and components considered are: nominal stress, structural hot-spot stress, effective notch stress, fracture mechanics and component testing.

1.6 Necessity of Fatigue Assessment

Fatigue assessment is generally required for components subject to fluctuating loads.

In the following cases, detailed fatigue assessment is **not** usually required. If there is any doubt that these criteria apply, a fatigue assessment is recommended:

(a) The highest nominal design stress range satisfies for $N \leq 2e6$

$$\text{Steel} \quad : \Delta\sigma_{S,d} \leq 36\,\text{MPa}/\gamma_M \tag{1.1}$$

$$\text{Aluminium} : \Delta\sigma_{S,d} \leq 12\,\text{MPa}/\gamma_M \tag{1.2}$$

$\boldsymbol{\gamma_M}$ should be taken from an applicable design code. This paragraph is not applicable to tubular joints.

(b) The Miner sum **D** (Sect. 4.3.1) is less than or equal to **D = 0.5** when evaluated using either fatigue class FAT 36 for steel or FAT 12 for aluminium

(c) For a detail for which a constant amplitude fatigue limit $\boldsymbol{\Delta\sigma_{R,L}}$ is specified and all design stress ranges are under an assumed or specified design resistance fatigue limit (Sect. 3.2)

$$\Delta\sigma_{S,d} \leq \Delta\sigma_{R,L} / \gamma_M \tag{1.3}$$

(d) For a crack, at which all design stress intensity factors are under an assumed or specified crack propagation threshold level $\mathbf{\Delta K_{th}}$.

$$\Delta K_{S,d} \leq \Delta K_{th} / \gamma_M \tag{1.4}$$

for steel $\Delta K_{th} = 2.0\ MPa\sqrt{m} = 63\ N\cdot mm^{-3/2}$
for aluminium $\Delta K_{th} = 0.7\ MPa\sqrt{m} = 21\ N\cdot mm^{-3/2}$

1.7 Application of the Document

Various assessment procedures are presented of which the choice is depending on the initial information about the welded joint and the applied loading. Then, the fatigue action data (e.g. stress type) and the fatigue resistance data are determined according to the assessment procedure. The corresponding types of fatigue action and resistance are summarized in Tables 1.1 and 1.2.

The chosen procedure may need to be performed using appropriate safety factors.

Table 1.1 Presentation of fatigue actions and resistances versus assessment procedure

Fatigue action	Fatigue resistance	Assessment procedure
Forces on component	Resistance determined by test of component	Component testing
Nominal stress in section	Resistance given by tables of structural details in terms of a set of S-N curves	Summation of cumulative damage
Structural hot-spot stress at weld toe	Resistance against structural hot-spot stress in terms of S-N curves	
Effective notch stress in weld notch	Resistance against effective notch stress in terms of a universal S-N curve	
Stress intensity at crack tip	Resistance against crack propagation in terms of the material parameters of the crack propagation law	Summation of crack increments

Table 1.2 General guidance for the application of the document

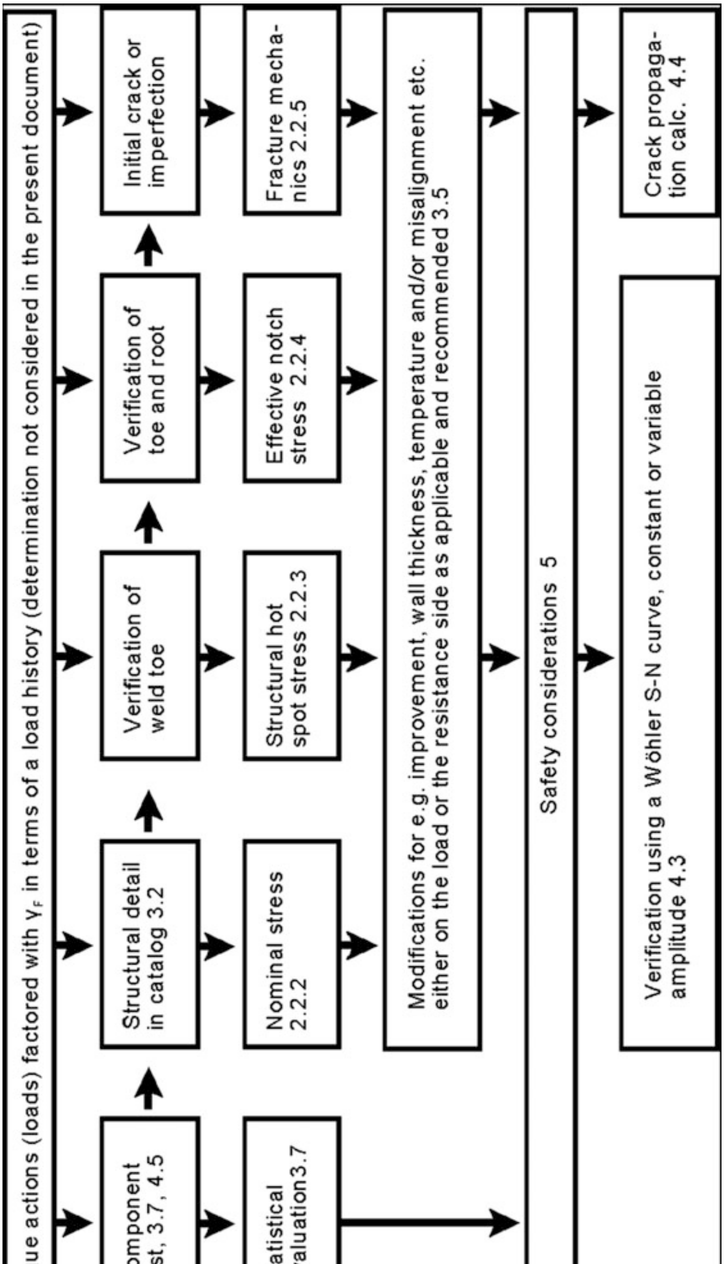

Chapter 2
Fatigue Actions (Loading)

All types of fluctuating load acting on the component and the resulting stresses at potential sites for fatigue have to be considered. Stresses or stress intensity factors then have to be determined according to the fatigue assessment procedure applied.

The actions originate from live loads, dead weights, snow, wind, waves, pressure, accelerations, dynamic response etc. Actions due to transient temperature changes should also be considered. Improper knowledge of fatigue actions is one of the major sources of fatigue damage.

Tensile residual stresses due to welding and other manufacturing processes decrease the fatigue resistance. However, the influence of high tensile residual stresses is already included in the fatigue resistance data given in Chap. 3.

2.1 Basic Principles

2.1.1 Determination of Fatigue Actions (Loading)

In assessing fatigue performance, a safe estimate of fatigue loading to be endured throughout the life of the structure or component under consideration is crucial. All types of varying loading should be considered. Fluctuating loading from different sources may be significant at different phases of the life, e.g. construction, transportation, installation, in-service, and may involve different frequencies. The design load spectrum should be selected on the basis that it is an upper bound estimate of the accumulated service conditions over the full design life of the structure or component concerned. If relevant, this may be based on characteristic load data and partial safety factors γ_F specified in the application code giving design values for the fatigue loading.

No guidance is given in this document for the establishing of design values for actions (loads), nor for partial safety factors γ_F on actions (loads).

A.F. Hobbacher, *Recommendations for Fatigue Design of Welded Joints and Components*, IIW Collection, DOI 10.1007/978-3-319-23757-2_2

2.1.2 Stress Range

Fatigue assessment is usually based on stress range or stress intensity factor range. Thus, the fatigue loading (actions) needs to be expressed in these terms.

$$\Delta\sigma = \sigma_{\max} - \sigma_{\min} \tag{2.1}$$

$$\Delta K = K_{\max} - K_{\min} \tag{2.2}$$

The maximum and minimum stresses should be calculated from the superposition of all non permanent, i.e. fluctuating loads:

(a) Fluctuations in the magnitudes of loads
(b) Movement of loads on the structure
(c) Changes in loading directions
(d) Structural vibrations due to loads and dynamic response
(e) Temperature transients

Fatigue analysis is based on the cumulative effect of all stress range occurrences during the anticipated service life of the structure.

2.1.3 Types of Stress Concentrations and Notch Effects

The stress required to assess the fatigue resistance of a particular stress concentration feature depends on the type and the fatigue assessment procedure used, see Table 2.1.

Figure 2.1 shows an example of different stress definitions, such as gross nominal stress and modified or local nominal stress. Figure 2.2 shows the increase in stress in the vicinity of the notch, caused by the structural detail and the weld toe.

2.2 Determination of Stresses and Stress Intensity Factors

2.2.1 Definition of Stress Components

In the vicinity of a notch the stress distribution over the plate thickness is non-linear (Fig. 2.3).

The stress components of the notch stress $\boldsymbol{\sigma_{nl}}$ are [2]:

$\boldsymbol{\sigma_m}$ membrane stress
$\boldsymbol{\sigma_b}$ shell bending stress
$\boldsymbol{\sigma_{nl}}$ non-linear stress peak

Table 2.1 Stress concentrations and notch effects considered

Type	Stress concentrations	Stress determined	Assessment procedure
A	None	Gross average stress from sectional forces, calculated using general theories, e.g. beam theory	Not applicable for fatigue analysis of joints, only for component testing
B	Macro-geometrical effects due to the design of the component, but excluding stress concentrations due to the welded joint itself.	Range of nominal stress (also modified or local nominal stress)	Nominal stress approach
C	B + structural discontinuities due to the structural detail of the welded joint, but excluding the notch effect of the weld toe transition	Range of structural hot-spot stress	Structural hot-spot stress approach
D	A + B + C + notch stress concentration due to the weld bead notches (a) actual notch stress (b) effective notch stress	Range of elastic notch stress (total stress)	(a) Fracture mechanics approach (b) Effective notch stress approach

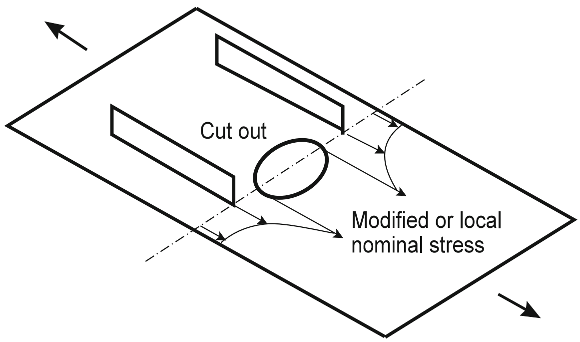

Fig. 2.1 Modified or local nominal stress

If a refined stress analysis method is used, which gives a non-linear stress distribution, the stress components can be separated by the following method:

The membrane stress $\boldsymbol{\sigma_m}$ is equal to the average stress calculated through the thickness of the plate. It is constant through the thickness.
The shell bending stress $\boldsymbol{\sigma_b}$ is linearly distributed through the thickness of the plate. It is found by drawing a straight line through the point **O** in Fig. 2.3 where the membrane stress intersects the mid-plane of the plate. The gradient of the shell bending stress is chosen such that the remaining non-linearly distributed component is in equilibrium.

Fig. 2.2 Notch stress and structural hot-spot stress

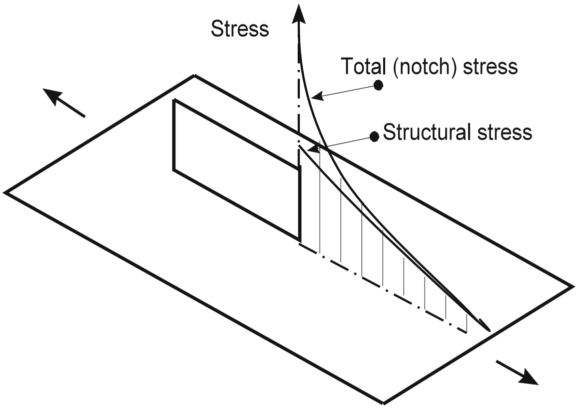

The non-linear stress peak $\boldsymbol{\sigma_{nl}}$ is the remaining component of the stress.

The stress components can be separated analytically for a given through thickness stress distribution $\boldsymbol{\sigma(x)}$ from $\mathbf{x = 0}$ at the surface to $\mathbf{x = t}$:

$$\sigma_m = \frac{1}{t} \cdot \int_{x=0}^{x=t} \sigma(x) \cdot dx \tag{2.3}$$

$$\sigma_b = \frac{6}{t^2} \cdot \int_{x=0}^{x=t} (\sigma(x) - \sigma_m) \cdot (\frac{t}{2} - x) \cdot dx \tag{2.4}$$

$$\sigma_{nl}(x) = \sigma(x) - \sigma_m - (1 - \frac{2x}{t}) \cdot \sigma_b \tag{2.5}$$

Note: In Fig. 2.3 and at formulae (2.3)–(2.5) a linear distribution of bending stress according to the Bernoulli theory of beams was assumed. Prior to an application of the formulae, that condition should be checked.

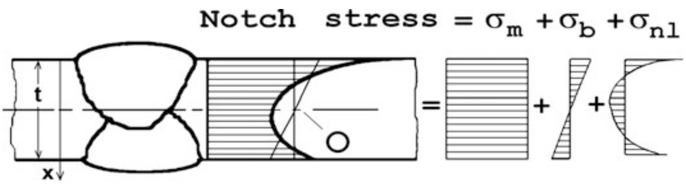

Fig. 2.3 Non-linear stress distribution separated to stress components

2.2.2 *Nominal Stress*

2.2.2.1 General

Nominal stress is the stress calculated in the sectional area under consideration, disregarding the local stress raising effects of the welded joint, but including the stress raising effects of the macro-geometric shape of the component in the vicinity of the joint, such as e.g. large cutouts. Overall elastic behaviour is assumed.

The nominal stress may vary over the section under consideration. For example at a beam-like component, the modified (also local) nominal stress and the variation over the section can be calculated using simple beam theory. Here, the effect of a welded on attachment is ignored (Fig. 2.4).

The effects of macro-geometric features of the component and stress fields in the vicinity of concentrated loads must be included in the nominal stress. Both may cause significant redistribution of the membrane stresses across the section. Significant shell bending stress may also be generated, as in curling of a flange, or distortion of a box section (Figs. 2.5, 2.6a, b).

The secondary bending stress caused by axial or angular **misalignment** (e.g. as considered to be acceptable in the fabrication specification) needs to be considered if the misalignment exceeds the amount which is already covered by the fatigue

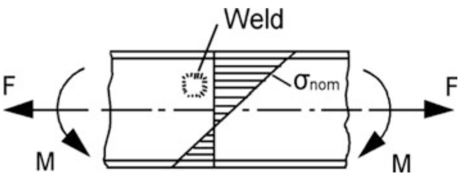

Fig. 2.4 Nominal stress in a beam-like component

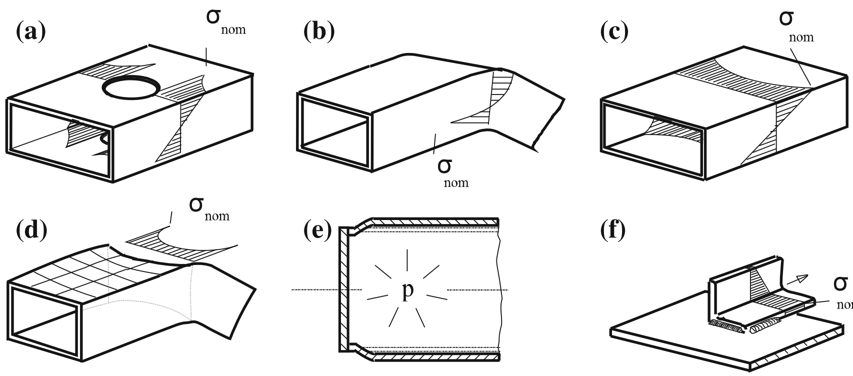

Fig. 2.5 Examples of macrogeometric effects. Stress concentrations at **a** cut-outs, **b** curved beams, **c** wide plates, **d** curved flanges, **e** concentrated loads, **f** excentricities

resistance S-N curve for the structural detail. This is done by the application of an additional stress magnification factor $\mathbf{k}_{m,eff}$ (see Sect. 3.8.2). Either the applied stress is multiplied by $\mathbf{k}_{m,eff}$ or the fatigue resistance (stress) is divided by it.

2.2.2.2 Calculation of Nominal Stress

In simple components the nominal stress can be determined using elementary theories of structural mechanics based on linear-elastic behaviour. Nominal stress is the average stress in the weld throat or in the plate at the weld toe as indicated in the tables of structural details. A possible misalignment shall be considered either in analysis or in resistance data (Fig. 2.7a)

The weld throat is determined at (Fig. 2.7b)

Butt welds	Wall thickness of the plates, at dissimilar wall thicknesses, the smaller wall thickness has to be taken
Fillet welds	The smallest distance from the root or deepest point of penetration to the surface of the fillet weld bead

The stress $\boldsymbol{\sigma}_w$ or $\boldsymbol{\tau}_w$ in weld throat **a** for a weld of length $\mathbf{l}_w$ and a force in the weld **F** becomes

$$\sigma_w \quad or \quad \tau_w = \frac{F}{A_w} = \frac{F}{a \cdot l_w} \tag{2.6}$$

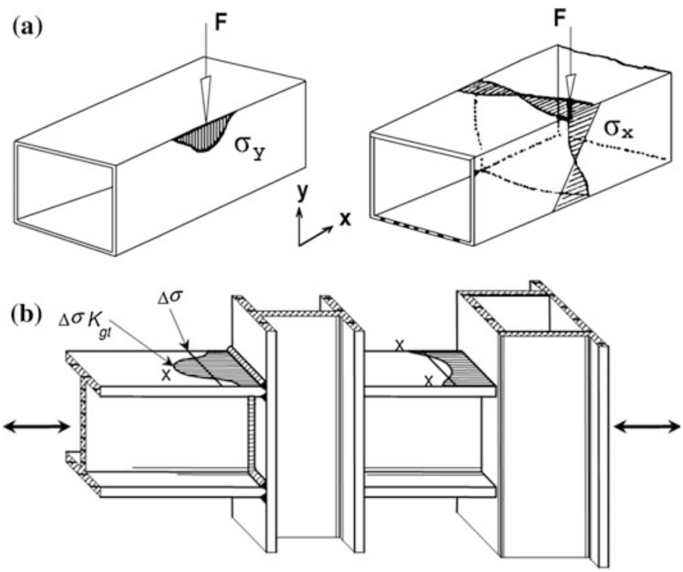

Fig. 2.6 **a** Modified (local) nominal stress near concentrated loads. **b** Modified (local) nominal stress at hard spots

Fig. 2.7 **a** Axial and angular misalignment. **b** Weld throat

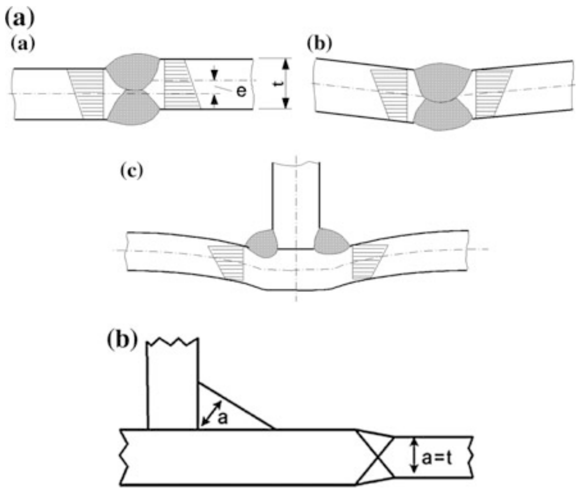

In other cases, finite element method (FEM) modelling may be used. This is primarily the case in

(a) complex statically over-determined (hyperstatic) structures
(b) structural components incorporating macro-geometric discontinuities, for which no analytical solutions are available

If the finite element method is used, meshing can be simple and coarse. Care must be taken to ensure that all stress concentration effects from the structural detail of the welded joint are excluded when calculating the **modified (local) nominal stress**.

If nominal stresses are calculated for fillet welds by coarse finite element meshes, nodal forces rather than element stresses should be used in a section through the weld in order to avoid stress underestimation.

When a nominal stress is intended to be calculated by finite elements, the more precise option of the structural hot spot stress determination should be considered.

2.2.2.3 Measurement of Nominal Stress

The fatigue resistance S-N curves of classified structural details are based on nominal stress, disregarding the stress concentrations due to the welded joint. Therefore the measured nominal stress must exclude the stress or strain concentration due to the corresponding discontinuity in the structural component. Thus, strain gauges must be placed outside the stress concentration field of the welded joint.

In practice, it may be necessary first to evaluate the extent and the stress gradient of the field of stress concentration (see Sect. 2.2.3.4) due to the welded joint. For further measurements, simple strain gauge application outside this field is sufficient.

When a nominal stress is intended to be measured by strain gauges, the more precise option of the structural hot spot stress measurement should be considered.

2.2.3 Structural Hot Spot Stress

2.2.3.1 General

The structural or geometric stress $\boldsymbol{\sigma}_{\mathbf{hs}}$ at the hot spot includes all stress raising effects of a structural detail excluding that due to the local weld profile itself. So, the non-linear peak stress $\boldsymbol{\sigma}_{\mathbf{nl}}$ caused by the local notch, i.e. the weld toe, is excluded from the structural stress. The structural stress is dependent on the global dimensional and loading parameters of the component in the vicinity of the joint (type **C** in Sect. 2.1.3 Table 2.1). It is determined on the surface at the hot spot of the component which is to be assessed. Structural hot spot stresses $\boldsymbol{\sigma}_{\mathbf{hs}}$ are generally defined for plate, shell and tubular structures. Figure 2.8 shows examples of structural discontinuities and details together with the structural stress distribution.

The structural hot spot stress approach is typically used where there is no clearly defined nominal stress due to complex geometric effects, or where the structural discontinuity is not comparable to a classified structural detail [9, 11–13].

The structural hot-spot stress can be determined using reference points by extrapolation to the weld toe under consideration from stresses at reference points

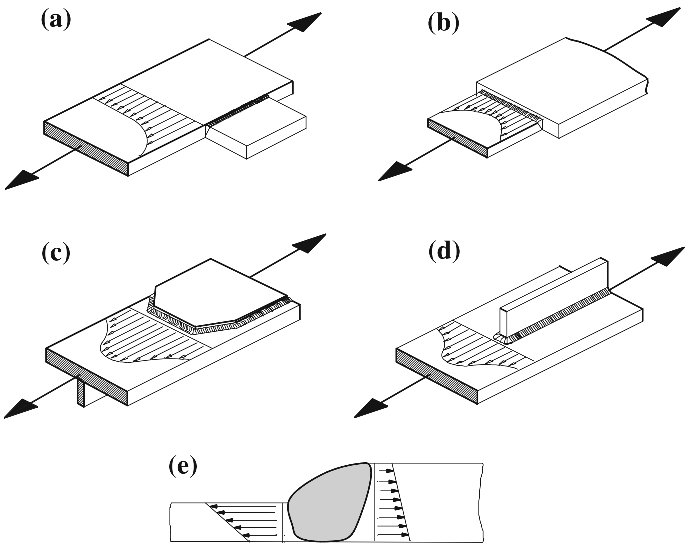

Fig. 2.8 Structural details and structural stress, e.g. at **a** end of longitudinal lateral attachment, **b** joint of plates with unequal width, **c** end of cover plate, **d** end of longitudinal attachment, **e** joint with unequal thickness

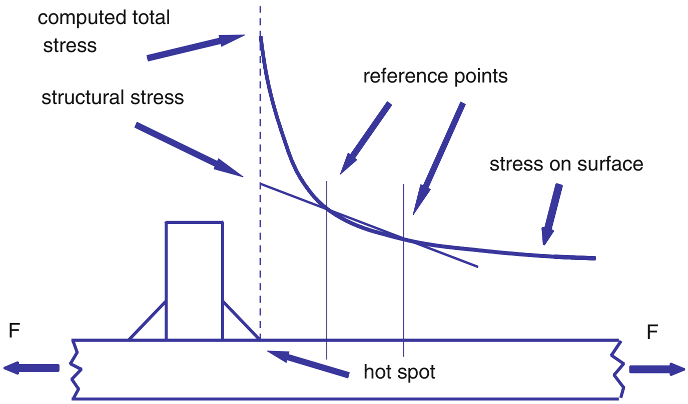

Fig. 2.9 Definition of structural hot-spot stress

(Fig. 2.9). Strictly speaking, the method as defined here is limited to the assessment of the weld toe, i.e. cases **a** to **e** in Fig. 2.10. However, the approach may be extended to the assessment of other potential fatigue crack initiation sites including the weld root, by using the structural hot spot stress on the surface as an indication of that in the region of interest. The S-N curves or the stress concentration factors used for verification in such cases depend largely on the geometric and dimensional parameters and are only valid in the range of these parameters.

In the case of a biaxial stress state at the plate surface, it is recommended that the principal stress which acts approximately in line with the perpendicular to the weld toe, i.e. within ±60° (Fig. 2.11) is used. The other principal stress may need to be analysed, if necessary, using the fatigue class in the nominal stress approach for welds parallel to the stress.

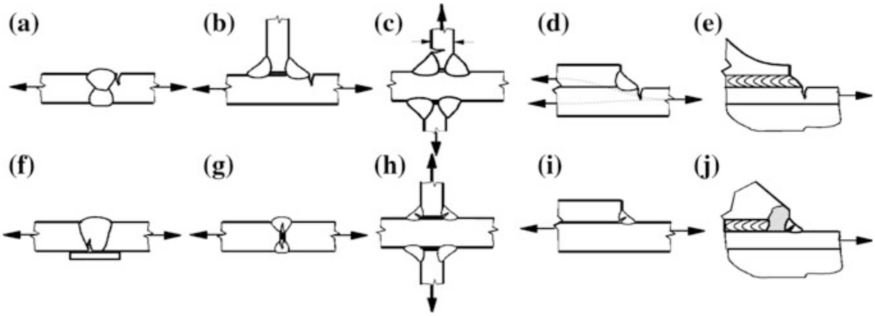

Fig. 2.10 Various locations of crack propagation in welded joints. **a–e** with weld toe cracks, **f–j** with weld root cracks

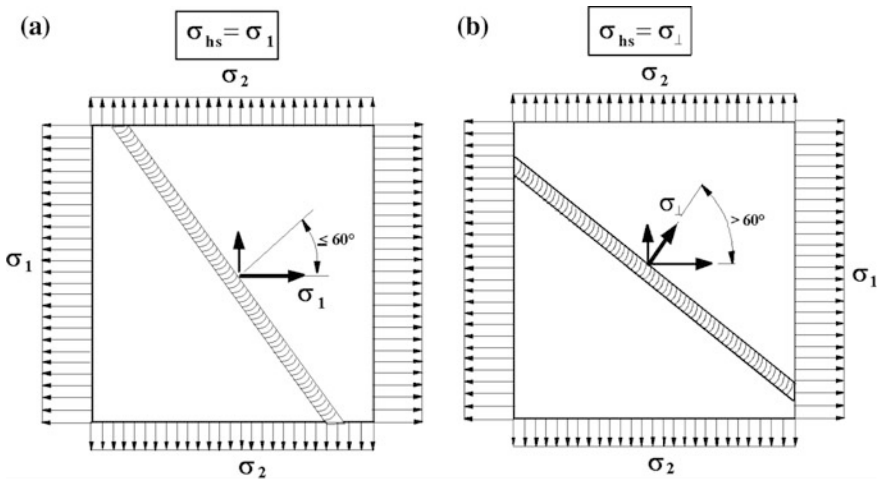

Fig. 2.11 Biaxial stresses at weld toe, principle stress within (**a**) and without (**b**) an angle of 60° perpendicular to the weld

2.2.3.2 Types of Hot Spots

Besides the definitions of structural hot spot stress as given above, two types of hot spots are defined according to their location on the plate and their orientation in respect to the weld toe as defined in Fig. 2.12, Table 2.2:

The structural stress acts normal to the weld toe in each case and is determined either by a special FEA procedure or by extrapolation from measured stresses.

Fig. 2.12 Types of hot spots

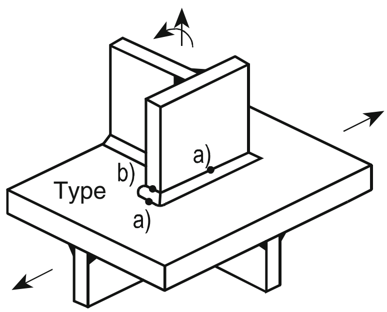

Table 2.2 : Types of hot spots

Type	Description	Determination
a	Weld toe on plate surface	FEA or measurement and extrapolation
b	Weld toe at plate edge	FEA or measurement and extrapolation

2.2.3.3 Determination of Structural Hot Spot Stress

The structural hot spot stress can be determined either by measurement or by calculation. Here the non-linear peak stress is eliminated by linearization of the stress through the plate thickness (see Sect. 2.2.1) or by extrapolation of the stress at the surface to the weld toe. The following considerations focus on surface stress extrapolation procedures of the surface stress, which are essentially the same for both measurement and calculation.

The procedure is first to establish the reference points and then to determine the structural hot spot stress by extrapolation to the weld toe from the stresses of those reference points. Depending on the method, there may be two or three reference points.

The reference point closest to the weld toe must be chosen to avoid any influence of the notch due to the weld itself (which leads to a non-linear stress peak). This is practically the case at a distance of **0.4 t** from the weld toe, where **t** is plate thickness. The structural hot spot stress at the weld toe is then obtained by extrapolation.

Identification of the critical points (hot spots) can be made by:

(a) Measuring several different points
(b) Analysing the results of a prior FEM analysis
(c) Experience of existing components, especially if they failed

2.2.3.4 Calculation of Structural Hot Spot Stress

In general, analysis of structural discontinuities and details to obtain the structural hot spot stress is not possible using analytical methods. Parametric formulae are rarely available. Thus, finite element analysis (FEA) is generally applied.

Usually, structural hot spot stress is calculated on the basis of an idealized, perfectly aligned welded joint. Consequently, any possible misalignment has to be taken explicitly into consideration explicitly in the FEA model or by applying an appropriate stress magnification factor k_m, see also Sect. 3.8.2. This applies particularly to butt welds, cruciform joints and one-sided transverse fillet welded attachments on one side of an unsupported plate.

The extent of the finite element model has to be chosen such that constraining boundary effects of the structural detail analysed are comparable to the actual structure.

Models with either thin plate or shell elements or with solid elements may be used. It should be noted that on the one hand the arrangement and the type of the elements must allow for steep stress gradients and for the formation of plate bending, but on the other hand, only the linear stress distribution in the plate thickness direction needs to be evaluated with respect to the definition of the structural hot spot stress. The stresses should be determined at the specified reference points.

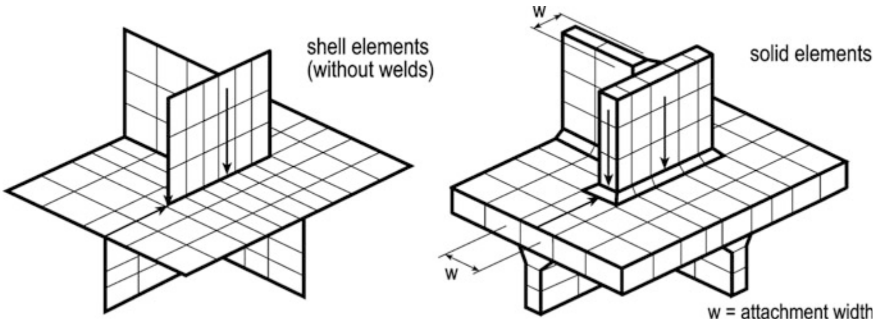

Fig. 2.13 Typical meshes and stress evaluation paths for a welded detail

A reasonably high level of expertise is required on the part of the FEA analyst. Guidance is given in [11]. In the following, only some rough recommendations are given:

In a **plate or shell element** model (Fig. 2.13, left part), the elements are arranged in the mid-plane of the structural components. 8-noded elements are recommended particularly in regions of steep stress gradients. In simplified models, the welds are not modelled, except for cases where the results are affected by local bending, e. g. due to an offset between plates or due to a small distance between adjacent welds. Here, the welds may be included by vertical or inclined plate elements having appropriate stiffness or by introducing constraint equations or rigid links to couple node displacements. Thin-shell elements naturally provide a linear stress distribution through the shell thickness, suppressing the notch stress at weld toes. Nevertheless, the structural hot-spot stress is frequently determined by extrapolation from the reference points mentioned before, particularly at points showing an additional stress singularity such as stiffener ends.

Alternatively, particularly for complex cases, prismatic **solid elements** which have a displacement function allowing steep stress gradients as well as plate bending with linear stress distribution in the plate thickness direction may be used. An example is isoparametric 20-node elements with mid-side nodes at the edges, which allow only one element to be arranged in the plate thickness direction due to the quadratic displacement function and the linear stress distribution. By reduced integration, the linear part of the stresses can be directly evaluated at the shell surface and extrapolated to the weld toe. Modelling of welds is generally recommended as shown in Fig. 2.13 (right part). The alternative with a multi-layer arrangement of solid elements allows to linearize the stresses over the plate thickness directly at the weld toe.

Surface Stress Extrapolation Methods:

If the structural hot-spot stress is determined by extrapolation, the **element lengths** are determined by the reference points selected for stress evaluation. In order to avoid an influence of the stress singularity, the stress closest to the hot spot is usually evaluated at the first nodal point. Therefore, the length of the element at the hot spot corresponds to its distance from the first reference point. If finer meshes are used, the refinement should be introduced in the thickness direction as well.

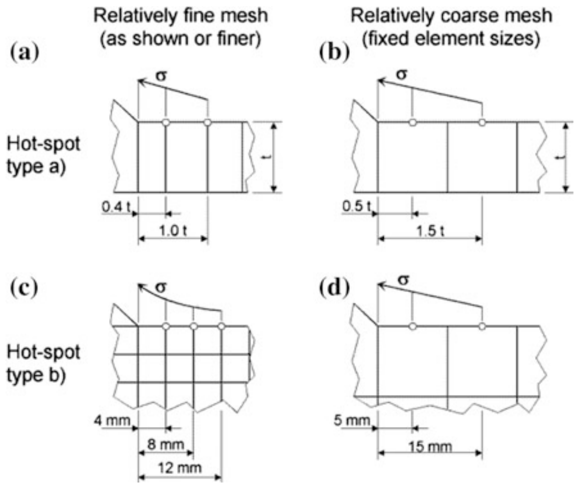

Fig. 2.14 Reference points at different types of meshing. Stress type "**a**" (**a**, **b**), type "**b**" (**c**, **d**)

Coarser meshes are also possible with higher-order elements and fixed lengths, as explained further below.

Appropriate element widths are important, particularly in cases with steep stress gradients. The width of the solid element or the two shell elements in front of the attachment should not exceed the attachment width '**w**', i. e. the attachment thickness plus two weld leg lengths as indicated in Fig. 2.13.

Typical extrapolation paths for determining the structural hot spot stress components on the plate surface or edge are shown by arrows in Fig. 2.13. If the weld is not modelled, extrapolation to the structural intersection point is recommended in order to avoid stress underestimation due to the missing stiffness of the weld.

Type "a" Hot Spots:

The structural hot spot stress $\boldsymbol{\sigma}_{\mathbf{hs}}$ is determined using the reference points and extrapolation equations as given below (see also Fig. 2.14).

(1) Fine mesh with element length not more than **0.4 t** at the hot spot: Evaluation of nodal stresses at two reference points **0.4 t** and **1.0 t**, and linear extrapolation (Eq. 2.7).

$$\sigma_{hs} = 1.67 \cdot \sigma_{0.4 \cdot t} - 0.67 \cdot \sigma_{1.0 \cdot t} \tag{2.7}$$

(2) Fine mesh as defined in (1) above: Evaluation of nodal stresses at three reference points **0.4 t**, **0.9 t** and **1.4 t**, and quadratic extrapolation (Eq. 2.8). This method is recommended for cases of pronounced non-linear structural stress increase towards the hot spot, at sharp changes of direction of the applied force or for thick-walled structures.

$$\sigma_{hs} = 2.52 \cdot \sigma_{0.4 \cdot t} - 2.24 \cdot \sigma_{0.9 \cdot t} + 0.72 \cdot \sigma_{1.4 \cdot t} \tag{2.8}$$

(3) Coarse mesh with higher-order elements having lengths equal to plate thickness at the hot spot: Evaluation of stresses at mid-side points or surface centres respectively, i.e. at two reference points **0.5 t** and **1.5 t**, and linear extrapolation (Eq. 2.9).

$$\sigma_{hs} = 1.50 \cdot \sigma_{0.5 \cdot t} - 0.50 \cdot \sigma_{1.5 \cdot t} \qquad (2.9)$$

Application of the usual wall thickness correction, as given in Sect. 3.5.2 is required when the structural hot spot stress of type **"a"** is obtained by surface extrapolation. For circular tubular joints, the wall thickness correction exponent of **n = 0.4** is recommended.

Type "b" Hot Spots:

The stress distribution is not dependent on plate thickness. Therefore, the reference points are given at absolute distances from the weld toe, or from the weld end if the weld does not continue around the end of the attached plate.

(4) Fine mesh with element length of not more than 4 mm at the hot spot: Evaluation of nodal stresses at three reference points **4**, **8** and **12 mm** and quadratic extrapolation (Eq. 2.10).

$$\sigma_{hs} = 3 \cdot \sigma_{4\,mm} - 3 \cdot \sigma_{8\,mm} + \sigma_{12\,mm} \qquad (2.10)$$

(5) Coarse mesh with higher-order elements having length of **10 mm** at the hot spot: Evaluation of stresses at the mid-side points of the first two elements and linear extrapolation (Eq. 2.11).

$$\sigma_{hs} = 1.5 \cdot \sigma_{5\,mm} - 0.5 \cdot \sigma_{15\,mm} \qquad (2.11)$$

Table 2.3 Recommended meshing and extrapolation (see also Fig. 2.14)

Type of model and weld toe		Relatively coarse models		Relatively fine models	
		Type a	Type b	Type a	Type b
Element size	Shells	t x t max t x w/2[a]	10 × 10 mm	≤0.4 t x t or ≤0.4 t x w/2	≤4 × 4 mm
	Solids	t x t max t x w	10 × 10 mm	≤0.4 t x t or ≤0.4 t x w/2	≤4 × 4 mm
Extra-polation points	Shells	0.5 t and 1.5 t mid-side points[b]	5 and 15 mm mid-side points	0.4 t and 1.0 t nodal points	4, 8 and 12 mm nodal points
	Solids	0.5 and 1.5 t surface centre	5 and 15 mm surface centre	0.4 t and 1.0 t nodal points	4, 8 and 12 mm nodal points

[a]w = longitudinal attachment thickness +2 weld leg lengths

[b]surface centre at transverse welds, if the weld below the plate is not modelled (see left part of Fig. 2.13)

In the case of type **“b”** hot spots obtained by surface stress extrapolation, the wall thickness correction (see Sect. 3.5.2) is applied with an exponent of **n = 0.1** (Table 2.3).

Alternative Methods:

Alternative methods of estimation the structural hot spot stress may be useful in special cases. However, care is needed to ensure that they are compatible with the fatigue design resistance data recommended in this document. In the method after Haibach [15], the stress on the surface 2 mm away from the weld toe is determined. In the method after Xiao and Yamada [16], the stress 1 mm below the weld toe on the anticipated crack path is taken. Both methods are useful at sharp changes in the direction of the applied force or at thick-walled structures. In both methods no correction is required for wall thickness. The results from FEA can also be evaluated using nodal forces or through thickness integration to estimate the structural hot spot stress.

A further alternative procedure after Dong and Hong [12] uses a special stress parameter based partly on structural hot spot stress and partly on fracture mechanics analysis, with a consideration of wall thickness and stress gradient.

2.2.3.5 Measurement of Structural Hot Spot Stress

The recommended placement and number of strain gauges depends on the extent of shell bending stresses, the wall thickness and the type of structural stress.

The centre point of the first gauge, whose gauge length should not exceed **0.2 t**, is located at a distance of **0.4 t** from the weld toe. If this is not possible for example due to a small plate thickness, the leading edge of the gauge should be placed at a distance of **0.3 t** from the weld toe. The following extrapolation procedure and number of gauges are recommended (Fig. 2.15):

Type “a” Hot Spots:

(a) Two gauges at reference points **0.4 t** and **1.0 t** and linear extrapolation (Eq. 2.12).

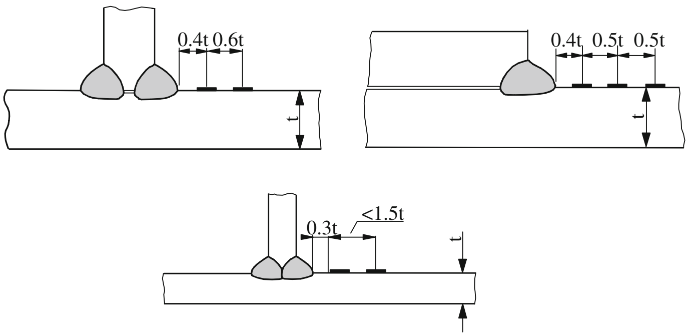

Fig. 2.15 Examples of strain gauges in plate structures

$$\varepsilon_{hs} = 1.67 \cdot \varepsilon_{0.4 \cdot t} - 0.67 \cdot \varepsilon_{1.0 \cdot t} \tag{2.12}$$

(b) Three gauges at reference points **0.4 t**, **0.9 t** and **1.4 t**, and quadratic extrapolation. This method is particularly suitable for cases of pronounced non-linear structural stress increase towards the hot spot (Eq. 2.13).

$$\varepsilon_{hs} = 2.52 \cdot \varepsilon_{0.4 \cdot t} - 2.24 \cdot \varepsilon_{0.9 \cdot t} + 0.72 \cdot \varepsilon_{1.4 \cdot t} \tag{2.13}$$

Precise positioning is not necessary if multi-grid strip gauges are used, since the results can be used to plot the stress distribution approaching the weld toe. The stresses at the required positions can then be read from the fitted curve.

Type "b" Hot Spots:

Three gauges are attached to the plate edge at reference points 4, 8 and 12 mm distant from the weld toe. The hot spot strain is determined by quadratic extrapolation to the weld toe (Eq. 2.14):

$$\varepsilon_{hs} = 3 \cdot \varepsilon_{4mm} - 3 \cdot \varepsilon_{8\,mm} + \varepsilon_{12\,mm} \tag{2.14}$$

Determination of Stress:

If the stress state is close to uniaxial, the approximation to the structural hot spot stress is obtained approximately from Eq. (2.15).

$$\sigma_{hs} = E \cdot \varepsilon_{hs} \tag{2.15}$$

For biaxial stress states, the actual stress may be up to 10 % higher than that obtained from Eq. (2.15). In this case, use of rosette strain gauges is recommended. If the ratio of longitudinal to transversal strains **$\varepsilon y/\varepsilon x$** is available, for example from FEA, the structural hot spot stress $\boldsymbol{\sigma_{hs}}$ can then be resolved from Eq. (2.16), assuming that this principal stress is approximately perpendicular to the weld toe.

$$\sigma_{hs} = E \cdot \varepsilon_x \cdot \frac{1 + \nu \dfrac{\varepsilon_y}{\varepsilon_x}}{1 - \nu^2} \tag{2.16}$$

The above equations also apply if strain ranges are measured, producing the range of structural hot spot stress $\boldsymbol{\Delta\sigma_{hs}}$.

2.2.3.6 Tubular Joints

Special recommendations exist for determining the structural hot spot stress in tubular joints [14]. In general these allow the use of linear extrapolation from the measured or calculated stresses at two reference points. The measurement of simple uni-axial stress is sufficient.

Parametric formulae have been established for the stress concentration factor $\mathbf{k_{hs}}$ in many joints between circular and rectangular section tubes, see Ref. [14]. Hence the structural hot spot stress $\boldsymbol{\sigma}_{\mathbf{hs}}$ becomes:

$$\sigma_{hs} = k_{hs} \cdot \sigma_{nom} \tag{2.17}$$

where $\boldsymbol{\sigma}_{\mathbf{nom}}$ is the nominal axial membrane or bending stress in the braces, calculated by elementary stress analysis or uni-axial measurement.

2.2.4 Effective Notch Stress

2.2.4.1 General

Effective notch stress is the total stress at the root of a notch, obtained assuming linear-elastic material behaviour. To take account of the variation of the weld shape parameters, as well as of the non-linear material behaviour at the notch root, the actual weld contour is replaced by an effective one (Fig. 2.16). For structural steels and aluminium alloys an effective notch root radius of **r = 1 mm** has been verified to give consistent results. For fatigue assessment, the effective notch stress is compared with a single fatigue resistance curve, although, as with other assessment methods, it is necessary to check that the fatigue resistance curve for parent metal is not exceeded in the direct vicinity of the weld [17–21].

The method is restricted to the assessment of welded joints with respect to potential fatigue failures from the weld toe or weld root (Fig. 2.17). The fatigue assessment must be additionally performed at the weld toes for the parent material using structural hot-spot stress (see Sect. 2.2.3) and the associated fatigue class (FAT) for the base material. Other modes of fatigue failure, such as crack growth from surface roughness or embedded defects, are not covered. The method is also not applicable if there is a significant stress component parallel to the weld.

The method is also restricted to assessment of naturally formed as-welded weld toes and roots (Fig. 2.18). At weld toes, an effective notch stress of at least **1.6** times the structural hot-spot stress should be assumed. This condition is usually given at welde roots. More details for practical application can be found in reference [23].

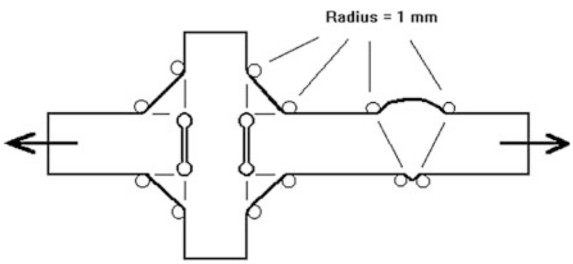

Fig. 2.16 Fictitious rounding of weld toes and roots

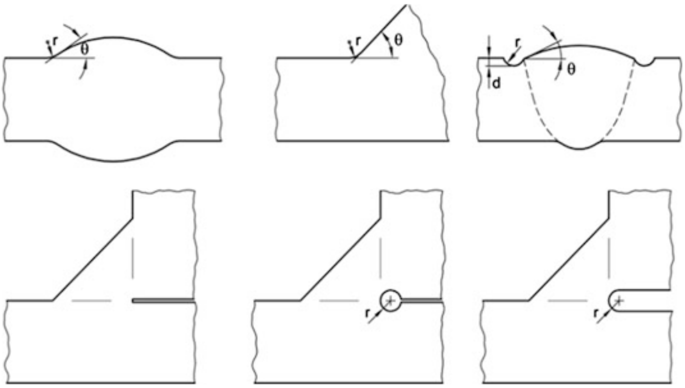

Fig. 2.17 Recommended rounding of weld toes and fillet weld roots

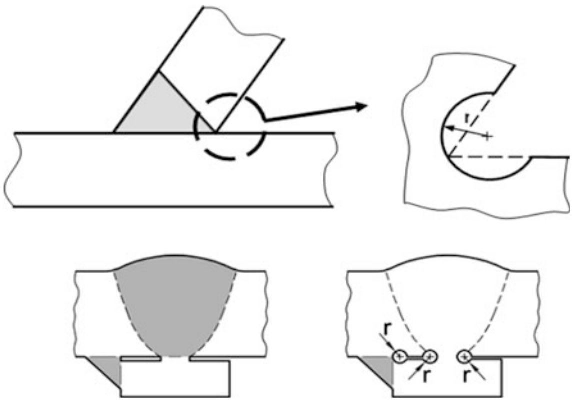

Fig. 2.18 Recommended rounding at Y-joint and backing bar roots

The method is well suited to the comparison of alternative weld geometries. Unless otherwise specified, it is suggested that welds should be modelled with flank angles of 30° for butt welds and 45° for fillet welds.

The method is limited to thicknesses **t ≥ 5 mm**, since the method has not yet been verified for smaller wall thicknesses.

Welds toes, machined or ground to a specified profile, shall be assessed using the notch stress of the actual profile in conjunction with the nominal stress based fatigue resistance curve for a butt weld ground flush to plate.

2.2.4.2 Calculation of Effective Notch Stress

Effective notch stresses or stress concentration factors can be calculated by parametric formulae, taken from diagrams or calculated by finite element or boundary element models. The effective notch radius is introduced such that the tip of the

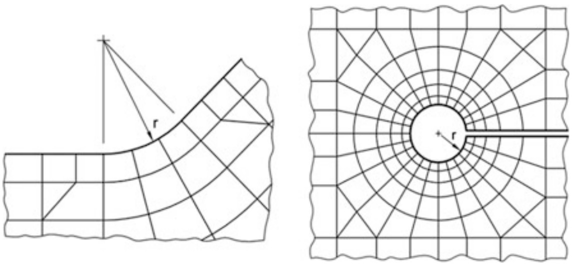

Fig. 2.19 Recommended meshing at weld toes and roots

Table 2.4 Recommended sizes of elements on surface

Element type	Relative size	Absolute size [mm]	No. of elements in 45° arc	No. of elements in 360° arc
Quadratic with mid-side nodes	≤r/4	≤0.25	≥3	≥24
Linear	≤r/6	≤0.15	≥5	≥40

radius coincides with the root of the real notch, e.g. the end of an unwelded root gap.

For the determination of effective notch stress by FEA, element sizes of not more that 1/6 of the radius are recommended in case of linear elements, and 1/4 of the radius in case of higher order elements (Fig. 2.19 and Table 2.4). These sizes have to be observed in the curved parts as well as in the beginning of the straight part of the notch surfaces in both directions, tangential and normal to the surface, see also Ref. [22].

Possible misalignment has to be considered explicitly in the calculations.

The model may be simplified from a 3-dimensional to a 2-dimensional one under the following conditions:

(a) The loading should be mainly perpendicular to the weld, i.e. normal and shear stress in direction of the weld are not existent or small and can be neglected.
(b) The loading and the geometry of the weld should not vary in the area to be assessed.

At an occurrence of multiaxial stress, the principles of Chap. 4 should be applied. If there is a proportional loading, i.e. all stress components are in a constant phase, then the maximum principle stress may be used, provided that the minimum principle stress has the same sign. Both should be either positive or negative. In all other cases the regulations of Sect. 4.3 should be applied.

2.2.4.3 Measurement of Effective Notch Stress

Because the effective notch radius is an idealization, it cannot be measured directly in the welded component. In contrast, the simple definition of the effective notch can be used for photo-elastic stress measurements in resin models.

2.2.5 *Stress Intensity Factors*

2.2.5.1 General

Fracture was developed to assess the behaviour of cracks or crack-like imperfections in components (Fig. 2.20). The methods are well established, but require an adequate level of knowledge and experience. It is recommended to perform the assessment procedures using the recommendations given here and consulting the actual compendia of the method [43, 53]. Fracture mechanics is used for several purposes as e.g.:

(a) Assessment of fracture, especially brittle fracture, in a component containing cracks or crack-like details.
(b) Assessment of fatigue properties in a component containing cracks or crack-like imperfection as e.g. in welded joints.
(c) Predicting the fatigue properties of severely notched components with no or a relatively short crack initiation phase. Welded joints behave as being severely notched. Predictions are made assuming small initial defects.

The fatigue assessment procedure as in (b) and (c) is performed by the calculation of the growth of an initial crack $\mathbf{a_i}$ to a final size $\mathbf{a_f}$. Since crack initiation occupies only a small proportion of the lives of welded joints in structural metals, the method is suitable for assessment of fatigue life, inspection intervals, crack-like weld imperfections and the effect of variable amplitude loading. The final crack $\mathbf{a_f}$ may be estimated as about one half wall thickness, since there is a rapid onset of crack propagation. Only a few and insignificant numbers of cycles are spent in that phase of fatigue.

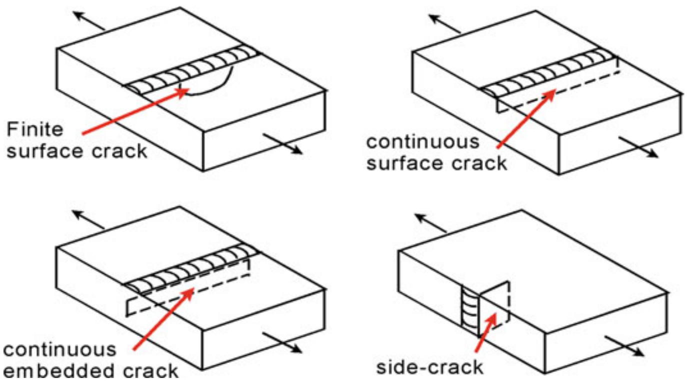

Fig. 2.20 Examples for different categories of cracks

2.2.5.2 Determination of Stress Intensity Factors

The parameter which describes the fatigue action at a crack tip in terms of crack propagation is the stress intensity factor (SIF) range **ΔK**. The starting crack configuration is the centre crack in an infinite plate. The stress intensity factor **K** is defined by the formula $K = \sigma \cdot \sqrt{\pi \cdot a}$. Where **σ** is the remote stress in the plate and **a** is the crack parameter, here the half distance from tip to tip.

2.2.5.2.1 Standard Configurations

In existing components, there are various crack configurations and geometrical shapes. So, corrections are needed for the deviation from the centre cracked plate. The formula for the stress intensity factor has to be expanded by a correction function $Y_u(a)$. These corrections take into account the following parameters and crack locations:

(a) Free surface of a surface crack.
(b) Embedded crack located inside of a plate.
(c) Limited width or wall thickness.
(d) Shape of a crack, mostly taken as being elliptic.
(e) Distance to an edge.

For a variety of crack configurations, parametric formulae for the correction function $\mathbf{Y_u(a)}$ have been developed (see Appendix 6.2 and references [25, 53]). These correction functions are based on different applied stress types (e.g. membrane, bending, structural hot spot stress, nominal stress). The one used must correspond to the stress type under consideration.

2.2.5.2.2 Stress Intensity Factor for Weld Toes

Fracture mechanics calculations related to welded joints are generally based on the total stress at the notch root, e.g. at the weld toe. The universal correction function $\mathbf{Y_u(a)}$ may be separated into the correction of a standard configuration **Y(a)** and an additional correction for the local notch of the weld toe $\mathbf{M_k(a)}$. A further separation into membrane stress and shell bending stress was done at most of the parametric formulae for the functions **Y(a)** and $\mathbf{M_k(a)}$ [32, 34].

$$K = \sigma \cdot \sqrt{\pi \cdot a} \cdot Y_u(a) \tag{2.18}$$

In practical application, first the relevant applied stress (usually the local nominal or the structural hot spot stress) at the location of the crack is determined, assuming that no crack is present. If required, the stress should be separated into membrane and shell bending stress components. The stress intensity factor (SIF) **K** then results as a superposition of the effects of both stress components. The effects of the crack shape and size are covered by the correction function **Y**. The effects of the any remaining stress raising discontinuity or notch from the weld toe (non-linear peak stress) can to be covered by additional factors $\mathbf{M_k}$, while

$$K = \sqrt{\pi \cdot a} \cdot (\sigma_m \cdot Y_m(a) \cdot M_{k,m}(a) + \sigma_b(a) \cdot Y_b(a) \cdot M_{k,b}(a)) \tag{2.18a}$$

where

K	stress intensity factor
$\boldsymbol{\sigma_m}$	membrane stress
$\boldsymbol{\sigma_b}$	shell bending stress
$\mathbf{Y_m}$	correction function for membrane stress intensity factor
$\mathbf{Y_b}$	correction function for shell bending stress intensity factor
$\mathbf{M_{k,m}}$	correction for non-linear stress peak in terms of membrane action
$\mathbf{M_{k,b}}$	Correction for non-linear stress peak in terms of shell bending

The correction functions $\mathbf{Y_m}$ and $\mathbf{Y_b}$ can be found in the literature. The solutions in Ref. [25–30] are particularly recommended. For most cases, the formulae for stress intensity factors given in Appendix 6.2 are adequate. $\mathbf{M_k}$-factors may be found in references [31, 32].

2.2.5.2.3 Weight Function Approach

The weight function approach is based on the idea that a given stress distribution can discretized into differential pairs of split forces which open a crack. The action of each differential force on a crack can be described by a function, the so called weight function **h(x, a)**. The determination of the stress intensity factor is thus reduced into an integration over the crack length. By this method, arbitrary stress distributions can be assessed. The basic formulation of the weight function approach is

$$K = \int_{x=0}^{x=a} \sigma(x) \cdot h(x,a) \cdot dx \tag{2.19}$$

Weight functions have been developed for 2-dimensional (Fett and Munz Ref. [39]) and 3-dimensional problems (Glinka et al., see Appendix 6.2 and Ref. [40]). More weight functions may be found in literature (Ref. [43]).

The application of weight functions requires an integration process to obtain the stress intensity factor. Here it must be observed that several weight functions lead to improper integrals, i.e. integrals with infinite boundaries but finite solutions. There are two ways to overcome. Firstly to use very fine steps near the singularity, or secondly to integrate analytically, if possible, and to calculate small stripes, which are later summed up for the number of cycles.

For transverse loaded welds, parametric formulae for the stress distribution in the plate have been developed. In these cases a finite element calculation may not be necessary (Hall et al. Ref. [41])

2.2.5.2.4 Finite Element Programs

The determination of stresses and stress distributions finite element programs may be used. It must be made sure that the refinement of the meshing corresponds to method, which is used for deriving the stress intensity factors.

For the use of standard solutions and existing $\mathbf{M_k}$ formulae, a coarse meshing may be sufficient to determine the membrane and the shell bending stress. If a weight function approach is used, a fine meshing is needed for a full information about the stress distribution at the weld toe or root, whichever is considered.

Several program systems exist which provide a direct determination of stress intensity factors. The meshing should be made according to the method used and to the recommendations of the program manual.

2.2.5.2.5 Aspect Ratio

The aspect ratio **a:c** is a significant parameter for the stress intensity factor (Fig. 2.21). It has to be taken into consideration at fracture mechanics calculations. This consideration can be done in different ways:

(a) Direct determination and calculation of crack growth in **c**-direction, e.g. by 3-dimensional weight functions or $\mathbf{M_k}$-formulae. These formulae give the stress intensity factor at the surface, which governs the crack propagation in **c**-direction.
(b) Application of formulae and values which have been derived from toes of fillet welds by fitting of experimental data, a possible example is given by Engesvik [44].

$$2 \cdot c = -0.27 + 6.34 \cdot a \ \text{if} \ a > 0.1 < a < 3 \ \text{mm} \tag{2.20}$$

$$a/(2 \cdot c) = 0 \ \text{if} \ a > 3 \ \text{mm}$$

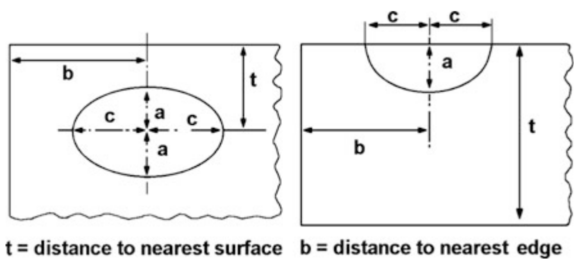

Fig. 2.21 Crack parameters

(c) If only 2-dimensional Mk values are given, then the crack depth of a = 0.15 or 0.1 mm may be used to calculate the effective stress intensity factor at the surface for the crack propagation in "**c**"-direction [53].
(d) A constant aspect ratio of **a:c = 0.1** may be taken as a conservative approach.

2.2.5.2.6 Assessment of Welded Joints Without Detected Imperfections

Fracture mechanics may be used to assess the fatigue properties of welded joints in which no imperfections have been detected. In such cases it is necessary to assume the presence of an initial crack, for example based on prior metallurgical evidence, the detection limit of the used inspection method or fitting from fatigue data, and then to calculate the stress intensity factor as above.

In case of post-weld treatment there is a possibly larger number of cycles for crack initiation. That shall be assessed and/or considered by a appropriate calculation procedure, which might be taken from the relevant literature.

For cracks starting from a weld toe, in absences of other evidence, it is recommended that an initial crack depth of at **a = 0.1 mm** and an aspect ratio as given above might be taken considering that there might be multiple spots for crack initiation. The initial cracks have been derived from fitting the assessment procedure to experimental data, disregarding possible fracture mechanics short crack effects. If possible, the calculations should be compared or calibrated at similar joint details with known fatigue properties.

If no weld toe radius **ρ** was specified or determined by measuring, it is recommended to assume a sharp corner i.e. a toe radius of **ρ = 0** to **ρ = 0.2 mm**.

For root gaps in load-carrying fillet welded cruciform joints, the actual root gap should be taken as the initial crack.

It is convenient to disregard the threshold properties. Later the obtained fatigue cycles may be converted into a FAT class and to proceed using that S-N curve.

$$FAT = \Delta\sigma_{applied} \cdot \sqrt[m]{\frac{N}{2 \cdot 10^6}} \tag{2.21}$$

2.3 Stress History

2.3.1 General

The fatigue design data presented in Chap. 3 were obtained from tests performed under constant amplitude loading. However, loads and the resulting fatigue actions (i.e. stresses) in real structures usually fluctuate in an irregular manner and give rise to variable amplitude loading. The stress range may vary in both magnitude and period from cycle to cycle.

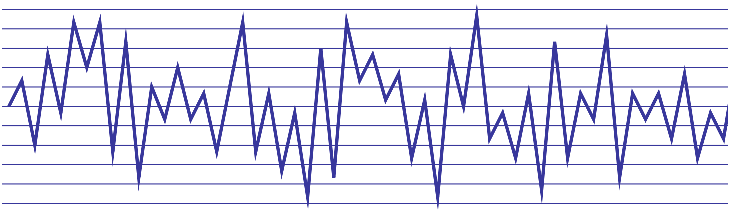

Fig. 2.22 Stress time history illustration

The stress history is a record and/or a representation of the fluctuations of the fatigue actions in the anticipated service time of the component. It is described in terms of successive maxima and minima of the stress caused by the fatigue actions (Fig. 2.22). It should aim to cover all loading events and the corresponding induced dynamic response in a conservative way.

In most cases, the stress-time history is stationary and ergodic, which allows the definition of a mean range and its variance, a statistical histogram and distribution, an energy spectrum and a maximum values probabilistic distribution from a representation covering a limited period of operation. Therefore, the data needed to perform a fatigue analysis can be determined from service load measurements or observations conducted over a limited time, as long as it is reasonably representative of the loading to be experienced during the whole fatigue life.

A stress history may be given as

(a) a record of successive maxima and minima of stress measured in a comparable structure for comparable loading and service life, or a typical sequence of load events.
(b) a two dimensional transition matrix of the stress history derived from a).
(c) a one- or two-dimensional stress range histogram (stress range occurrences) obtained from a) by a specified counting method.
(d) a one-dimensional stress range histogram (stress range exceedences, stress range spectrum) specified by a design code.

The representations (a) and (b) may be used for component testing, while (c) and (d) are most useful for fatigue assessment by calculation.

2.3.2 Cycle Counting Methods

Cycle counting is the process of converting a variable amplitude stress sequence into a series of constant amplitude stress range cycles that are equivalent in terms of damage to the original sequence. Various methods are available including zero crossing counting, peak counting, range pair counting and rainflow counting. For welded components, the ‘rainflow’ or similar ‘reservoir’ methods are recommended for counting stress ranges [58, 59].

2.3.3 Cumulative Frequency Diagram (Stress Spectrum)

The cumulative frequency diagram (stress spectrum) corresponds to the cumulative probability of stress range expressed in terms of stress range level exceedences versus the number of cycles. The curve is therefore continuous.

It is usually more convenient to represent the spectrum by a table of discrete blocks of cycles of constant amplitude stress range, typically up to 20 different stress levels. The assumed magnitude of the stress range in a given block would then depend on the conservatism required. Typical values would be the maximum or the mean of the stress range in the block.

Besides the representation in probabilities, a presentation of the number of occurrences or exceedances in a given number of cycles, e.g. 1 million, is used. An example showing a Gaussian normal distribution is given below (Table 2.5 and Fig. 2.23):

Table 2.5 Example of a stress range occurrence table (stress histogram or frequency)

Block No.	Relative stress range	Occurrence (frequency)
1	1.000	2
2	0.950	16
3	0.850	280
4	0.725	2720
5	0.575	20000
6	0.425	92000
7	0.275	280000
8	0.125	605000

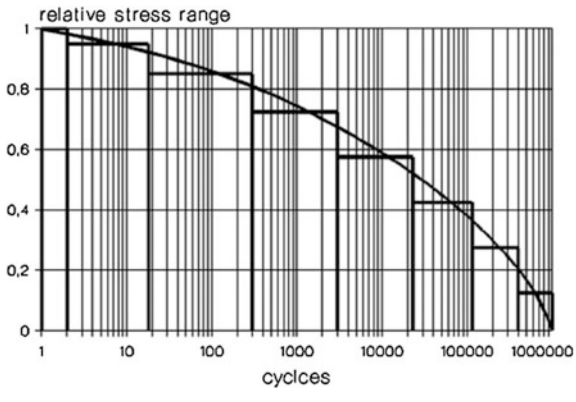

Fig. 2.23 Example of a cumulative frequency diagram (stress spectrum)

Chapter 3
Fatigue Resistance

3.1 Basic Principles

Fatigue resistance is usually derived from constant or variable amplitude tests. The fatigue resistance data given here are based on published results from constant amplitude tests. Guidance on the direct use of fatigue test data is given in Sects. 3.7 and 4.5.

As generally required, the fatigue resistance data presented here are expressed in terms of the same type of stress as that, used to determine the test data upon which they are based.

The present fatigue endurance resistance data for welded joints are expressed as S-N curves. However, there are different definitions of failure in conventional fatigue endurance testing. In general, small welded specimens are tested to complete rupture, which is usually very close to through-thickness cracking. In large components or vessels, the observation of a larger or through-wall crack is usually taken as a failure. The fatigue failure according to the present S-N curves effectively corresponds to through-section cracking. The S-N curves are of the form:

$$N = \frac{C}{\Delta\sigma^m} \quad \text{or} \quad N = \frac{C}{\Delta\tau^m} \tag{3.1}$$

where the slope **m** may adopt different values over the range of possible fatigue lives, from the low endurance to the high cycle regime (see Sect. 3.2).

For fracture mechanics analyses, the fatigue resistance data are in the form of relationships between **ΔK** and the rate of fatigue crack propagation (**da/dN**). The fatigue crack growth rate data are derived by monitoring crack propagation in tests.

The original version of this chapter was revised. Belated correction has been updated. An erratum to this chapter is available at DOI 10.1007/978-3-319-23757-2_8

The original version of this chapter was revised. An erratum to this chapter can be found at DOI 10.1007/978-3-319-23757-2_7

A.F. Hobbacher, *Recommendations for Fatigue Design of Welded Joints and Components*, IIW Collection, DOI 10.1007/978-3-319-23757-2_3

All fatigue resistance data are given as characteristic values, which are assumed to represent a survival probability of at least 95 %, calculated from the mean value on the basis of two-sided 75 % tolerance limits of the mean, unless otherwise stated (see Sect. 3.7). Other existing definitions as e.g. a survival probability of 95 % on the basis of 95 % one-sided limit of the mean or mean minus two standard deviations corresponding to a survival probability of 97.7 % are practically equal for engineering applications.

The (nominal) stress range should be within the limits of the elastic properties of the material. The range of the design values of the stress range shall not exceed $\mathbf{1.5 \cdot f_y}$ for nominal normal stresses or $\mathbf{1.5 \cdot f_y/\sqrt{3}}$ for nominal shear stresses.

The fatigue resistance of a welded joint is also limited by the fatigue resistance of the parent material.

3.2 Fatigue Resistance of Classified Structural Details

The fatigue assessment of classified structural details and welded joints is based on the nominal stress range. In most cases, structural details are assessed on the basis of the maximum principal stress range in the section where potential fatigue cracking is considered. However, guidance is also given for the assessment of shear loaded details, based on the maximum shear stress range. Separate S-N curves are provided for consideration of normal or shear stress ranges, as illustrated in Figs. 3.1, 3.2 and 3.3 respectively.

Care must be taken to ensure that the stress used for the fatigue assessment is the same as that given in the tables of the classified structural details. Macro-structural hot

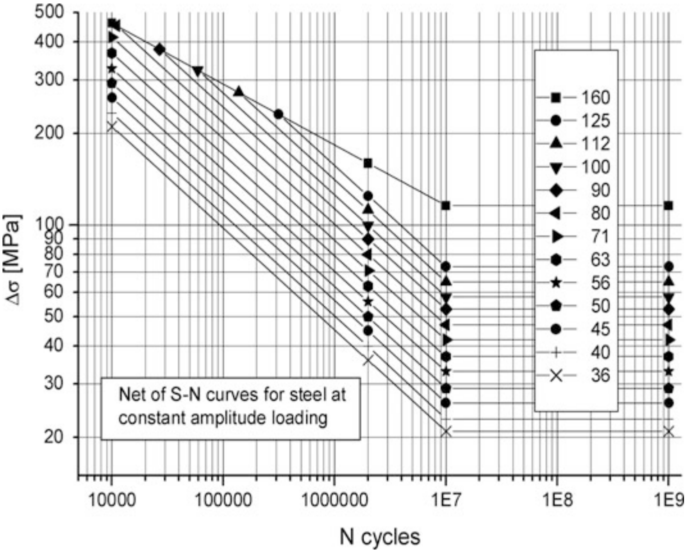

Fig. 3.1 Fatigue resistance S-N curves for steel, normal stress, standard applications

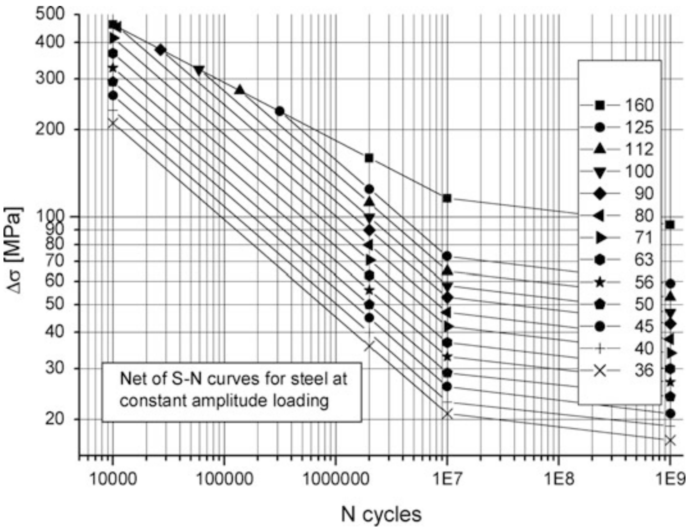

Fig. 3.2 Fatigue resistance S-N curves for steel, normal stress, very high cycles applications

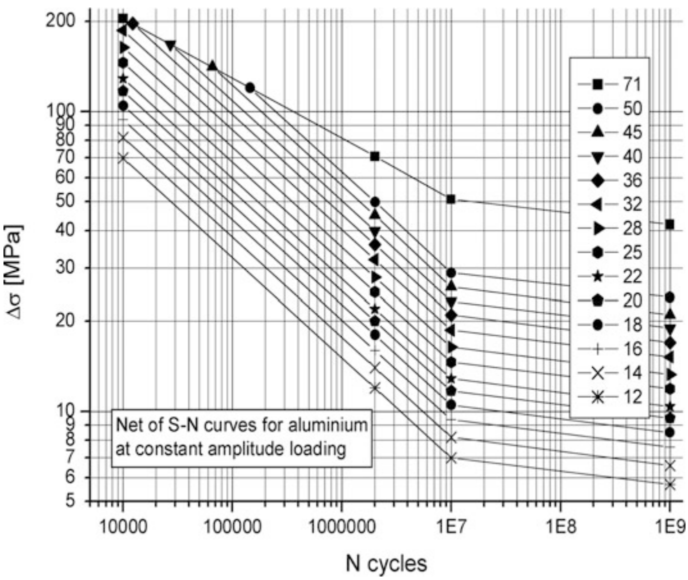

Fig. 3.3 Fatigue resistance S-N curves for aluminium, normal stress

spot stress concentrations not covered by the structural detail of the joint itself, e.g. large cut-outs in the vicinity of the joint, have to be accounted for by the use of a detailed stress analysis, e.g. finite element analysis, or appropriate stress concentration factors (see Sect. 2.2.2).

The fatigue curves are based on representative experimental investigations and thus include the effects of:

- structural hot spot stress concentrations due to the detail shown
- local stress concentrations due to the weld geometry
- weld imperfections consistent with normal fabrication standards
- direction of loading
- high residual stresses
- metallurgical conditions
- welding process (fusion welding, unless otherwise stated)
- inspection procedure (NDT), if specified
- post weld treatment, if specified

Furthermore, within the limits imposed by static strength considerations, the fatigue curves of welded joints are independent of the tensile strength of the material.

Each fatigue strength S-N curve is identified by the characteristic fatigue strength of the detail in MPa at 2 million cycles. This value is the fatigue class (FAT).

The slope of the fatigue strength S-N curves for details assessed on the basis of normal stresses (Fig. 3.1) is **m = 3.00** if not stated expressly otherwise. The constant amplitude knee point is assumed to correspond to **N = 10^7 cycles**.

The slope of the fatigue strength curves for details assessed on the basis of shear stresses (Figs. 3.2, 3.4, 3.5 and 3.6) is **m = 5.00**, but in this case the knee point is assumed to correspond to **N = 10^8 cycles**.

The conventional assumption is that the S-N curves terminate at a fatigue limit, below which failure will not occur, or in which case the S-N curve becomes a horizontal line. Traditionally, this constant amplitude fatigue limit (CAFL), also referred as ‘knee point’, is defined in terms of the corresponding fatigue endurance on the S-N curve, $N = 10^7$ being the most common assumption (see Fig. 3.1). However, new experimental data indicate that a CAFL does not exist and the S-N curve should continue on the basis of a further decline in stress range of about 10 % per decade in terms of cycles, which corresponds to a slope of **m = 22**.

This issue is only relevant if a design is expected to withstand very large numbers of stress cycles, such as for example at rotating welded machine parts. The matter is still under development and users should consult the latest relevant literature. Meanwhile, the nominal stress-based characteristic S-N curves are presented with the extrapolation beyond 10^7 cycles at a slope of m = 22 in Figs. 3.2 and 3.3.

The descriptions of the structural details only partially include information about the weld size, shape and quality. The data refer to a standard quality as given in codes and standard welding procedures. For higher or lower qualities, conditions of welding may be specified and verified by test (Sect. 3.7).

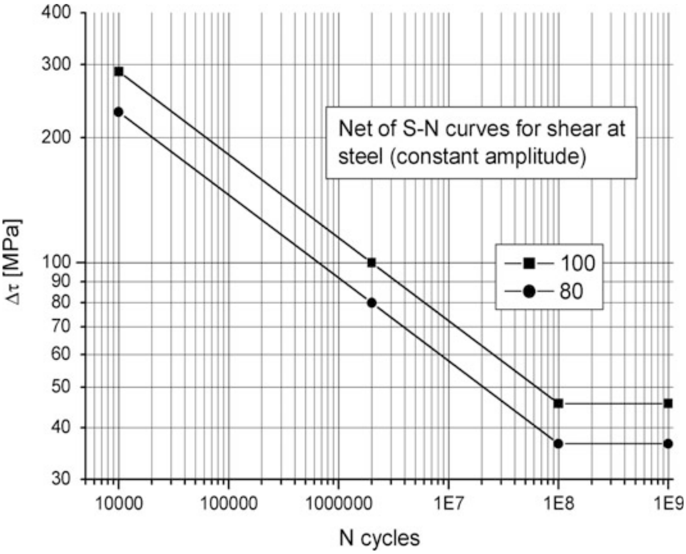

Fig. 3.4 Fatigue resistance S-N curve for shear at steel, standard applications

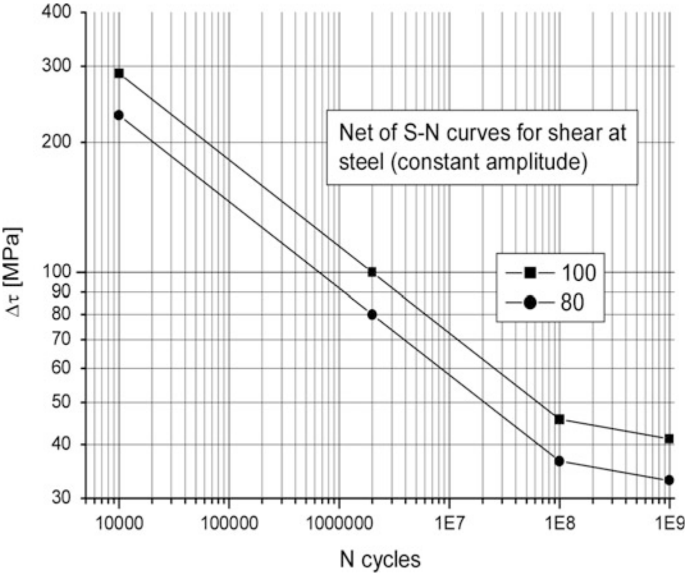

Fig. 3.5 Fatigue resistance S-N curves for shear at steel, very high cycle applications

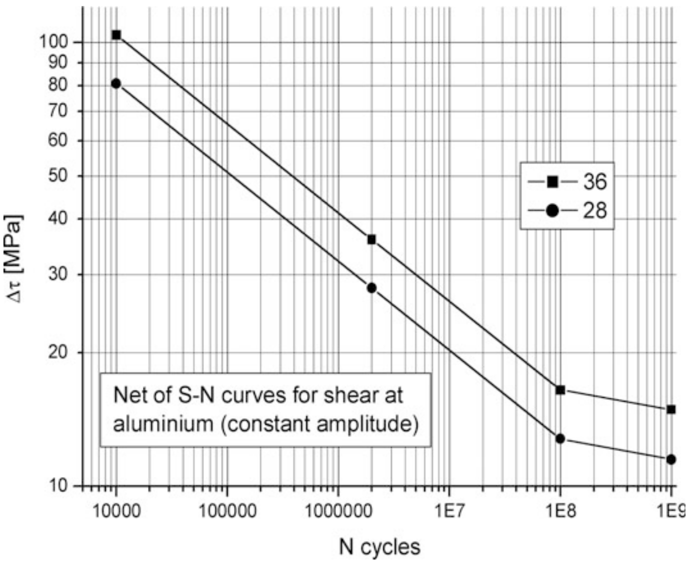

Fig. 3.6 Fatigue resistance S-N curve for shear at aluminium

As appropriate, the fatigue classes given in Table 3.1 shall be modified according to Sect. 3.5. The limitations on weld imperfections shall be considered (Sect. 3.8).

All butt weld joints shall be fully fused and have full penetration welds, unless otherwise stated.

All the S-N curves for weld details are limited by the S-N curve for the parent metal, which may vary with material tensile strength. It is recommended that a higher fatigue class for the material than stated (i.e. FAT 160 for steel or FAT 71 for aluminium alloys) should only be assumed if verified by test.

The S-N curves for weld details refer to specific failure modes, generally fatigue crack growth from the weld toe through the base material, from the weld root trough the weld throat, or from the weld surface through the weld and then into the base material. In an assessment of a given weld detail it is important to consider all possible potential failure modes for the direction of loading. E.g. at cruciform joints with fillet welds, both potential failure modes, such as toe crack through plate and root crack through weld throat, have to be assessed.

Table 3.1 Fatigue resistance values for structural details in steel and aluminium assessed on the basis of nominal stresses

No.	Structural Detail	Description (St. = steel; Al. = aluminium)	FAT St.	FAT Al.	Requirements and remarks
100	Unwelded parts of a component				
111	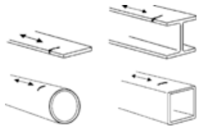	Rolled or extruded products, components with machined edges, seamless hollow sections m = 5			No fatigue resistance of any detail to be higher at any number of cycles Sharp edges, surface and rolling flaws to be removed by grinding. Any machining lines or grooves to be parallel to stresses
		Steel: A higher FAT class may be used if verified by test or specified by applicable code	160		
		Al.: AA 5000/6000 alloys		71	
		AA 7000 alloys		80	
121	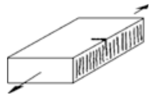	Machine gas cut or sheared material with subsequent dressing, no cracks by inspection, no visible imperfections m = 3	140	—	All visible signs of edge imperfections to be removed. The cut surfaces to be machined or ground, all burrs to be removed No repair by welding refill Notch effects due to shape of edges shall be considered
122	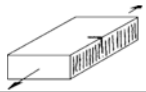	Machine thermally cut edges, corners removed, no cracks by inspection m = 3	125	40	Notch effects due to shape of edges shall be considered
123	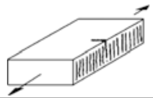	Manually thermally cut edges, free from cracks and severe notches m = 3	100	–	Notch effects due to shape of edges shall be considered
124	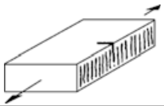	Manually thermally cut edges, uncontrolled, no notch deeper than 0.5 mm m = 3	80	–	Notch effects due to shape of edges shall be considered

(continued)

Table 3.1 (continued)

No.	Structural Detail	Description (St. = steel; Al. = aluminium)	FAT St.	FAT Al.	Requirements and remarks
200	**Butt welds, transverse loaded**				
211		Transverse loaded butt weld (X-groove or V-groove) ground flush to plate, 100 % NDT	112	45	All welds ground flush to surface, grinding parallel to direction of stress. Weld run-on and run-off pieces to be used and subsequently removed. Plate edges ground flush in direction of stress. Welded from both sides. Misalignment <5 % of plate thickness Proved free from significant defects by appropriate NDT
212		Transverse butt weld made in shop in flat position, NDT weld reinforcement <0.1 A thickness	90	36	Weld run-on and run-off pieces to be used and subsequently removed. Plate edges ground flush in direction of stress. Welded from both sides. Misalignment <5 % of plate thickness
213		Transverse butt weld not satisfying conditions of 212, NDT Al.: Butt weld with toe angle ≤ 50° Butt welds with toe angle > 50°	80	 32 25	Weld run-on and run-off pieces to be used and subsequently removed. Plate edges ground flush in direction of stress. Welded from both sides. Misalignment <10 % of plate thickness
214		Transverse butt weld, welded on non-fusible temporary backing, root crack	80	28	Backing removed, root visually inspected Misalignment <10 % of plate thickness
215		Transverse butt weld on permanent backing bar	71	25	Misalignment <10 % of plate thickness
216	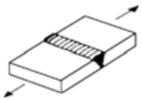	Transverse butt welds welded from one side without backing bar, full penetration Root checked by appropriate NDT including visual inspection NDT without visual inspection No NDT	 71 63 36	 28 20 12	Misalignment <10 % of plate thickness

(continued)

Table 3.1 (continued)

No.	Structural Detail	Description (St. = steel; Al. = aluminium)	FAT St.	FAT Al.	Requirements and remarks
217		Transverse partial penetration butt weld, analysis based on stress in weld throat sectional area, weld overfill not to be taken into account	36	12	The detail is not recommended for fatigue loaded members Assessment by notch stress or fracture mechanics is preferred
221	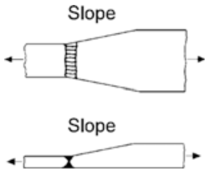	Transverse butt weld ground flush, NDT, with transition in thickness and width Slope 1:5 Slope 1:3 Slope 1:2	 112 100 90	 45 40 32	All welds ground flush to surface, grinding parallel to direction of loading. Weld run-on and run-off pieces to be used and subsequently removed. Plate edges to be ground flush in direction of stress Misalignment due to deliberate thickness step to be considered, see Sect. 3.8.2. Additional misalignment due to fabrication imperfection < 5 % of plate thickness
222	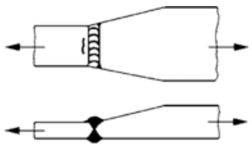	Transverse butt weld made in shop, welded in flat position, weld profile controlled, NDT, with transition in thickness and width: Slope 1:5 Slope 1:3 Slope 1:2	90 80 72	32 28 25	Weld run-on and run-off pieces to be used and subsequently removed. Plate edges ground flush in direction of stress Misalignment due to deliberate thickness step to be considered, see Sect. 3.8.2. Additional misalignment due to fabrication imperfection < 5 % of plate thickness
223	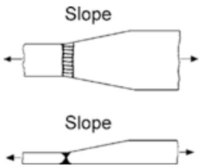	Transverse butt weld, NDT, with transition on thickness and width Slope 1:5 Slope 1:3 Slope 1:2	 80 71 63	 25 22 20	Weld run-on and run-off pieces to be used and subsequently removed. Plate edges ground flush in direction of stress Misalignment due to deliberate thickness step to be considered, see Sect. 3.8.2. Additional misalignment due to fabrication imperfection < 10 % of plate thickness

(continued)

Table 3.1 (continued)

No.	Structural Detail	Description (St. = steel; Al. = aluminium)	FAT St.	FAT Al.	Requirements and remarks
224		Transverse butt weld, different thicknesses without transition, centres aligned In cases, where weld profile is equivalent to a moderate slope transition, see no. 222	71	22	Misalignment < 10 % of plate thickness If centers are deliberately misaligned, this misalignment has to be considered, see Sect. 3.8.2
225		Three plate connection, potential cracking from root	71	22	Misalignment < 10 % of plate thickness
226	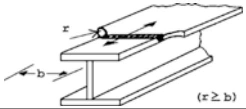	Transverse butt weld flange splice in built-up section welded prior to the assembly, ground flush, with radius transition, NDT	100	40	All welds ground flush to surface, grinding parallel to direction of stress. Weld run-on and run-off pieces to be used and subsequently removed. Plate edges ground flush in direction of stress
231	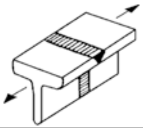	Transverse butt weld splice in rolled section or bar besides flats, ground flush, NDT	80	28	All welds ground flush to surface, grinding parallel to direction of stress. Weld run-on and run-off pieces to be used and subsequently removed. Plate edges ground flush in direction of stress
232	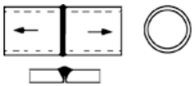	Transverse butt weld splice in circular hollow section, welded from one side, full penetration, potential failure from root root inspected by NDT no NDT	 71 36	 28 12	Welded in flat position Axial misalignment < 5 % of wall thickness
233	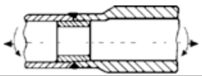	Tubular joint with permanent backing	71	28	Full peneration weld
234	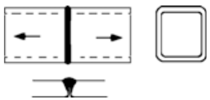	Transverse butt weld splice in rectangular hollow section, welded from one side, full penetration, root crack root inspected by NDT, t >=8 mm root inspected by NDT, t < 8 mm no NDT	 71 56 36	 28 25 12	Welded in flat position

(continued)

Table 3.1 (continued)

No.	Structural Detail	Description (St. = steel; Al. = aluminium)	FAT St.	FAT Al.	Requirements and remarks
241	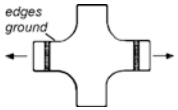	Transverse butt weld ground flush, weld ends and radius ground, 100 % NDT at crossing flanges, radius transition	100	40	All welds ground flush to surface, grinding parallel to direction of stress. Weld run-on and run-off pieces to be used and subsequently removed. Plate edges ground flush in direction of stress Welded from both sides. No misalignment
242	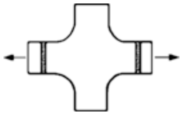	Transverse butt weld made in shop at flat position, weld profile controlled, NDT, at crossing flanges, radius transition	90	36	Weld run-on and run-off pieces to be used and subsequently removed. Plate edges ground flush in direction of stress Welded from both sides.Misalignment < 5 % of plate thickness
243	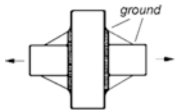	Transverse butt weld at intersecting flange, weld ground flush, NDT, at crossing flanges with welded triangular transition plates, weld ends ground Crack starting at butt weld For crack of continuous flange see details 525 and 526	80	32	All welds ground flush to surface, grinding parallel to direction of stress. Plate edges ground flush in direction of stress Welded from both sides. Misalignment < 10 % of plate thickness
244	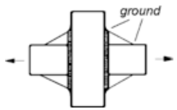	Transverse butt weld at intersecting flange, NDT, at crossing flanges, with welded triangular transition plates, weld ends ground Crack starting at butt weld For crack of continuous flange see details 525 and 526	71	28	Plate edges ground flush in direction of stress Welded from both sides. Misalignment < 10 % of plate thickness
245	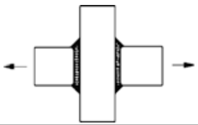	Transverse butt weld at intersecting flange Crack starting at butt weld For crack of continuous flange see details 525 and 526	50	20	Welded from both sides. Misalignment < 10 % of plate thickness

(continued)

Table 3.1 (continued)

No.	Structural Detail	Description (St. = steel; Al. = aluminium)	FAT St.	FAT Al.	Requirements and remarks
300	**Longitudinal load-carrying welds**				
311		Automatic longitudinal seam welds without stop/start positions in hollow sections with stop/start positions	125 90	50 36	
312	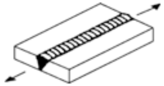	Longitudinal butt weld, both sides ground flush parallel to load direction, or continuous automatic longitudinal butt weld without start/stop positions proved free from significant defects by appropriate NDT	125	50	
313	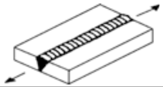	Longitudinal butt weld, without stop/start positions, NDT with stop/start positions	112 90	45 36	
321	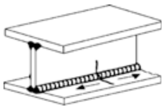	Continuous automatic longitudinal fully penetrated K-butt weld without stop/start positions (based on stress range in flange) NDT	125	50	No stop-start position is permitted except when the repair is performed by a specialist and inspection is carried out to verify the proper execution of the weld
322	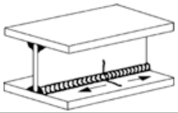	Continuous automatic longitudinal double sided fillet weld without stop/start positions (based on stress range in flange)	112	45	
323	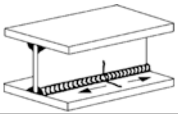	Continuous manual longitudinal fillet or butt weld (based on stress range in flange)	90	36	

(continued)

Table 3.1 (continued)

No.	Structural Detail	Description (St. = steel; Al. = aluminium)	FAT St.	FAT Al.	Requirements and remarks
324	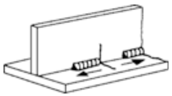	Intermittent longitudinal fillet weld (based on normal stress in flange **σ** and shear stress in web **τ** at weld ends)			Analysis based on normal stress in flange and shear stress in web at weld ends Representation by formula: Steel: FAT = 80 · (1 - Δτ/Δσ) but not lower than 36 Alum.: FAT = 32 · (1 - Δτ/Δσ) but not lower than 14
		τ/σ = 0	80	32	
		0.0–0.2	71	28	
		0.2–0.3	63	25	
		0.3–0.4	56	22	
		0.4–0.5	50	20	
		0.5–0.6	45	18	
		0.6–0.7	40	16	
		>0.7	36	14	
325	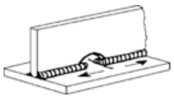	Longitudinal butt weld, fillet weld or intermittent weld with cope holes (based on normal stress in flange **σ** and shear stress in web **τ** at weld ends), cope holes not higher than 40 % of web			Analysis based on normal stress in flange and shear stress in web at weld ends Representation by formula: Steel: FAT = 71 · (1 − Δτ/Δσ) but not lower than 36 Alum.: FAT = 28 . (1 − Δτ/Δσ) but not lower than 14
		τ/σ = 0	71	28	
		0.0–0.2	63	25	
		0.2–0.3	56	22	
		0.3–0.4	50	20	
		0.4–0.5	45	18	
		0.5–0.6	40	16	
		>0.6	36	14	

(continued)

Table 3.1 (continued)

No.	Structural Detail	Description (St. = steel; Al. = aluminium)	FAT St.	FAT Al.	Requirements and remarks
331	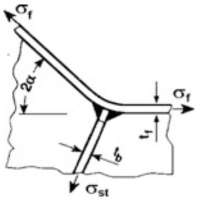	Joint at stiffened knuckle of a flange to be assessed according to no. 411–414, depending on type of joint Stress in stiffener plate: $\sigma = \sigma_f \cdot \frac{A_f}{\sum A_{st}} \cdot 2 \cdot \sin\alpha$ A_f = area of flange A_{st} = area of stiffener Stress in weld throat: $\sigma = \sigma_f \cdot \frac{A_f}{\sum A_w} \cdot 2 \cdot \sin\alpha$ A_w = area of weld throat	—	—	
332	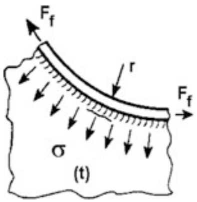	Unstiffened curved flange to web joint, to be assessed according to no. 411–414, depending on type of joint Stress in web plate: $\sigma = \frac{F_f}{r \cdot t}$ Stress in weld throat: $\sigma = \frac{F_f}{r \cdot \Sigma a}$ $\mathbf{F_f}$ axial force in flange **t** thickness of web plate **a** weld throat	—	—	The resulting force of F_f-left and F_f-right will bend the flange perpendicular to the plane of main loading. In order to minimize this additional stressing of the welds, it is recommended to minimize the width and to maximize the thickness of the flange Stress parallel to the weld is to be considered. For additional shear, principal stress in web is to be consired (see 321–323)
400	**Cruciform joints and/or T-joints**				
411	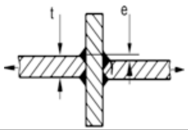	Cruciform joint or T-joint, K-butt welds, full penetration, weld toes ground, potential failure from weld toe Single sided T-joints	80 90	28 32	Advisable to ensure that intermediate plate was checked against susceptibility to lamellar tearing Misalignment < 15 % of primary plate thickness in cruciform joints

(continued)

Table 3.1 (continued)

No.	Structural Detail	Description (St. = steel; Al. = aluminium)	FAT St.	FAT Al.	Requirements and remarks
412	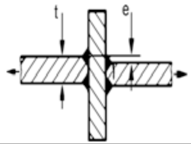	Cruciform joint or T-joint, K-butt welds, full penetration, potential failure from weld toe Single sided T-joints	71 80	25 28	Advisable to ensure that intermediate plate was checked against susceptibility to lamellar tearing Misalignment < 15 % of primary plate thickness in cruciform joints
413	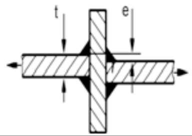	Cruciform joint or T-joint, fillet welds or partial penetration K-butt welds, potential failure from weld toe Single sided T-joints	63 71	22 25	Advisable to ensure that intermediate plate was checked against susceptibility to lamellar tearing Misalignment < 15 % of primary plate thickness in cruciform joints Also to be assessed as 414
414	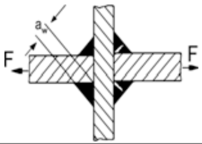	Cruciform joint or T-joint, fillet welds or partial penetration K-butt welds including toe ground joints, potential failure from weld root For a/t <=1/3	36 40	12 14	Analysis based on stress in weld throat $\sigma_w = F/\sum(a_w \cdot l)$ l = length of weld, a_w = load carrying weld throat. Also to be assessed as 413
415	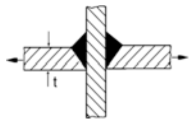	Cruciform joint or T-joint, single-sided arc or laser beam welded V-butt weld, full penetration, potential failure from weld toe. Full penetration checked by inspection of root If root is not inspected, then root crack	71 36	25 12	Advisable to ensure that intermediate plate was checked against susceptibility to lamellar tearing Misalignment < 15 % of primary plate thickness in cruciform joints
416	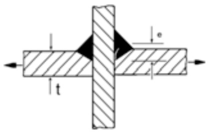	Cruciform joint or T-joint, single-sided arc welded fillet or partial penetration Y-butt weld, no lamellar tearing, misalignment of plates $e < 0.15 \cdot t$, stress at weld root. Penetration verified **Attention:** Bending by excenricity **e** must be consired!	71	25	Analysis based on axial and bending stress in weld throat. Excentricity **e** to be considered in analysis. Stress at weld root: $\boldsymbol{\Delta\sigma_{w,\,root} = \Delta\sigma_{w,\,nom} \cdot (1 + 6e/a)}$ **e** = excentricity between midpoints plate and weld throat **a** (inclusive penetration), rotated into vertical leg plane using root tip as pivot An analysis by effective notch stress procedure is recommended

(continued)

Table 3.1 (continued)

No.	Structural Detail	Description (St. = steel; Al. = aluminium)	FAT St.	FAT Al.	Requirements and remarks
421	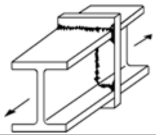	Splice of rolled section with intermediate plate, fillet welds, potential failure from weld root	36	12	Analysis based on stress in weld throat
422	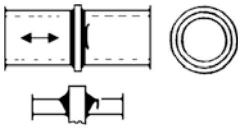	Splice of circular hollow section with intermediate plate, singlesided butt weld, potential failure from toe wall thickness > 8 mm wall thickness < 8 mm	 56 50	 22 20	NDT of welds in order to ensure full root penetration
423	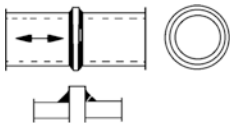	Splice of circular hollow section with intermediate plate, fillet weld, potential failure from root. Analysis based on stress in weld throat wall thickness >8 mm wall thickness <8 mm	 45 40	 16 14	
424	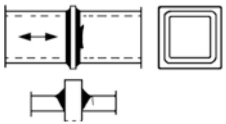	Splice of rectangular hollow section, single-sided butt weld, potential fairure from toe wall thickness > 8 mm wall thickness < 8 mm	 50 45	 20 18	NDT of welds in order to ensure full root penetration
425	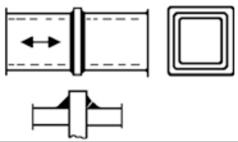	Splice of rectangular hollow section with intermediate plate, fillet welds, potential failure from root wall thickness > 8 mm wall thickness < 8 mm	 40 36	 16 14	

(continued)

Table 3.1 (continued)

No.	Structural Detail	Description (St. = steel; Al. = aluminium)	FAT St.	FAT Al.	Requirements and remarks
431	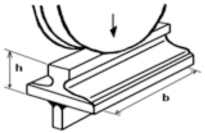	Weld connecting web and flange, loaded by a concentrated force in web plane perpendicular to weld. Force distributed on width **b = 2 · h + 50 mm** Assessment according to no. 411–414. A local bending due to eccentric load should be considered	–	–	
500	**Non-load-carrying attachments**				
511	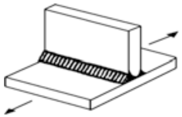	Transverse non-load-carrying attachment, not thicker than main plate K-butt weld, toe ground Two sided fillets, toe ground Fillet weld(s), as welded thicker than main plate	 100 100 80 71	 36 36 28 25	Grinding marks normal to weld toe An angular misalignment corresponding to $\mathbf{k_m = 1.2}$ is already covered
512	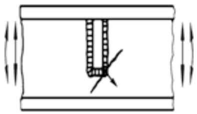	Transverse stiffener welded on girder web or flange, not thicker than main plate K-butt weld, toe ground Two-sided fillets, toe ground fillet weld(s): as welded thicker than main plate	 100 100 80 71	 36 36 28 25	
513	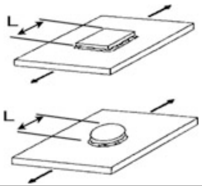	Non-loadcarrying rectangular or circular flat studs, pads or plates L ≤ 50 mm L > 50 and ≤ 150 mm L > 150 and ≤ 300 mm L > 300 mm	 80 71 63 50	 28 25 20 18	
514			71	25	

(continued)

Table 3.1 (continued)

No.	Structural Detail	Description (St. = steel; Al. = aluminium)	FAT St.	FAT Al.	Requirements and remarks
	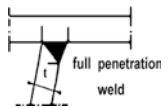	Trapezoidal stiffener to deck plate, full penetration butt weld, calculated on basis of stiffener thickness, out of plane bending			
515	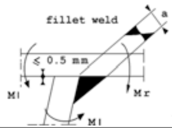	Trapezoidal stiffener to deck plate, fillet or partial penetration weld, out of plane bending	71	25	Calculation based on maximum out-of-plane bending stress range in weld throat or stiffener
521	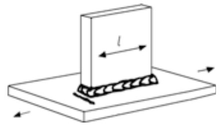	Longitudinal fillet welded gusset of length **l**. Fillet weld around end l < 50 mm l < 150 mm l < 300 mm l > 300 mm	 80 71 63 50	 28 25 20 18	For gusset on edge: see detail 525 Particularly suitable for assessment on the basis of structural hot spot stress approach
522	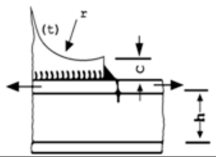	Longitudinal fillet welded gusset with radius transition, fillet weld around end and toe ground, c < 2 t, max 25 mm r > 150 mm	90	32	**t** = thickness of attachment Particularly suitable for assessment on the basis of structural hot spot stress approach
523	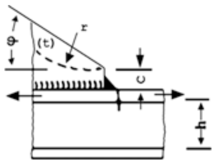	Longitudinal fillet welded gusset with smooth transition (sniped end or radius) welded on beam flange or plate, fillet weld around end. c < 2 t, max 25 mm r > 0.5 h r < 0.5 h or $\phi > 20°$	 71 63	 25 20	**t** = thickness of attachment If attachement thickness < 1/2 of base plat thickness, then one step higher allowed (not for welded on profiles!) Particularly suitable for assessment on the basis of structural hot spot stress approach
524		Longitudinal flat side gusset welded on plate edge or beam flange edge, with smooth transition			**t** = thickness of attachment For $t_2 < 0.7\ t_1$, FAT rises 12 %

(continued)

Table 3.1 (continued)

No.	Structural Detail	Description (St. = steel; Al. = aluminium)	FAT St.	FAT Al.	Requirements and remarks
	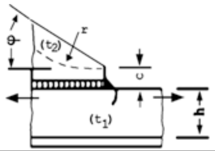	(sniped end or radius), fillet weld around end. $c < 2t_2$, max. 25 mm r > 0.5 h r < 0.5 h or ϕ > 20°	 50 45	 18 16	Particularly suitable for assessment on the basis of structural hot spot stress approach
525	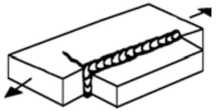	In-plane or out-of-plane longitudinal gusset welded to plate or beam flange edge, gusset length **l**: l < 150 mm l < 300 mm l > 300 mm	 50 45 40	 18 16 14	For $t_2 < 0.7\ t_1$, FAT rises 12 % t_1 is main plate thkcness t_2 is gusset thickness
526	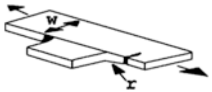	Longitudinal flat side gusset welded on edge of plate or beam flange, radius transition ground r > 150 or r/w > 1/3 1/6 < r/w < 1/3 r/w < 1/6	 90 71 50	 36 28 22	Smooth transition radius formed by grinding the weld area in transition in order to remove the weld toe completely. Grinding parallel to stress
531	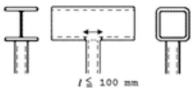	Circular or rectangular hollow section, fillet welded to another section. Section width parallel to stress direction < 100 mm, else like longitudinal attachment	71	28	Non load-carrying welds. Width parallel to stress direction < 100 mm
600	**Lap joints**				
611	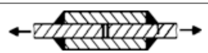	Transverse loaded lap joint with fillet welds Fatigue of parent metal Fatigue of weld throat	 63 45	 22 16	Stresses to be calculated in the main plate using a plate width equal to the weld length Buckling avoided by loading or design!

(continued)

Table 3.1 (continued)

No.	Structural Detail	Description (St. = steel; Al. = aluminium)	FAT St.	FAT Al.	Requirements and remarks
612	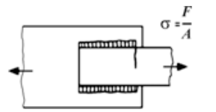	Longitudinally loaded lap joint with side fillet welds Fatigue of parent metal Fatigue of weld (calc. on max. weld length of 40 times the throat of the weld)	 50 50	 18 18	Buckling avoided by loading or design For verification of parent metal, the higher stresses of the two members must be taken
613	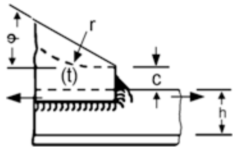	Lap joint gusset, fillet welded, non-load-carrying, with smooth transition (sniped end with $\phi < 20°$ or radius), welded to loaded element $c < 2\Delta t$, but $c <= 25$ mm to flat bar to bulb section to angle section	 63 56 50	 22 20 18	**t** = thickness of gusset plate
614	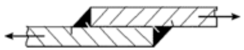	Transverse loaded overlap joint with fillet welds Stress in plate at weld toe (toe crack) Stress in weld throat (root crack)	 63 36	 22 12	Stresses to be calculated using a plate width equalling the weld length For stress in plate, eccentricity to be considered, as given in chapters 3.8.2 and 6.3 Both failure modes have to be assessed separately
700	**Reinforcements**				
711	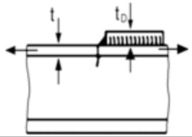	End of long doubling plate on I-beam, welded ends (based on stress range in flange at weld toe) $t_D \leq 0.8$ t $0.8\ t < t_D \leq 1.5$ t $t_D > 1.5$ t	 56 50 45	 20 18 16	End zones of single or multiple welded cover plates, with or without transverse welds If the cover plate is wider than the flange, a transverse weld is needed. No undercut at transverse welds
712	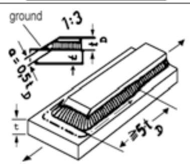	End of long doubling plate on beam, reinforced welded ends ground (based on stress range in flange at weld toe) $t_D \leq 0.8$ t $0.8\ t < t_D \leq 1.5$ t $t_D > 1.5$ t	 71 63 56	 28 25 22	Grinding parallel to stress direction

(continued)

Table 3.1 (continued)

No.	Structural Detail	Description (St. = steel; Al. = aluminium)	FAT St.	FAT Al.	Requirements and remarks
721	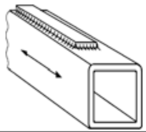	End of reinforcement plate on rectangular hollow section wall thickness: t < 25 mm	50	20	No undercut at transverse weld!
731	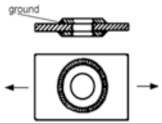	Fillet welded reinforcements Toe ground As welded	 80 71	 32 25	Grinding in direction of stress! Analysis based on modified nominal stress, however, structural hot spot stress approach recommended
800	**Flanges, branches and nozzles**				
811	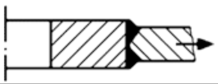	Stiff block flange, full penetration weld	71	25	
812	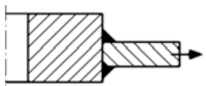	Stiff block flange, partial penetration or fillet weld toe crack in plate root crack in weld throat	 63 36	 22 12	
821	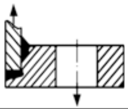	Flat flange with > 80 % full penetration butt welds, modified nominal stress in pipe, toe crack	71	25	Assessment by structural hot spot is recommended
822	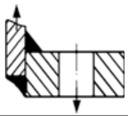	Fillet welded pipe to flat flange joint. Potential fatigue failure from weld toe in pipe	63	22	Analysis based on modified nominal stress. However, structural hot spot stress recommended
831	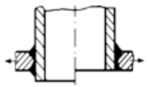	Tubular branch or pipe penetrating a plate, K-butt welds	80	28	If diameter > 50 mm, stress concentration of cutout has to be considered

(continued)

Table 3.1 (continued)

No.	Structural Detail	Description (St. = steel; Al. = aluminium)	FAT St.	FAT Al.	Requirements and remarks
					Analysis based on modified nominal stress. However, structural hot spot stress recommended
832	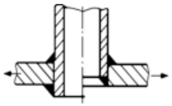	Tubular branch or pipe penetrating a plate, fillet welds. Toe cracks	71	25	If diameter > 50 mm, stress concentration of cutout has to be considered
		Root cracks (analysis based on stress in weld throat)	36	12	Analysis based on modified nominal stress. However, structural hot spot stress recommended
841	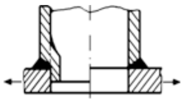	Nozzle welded on plate, root pass removed by drilling	71	25	If diameter >50 mm, stress concentration of cutout has to be considered Analysis based on modified nominal stress. However, structural hot spot stress recommended
842	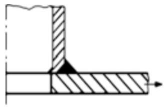	Nozzle welded on pipe, root pass as welded	63	22	If diameter > 50 mm, stress concentration of cutout has to be considered Analysis based on modified nominal stress. However, structural hot spot stress recommended
900	**Tubular joints**				
911	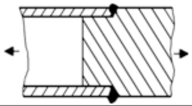	But welded circular tube or pipe to solid bar joint. Potential fatigue failure from weld toe or root in tube or pipe	63	22	Analysis based on stress in tube or pipe Full penetration of weld to solid bas is required
912			63	22	Analysis based on stress in tube or pipe Full penetration of weld to solid bas is required

(continued)

Table 3.1 (continued)

No.	Structural Detail	Description (St. = steel; Al. = aluminium)	FAT St.	FAT Al.	Requirements and remarks
	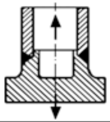	Butt welded joint between circular tube or pipe and flange with integral backing. Potential fatigue failure fromweld root			
913	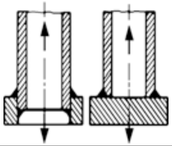	Fillet or partial penetration welded joint between circular tube or pipe and flange. Potential fatigue failure from weld root	50	18	Impairment of inspection of root cracks by NDT may be compensated by adequate safety considerations (see Sect. 3.5) or by downgrading by two FAT classes
921		Circular hollow section with welded on disc, potential fatigue failure from toe in hollow section K-butt weld, toe ground Fillet weld, toe ground Fillet welds, as welded	 90 90 71	 32 32 25	
931	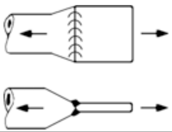	Tube-plate joint, tubes flattened, butt weld (X-groove) Tube diameter < 200 mm and plate thickness < 20 mm	63	18	
932	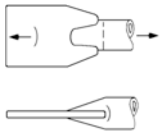	Tube-plate joint, tube slitted and welded to plate tube diameter < 200 mm and plate thickness < 20 mm tube diameter > 200 mm or plate thickness > 20 mm	 63 45	 18 14	

Table 3.2 Fatigue resistance values for structural details on the basis of shear stress

No	Description (St. = steel; Al. = aluminium)	FAT St.	FAT Al.
1	Parent metal or full penetration butt weld; **m = 5 down to 1E8** cycles	100	36
2	Fillet weld or partial penetration butt weld; **m = 5 down to 1E8** cycles	80	28

3.3 Fatigue Resistance Assessed on the Basis of Structural Hot Spot Stress

3.3.1 Fatigue Resistance Using Reference S-N Curve

The S-N curves for assessing the fatigue resistance of a detail on the basis of structural hot spot stress (Sect. 2.2.3) are given in the Table 3.3 for steel and aluminium, where the definition of the FAT class is given in Sect. 3.2. The resistance values refer to the as-welded condition unless stated otherwise. The effects of high tensile residual stress are included. Only small effects of misalignment are included, see also Sect. 3.8.2. The weld shape should be similar to that shown below (Table 3.3).

The design value of the structural hot spot stress range $\mathbf{\Delta\sigma_{hs}}$ shall not exceed $\mathbf{2 \cdot f_y}$. The fatigue resistance of a welded joint is limited by the fatigue resistance of the base material.

For hollow section joints, special hot-spot stress design *S-N* curves have been recommended by the IIW [14]. These tubular joint design curves should not be applied to other types of structure.

3.3.2 Fatigue Resistance Using a Reference Detail

The tables of the fatigue resistance of structural details given in Sect. 3.2, or fatigue data from other sources which refer to a comparable detail, may be used. The reference detail should be chosen to be as similar as possible to the detail to be assessed.

Thus, the procedure will be:

(a) Select a reference detail with known fatigue resistance, which is as similar as possible to the detail being assessed with respect to geometric and loading parameters.
(b) Identify the type of stress in which the fatigue resistance is expressed. This is usually the nominal stress (as in the tables in Sect. 3.2).
(c) Establish a FEA model of the reference detail and the detail to be assessed with the same type of meshing and elements following the recommendations given in Sect. 2.2.3.

Table 3.3 Fatigue resistance against structural hot spot stress

No.	Structural detail	Description	Requirements	FAT Steel	FAT Alu.
1	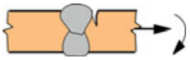	Butt joint	As welded, NDT	100	40
2	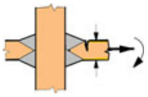	Cruciform or T-joint with full penetration K-butt welds	K-butt welds, no lamellar tearing	100	40
3	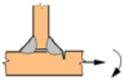	Non load-carrying fillet welds	Transverse non-load carrying attachment, not thicker than main plate, as welded	100	40
4	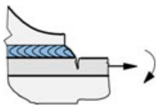	Bracket ends, ends of longitudinal stiffeners	Fillet welds welded around or not, as welded	100	40
5	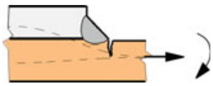	Cover plate ends and similar joints	As welded	100	40
6	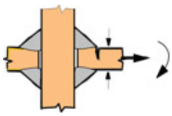	Cruciform joints with load-carrying fillet welds	Fillet welds, as welded	90	36
7	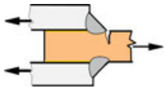	Lap joint with load carrying fillt welds	Fillet welds, as welded	90	36
8	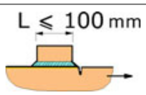	Type "b" joint with short attachment	Fillet or full penetration weld, as welded	100	40
9	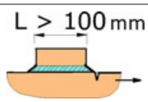	Type "b" joint with long attachment	Fillet or full penetration weld, as welded	90	36

Note 1 Table does not cover larger effects of misalignment than those specified in Sect. 3.8.2. They have to be considered explicitly in the determination of the hot spot stress range
Note 2 The nominally non- or partially load-carrying fillet welds shown under no. 3 and 5 in Table 3.3 may actually be load-carrying, in certain cases, e.g. for very large attachments or if the bending of the base plate is restrained. In these cases load-carrying fillet welds should be assumed with FAT classes given under no. 6 and 7 in Table 3.3. This may also apply to no. 4 without soft bracket end
Note 3 A further reduction by one FAT class is recommended for fillet welds having throat thicknesses of less than one third of the thickness of the base plate

(d) Load the reference detail and the detail to be assessed with the stress identified in b).
(e) Determine the structural hot spot stress $\boldsymbol{\sigma}_{\mathbf{hs,\ ref}}$ of the reference detail and the structural hot spot stress $\boldsymbol{\sigma}_{\mathbf{hs,\ assess}}$ of the detail to be assessed.
(f) The fatigue resistance for 2 million cycles of the detail to be assessed $\mathbf{FAT}_{\mathbf{assess}}$ is then calculated from fatigue class of the reference detail $\mathbf{FAT}_{\mathbf{ref}}$ by:

$$FAT_{assess} = \frac{\sigma_{hs,\ ref}}{\sigma_{hs,\ assess}} \cdot FAT_{ref} \tag{3.2}$$

3.4 Fatigue Resistance Assessed on the Basis of the Effective Notch Stress

3.4.1 Steel

The effective notch stress fatigue resistance against fatigue actions, as determined in Sect. 2.2.4 for steel [24], is given in Table 3.4. The definition of the FAT class is given in Sect. 3.2. The fatigue resistance value refers to the as-welded condition. The effect of high tensile residual stresses is included. The effect of possible misalignment is **not** included.

The fatigue resistance of a weld toe is additionally limited by the fatigue resistance of the parent material, which is determined by the use of the structural hot-spot stress and the FAT class of the non-welded parent material. This additional check shall be performed according to Sect. 2.2.3.

3.4.2 Aluminium

The same regulations apply as for steel (Table 3.5).

Table 3.4 Effective notch fatigue resistance for steel

No.	Quality of weld notch	Description	FAT
1	Effective notch radius equal to **1 mm** replacing weld toe and weld root notch	Notch as-welded, normal welding quality m = 3	225

Table 3.5 Effective notch fatigue resistance for aluminium

No.	Quality of weld notch	Description	FAT
1	Effective notch radius equal to **1 mm** replacing weld toe and weld root notch	Notch as-welded, normal welding quality m = 3	71

3.5 Fatigue Strength Modifications

3.5.1 *Stress Ratio*

3.5.1.1 Steel

For effective stress ratios, based on consideration of both applied and residual stresses, **R < 0.5** a fatigue enhancement factor **f(R)** may be considered by multiplying the fatigue class of classified details by **f(R)**. This factor depends on the level and direction of residual stresses. Here, all types of stress which are **not** considered in fatigue analysis and which are effective during service loading of the structure are regarded as residual stress. The ranking in categories I, II or III should be documented by the design office. If no reliable information on residual stress is available, an enhancement factor **f(R) = 1** is recommended. Other factors should only be used if reliable information or estimations of the residual stress level are available [47].

The following cases are to be distinguished (Fig. 3.7):

I. Unwelded base material and wrought products with negligible residual stresses (**<0.2 · f_y**), stress relieved welded components, in which the effects of constraints or secondary stresses have been considered in analysis. No constraints in assembly

$$\begin{aligned} f(R) &= 1.6 && \text{for } R < -1 \text{ or completely in compression} \\ f(R) &= -0.4 \cdot R + 1.2 && \text{for } -1 \le R \le 0.5 \\ f(R) &= 1 && \text{for } R > 0.5 \end{aligned} \tag{3.3}$$

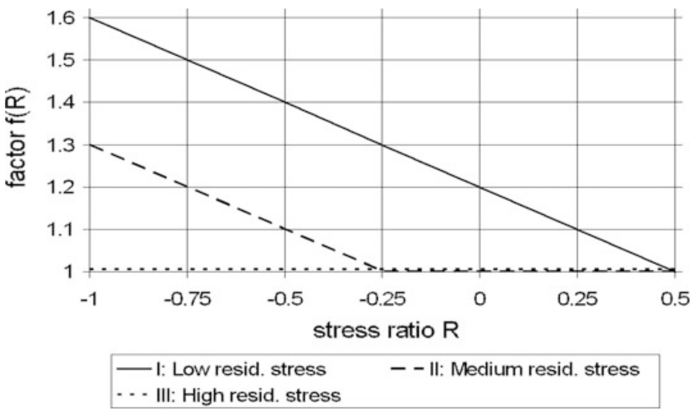

Fig. 3.7 Enhancement factor f(R)

II. Small-scale thin-walled simple structural elements containing short welds. Parts or components containing thermally cut edges. No constraints in assembly.

$$
\begin{aligned}
f(R) &= 1.3 && \text{for } R < -1 \text{ or completely in compression} \\
f(R) &= -0.4 \cdot R + 0.9 && \text{for } -1 \le R \le -0.25 \\
f(R) &= 1 && \text{for } R > -0.25
\end{aligned}
\tag{3.4}
$$

III. Complex two- or three-dimensional welded components, components with global residual stresses, thick-walled components. The normal case for welded components and structures.

$$f(R) = 1 \qquad \text{no enhancement} \tag{3.5}$$

It should be noted that stress relief in welded joints is unlikely to be fully effective, and additional residual stresses may be introduced by lack of fit during assembly of prefabricated welded components, by displacements of abutments or for other reasons. Consequently, it is recommended that values of **f(R) > 1** should only be adopted for welded components in very special circumstances. In several cases, stress relieving might reduce the fatigue properties as e.g. at TMCP steels by reduction of mechanical properties, or at weld roots in single sided butt welds or at fillet welds, by reduction of beneficial residual compressive stress.

Note: For unwelded or stress relieved steel structures, a simplified approach may be used, which consists in considering only 60 % of the stresses in compression.

3.5.1.2 Aluminium

The same regulations as for steel are recommended.

3.5.2 Wall Thickness

Fatigue resistance modifications are required at the nominal stress method (see Sect. 3.2) and the hot spot structural stress method of type "**a**" at surface extrapolation as described in Sect. 3.3. It is not required at the effective notch stress method and at the fracture mechanics method (see Sects. 3.4 and 3.6).

3.5.2.1 Steel

The influence of plate thickness on fatigue strength should be taken into account in cases where the site for potential fatigue cracking is the weld toe. The fatigue resistance values given here for steel refer to a wall thickness up to 25 mm. The lower fatigue strength for thicker members is taken into consideration by multiplying the FAT class of the structural detail by the thickness reduction factor **f(t)**:

$$f(t) = \left(\frac{t_{ref}}{t_{eff}}\right)^{n} \tag{3.6}$$

where the reference thickness $\mathbf{t_{ref} = 25\ mm}$. The thickness correction exponent **n** is dependent on the effective thickness $\mathbf{t_{eff}}$ and the joint category (see Table 3.6) [45]. In the same way a benign thinness effect might be considered, but this should be verified by component test.

The plate thickness correction factor is not required in the case of assessment based on effective notch stress procedure or fracture mechanics.

For the determination of $\mathbf{t_{eff}}$, the following cases have to be distinguished (Fig. 3.8):

$$\text{if} \quad \mathbf{L/t > 2} \quad \text{then} \quad \mathbf{t_{eff} = t} \tag{3.6a}$$

$$\text{if} \quad \mathbf{L/t \leq 2} \quad \text{then} \quad \mathbf{t_{eff} = 0.5 \cdot L} \text{ or } \mathbf{t_{eff} = t_{ref}} \text{ whichever is larger}$$

Table 3.6 Thickness correction exponents

Joint category	Condition	**n**
Cruciform joints, transverse T-joints, plates with transverse attachments, ends of longitudinal stiffeners	as-welded	0.3
Cruciform joints, transverse T-joints, plates with transverse attachments, ends of longitudinal stiffeners	toe ground	0.2
Transverse butt welds	as-welded	0.2
Butt welds ground flush, base material, longitudinal welds or attachments to plate edges	any	0.1

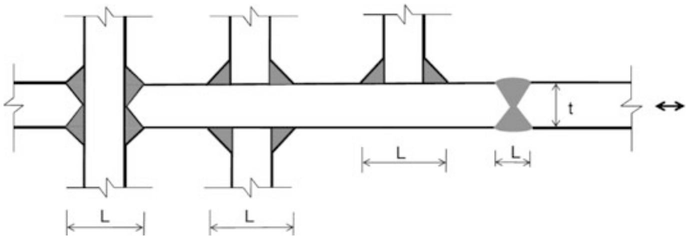

Fig. 3.8 Definition of toe distance L

3.5.2.2 Aluminium

The same rules as for steel are recommended.

3.5.3 Improvement Techniques

3.5.3.1 General

Post weld improvement techniques may increase the fatigue resistance, generally as a result of an improvement in the weld profile, the residual stress conditions or the environmental conditions of the welded joint. They may be used to increase the fatigue strength of new structures, notably if a weld detail is found to be critical, or as a part of repair or upgrading of an existing structure.

The main improvements techniques are:

(a) Methods for improvement of weld profile:

Machining or grinding of but weld flush to the surface
Machining or grinding of the weld transition at the toe
Remelting of the weld toe by TIG-, plasma or laser dressing

(b) Methods for improvement of residual stress conditions:

Peening (hammer-, needle-, shot-, brush-peening or ultrasonic treatment)
Overstressing (proof testing)
Stress relief

(c) Methods for improvement of environmental conditions:

Painting
Resin coating

The effects of all improvement techniques are sensitive to the method of application and the applied loading, being most effective in the low stress high cycle regime. They may also depend on the material, the structural detail, the applied stress ratio and the dimensions of the welded joint. Consequently, fatigue tests for the verification of the procedure in the endurance range of interest are recommended (Sects. 3.7 and 2.2.2).

Recommendations are given below for the following post-welding weld toe improvement methods: grinding, TIG dressing, hammer and needle peening.

3.5.3.2 Applicability of Improvement Methods

The recommendations apply to all arc welded steel or aluminium components subjected to fluctuating or cyclic stress and designed to a fatigue limit state criterion. They are limited to structural steels with specified yield strengths up to 900 MPa and to weldable structural aluminium alloys commonly used in welded structures, primarily of the AA 5000 and AA 6000 series but including weldable Al-Zn-Mg alloys.

The recommendations apply to welded joints in plates, sections built up of plates or similar rolled or extruded shapes, and hollow sections. Unless otherwise specified, the plate thickness range for steel is 6 to 150 mm, while that for aluminium is 4 to 50 mm.

The recommended levels of improvement in fatigue strength only apply when used in conjunction with the nominal stress or structural hot spot stress method. They do not apply to the effective notch stress or fracture mechanics method.

The application is limited to joints operating at temperatures below the creep range. In general, the recommendations do not apply for low cycle fatigue conditions, so the nominal stress range is limited to $\Delta\sigma \leq 1.5 \cdot f_y$. Additional restrictions may apply for specific improvement procedures. It is important to note that the fatigue resistance of an improved weld is limited by the fatigue resistance S-N curve of the base material.

The improvement procedures described below, apply solely to the weld toe and hence to a potential fatigue crack growth starting from this point. Thus, weld details of the type illustrated in Fig. 3.9 are suitable for treatment. However, the benefit of an improvement technique could be reduced as a result of intervention of fatigue cracking from the weld root. Thus, details of the kind shown in Fig. 3.10 are less suitable. In general, all potential alternative sites for fatigue crack initiation (e.g. weld root or imperfections) in treated welded joints should be assessed in order to establish the fatigue life of the weld detail under consideration.

The benefit factors due to the improvement techniques are presented as upgrades to the FAT class that applies to the as-welded joint. Alternative factors, including a possible change to a shallower, more favourable, slope of S-N curve for the improved weld, may be derived on the basis of special fatigue tests (see Sect. 4.5).

A profile improvement can sometimes assist in the application of a residual stress technique and vice versa (e.g. grinding before peening in the case of a poor

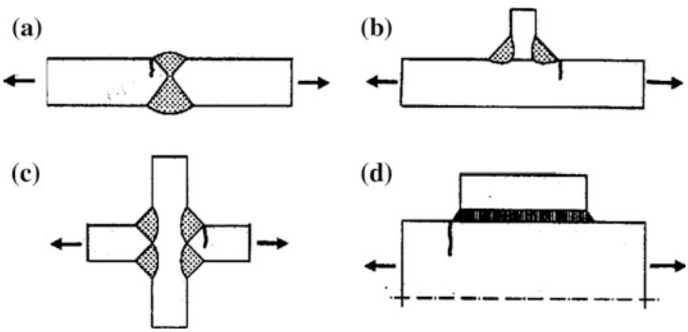

Fig. 3.9 Examples of joints suitable for improvement

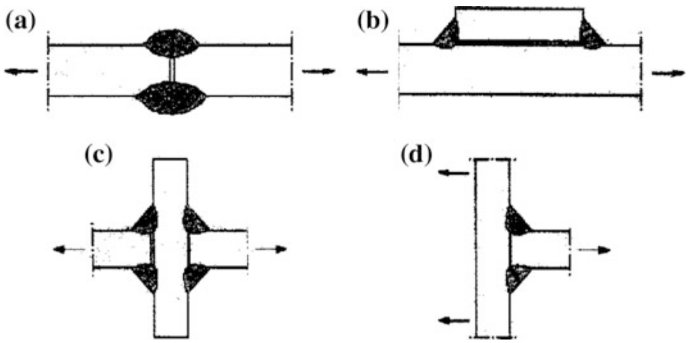

Fig. 3.10 Examples of joints, in which an improvement might be limited by a possible root crack

weld profile or shot peening a dirty surface before TIG dressing). However, a higher benefit factor than that applicable for the second technique alone can only be justified on the basis of special fatigue tests.

3.5.3.3 Grinding

Weld toe fatigue cracks initiate at undercut, cold laps or the sharp crack-like imperfections, just a few tenths of a millimetre deep, which are an inherent feature of most arc welds. The aim of grinding is firstly to remove these imperfections and secondly to create a smooth transition between weld and plate, thus, reducing the stress concentration. All embedded imperfections revealed by grinding must be repaired. For the details of the grinding procedure see Ref. [46].

The benefit of grinding is given as a factor on the stress range of the fatigue class of the non-improved joint, see Tables 3.7 and 3.8.

The thickness correction exponent according to Sect. 3.5.2 Table 3.6 is **n = 0.2**.

Table 3.7 FAT classes for use with nominal stress at joints improved by grinding

Area of application and maximum possible claim	Steel	Aluminium
Benefit at details classified in as-welded condition as FAT ≤ 90 for steel or FAT ≤ 32 for aluminium	1.3	1.3
Max possible FAT class after improvement	FAT 112	FAT 45

Table 3.8 FAT classes for use with structural hot-spot stress at joints improved by grinding

Material	Load-carrying fillet welds	Non-load-carrying fillet welds and butt welds
Mild steel, $f_y < 355$ MPa	112	125
Higher strength steel, $f_y \geq 355$ MPa	112	125
Aluminium alloys	45	50

3.5.3.4 TIG Dressing

By TIG (tungsten inert gas) dressing, the weld toe is remolten in order to remove the weld toe imperfections and to produce a smooth transition from the weld to plate surface, thus reducing the stress concentration. The recommendations (Tables 3.9 and 3.10) apply to partial or full penetration arc welded in steels with a specified yield strength up to 900 MPa and to wall thicknesses ≥ 10 mm operating in a non-corrosive environment or under conditions of corrosion protection. The details of the procedure are described in Ref. [46].

The thickness correction exponent according to chapter 3.5.2 Table 3.6 is **n = 0.2**.

A possible interaction between heat treatment and TIG dressing at aluminium alloys should be considered.

3.5.3.5 Hammer Peening

By hammer peening, the material is plastically deformed at the weld toe in order to introduce beneficial compressive residual stresses. The recommendations are restricted to steels with specified yield strengths up to 900 MPa and structural aluminium alloys, both operating in non-corrosive environments or under conditions of corrosion protection. The recommendations apply for plate thicknesses from 10 to 50 mm in steel and 5 to 25 mm in aluminium and to arc welded fillet welds with a minimum weld leg length of 0.1 × t, where t is the thickness of the stressed plate (Tables 3.11 and 3.12). The details of the procedure are described in Ref. [46].

Special requirements apply when establishing the benefit of hammer peening:

Table 3.9 FAT classes for use with nominal stress at joints improved by TIG dressing

Area of application and maximum possible claim	Steel	Aluminium
Benefit at details with FAT ≤ 90 at steel or FAT ≤ 32 at aluminium, as welded	1.3	1.3
Max possible FAT class after improvement	FAT 112	FAT 45

Table 3.10 FAT classes for use with structural hot-spot stress at joints improved by TIG dressing

Material	Load-carrying fillet welds	Non-load-carrying fillet welds and butt welds
Mild steel, $f_y < 355$ MPa	112	125
Higher strength steel, $f_y > 355$ MPa	112	125
Aluminium alloys	45	50

Table 3.11 FAT classes for use with nominal stress at joints improved by hammer peening

Area of application and maximum possible claim	Mild steel $f_y < 355$ MPa	Steel $f_y \geq 355$ MPa	Aluminium
Benefit at details with FAT ≤ 90 at steel or FAT ≤ 32 at aluminium, as welded	1.3	1.5	1.5
Max possible FAT after improvement	FAT 112	FAT 125	FAT 56

Table 3.12 FAT classes for use with structural hot-spot stress at joints improved by hammer peening

Material	Load-carrying fillet welds	Non-load-carrying fillet welds
Mild steel, $f_y < 355$ MPa	112	125
Higher strength steel, $f_y \geq 355$ MPa	125	140
Aluminium alloys	50	56

(a) Maximum amount of nominal compressive stress in load spectrum including proof loading <0.25 f_y (for aluminium, use f_y of heat affected zone)
(b) The S-N curve for the hammer peened weld is is used in conjunction with an effective stress range that depends on applied stress ratio R = minσ/maxσ as follows:

if $R < 0$	The S-N resistance curve is used with full stress range $\Delta\sigma$
if $0 < R \leq 0.4$	The S-N resistance curve is used with the maximum stress σ_{max}
if $R > 0.4$	Then there is no benefit

For wall thicknesses bigger than 25 mm, the thickness correction for as-welded joints still applies (see 3.5).

3.5.3.6 Needle Peening

By needle peening, the material is plastically deformed at the weld toe in order to introduce beneficial compressive residual stresses. The details of the procedure are described in [46].

Special requirements apply when establishing the benefit of needle peening:

(a) Maximum amount of nominal compressive stress in load spectrum including proof loading ≤ 0.25 f_y (for aluminium, use f_y of heat affected zone), see Tables 3.13 and 3.14.
(b) The S-N curve for needle peened weld is expressed in terms of an effective stress range that depends on applied R ratio as follows:

Table 3.13 FAT classes for use with nominal stress at joints improved by needle peening

Area of application and maximum possible claim	Mild steel fy < 355 MPa	Steel fy ≥ 355 MPa	Aluminium
Benefit at details with FAT ≤ 90 at steel or FAT ≤ 32 at aluminium, as welded	1.3	1.5	1.5
Max possible FAT after improvement	FAT 112	FAT 125	FAT 56

Table 3.14 FAT classes for structural hot-spot stress at joints improved by needle peening

Material	Load-carrying fillet welds	Non-load-carrying fillet welds
Mild steel, $f_y < 355$ MPa	112	125
Higher strength steel, $f_y > 355$ MPa	125	140
Aluminium alloys	50	56

if $R < 0$ The S-N resistance curve is used with full stress range $\Delta\sigma$

if $0 < R \leq 0.4$ The S-N resistance curve is used with the maximum stress σ_{max}

If $R > 0.4$ Then there is no benefit

For wall thicknesses bigger than 25 mm, the thickness correction for as-welded joints still applies (see 3.5).

3.5.4 *Effect of Elevated Temperatures*

One of the main material parameters governing the fatigue resistance is the modulus of elasticity **E** which decreases with increase in temperature. So the fatigue resistance at elevated temperatures (HT) may be calculated as

$$FAT_{HT} = FAT_{20^\circ C} \cdot \frac{E_{HT}}{E_{20^\circ C}} \tag{3.7}$$

3.5.4.1 Steel

For higher temperatures, the fatigue resistance data may be modified by the reduction factor given in Fig. 3.11. This fatigue reduction factor is a conservative approach and might be relaxed according to test evidence or applicable codes. Creep effects are not covered here.

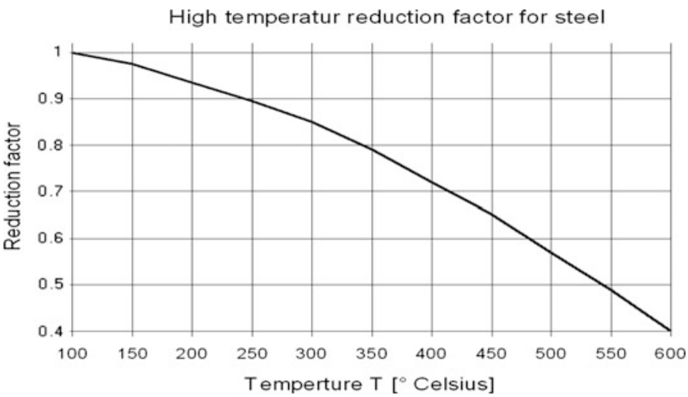

Fig. 3.11 Fatigue strength reduction factor for steel at elevated temperatures

3.5.4.2 Aluminium

The fatigue data given here refer to operation temperatures lower than 70 °C. This value is a conservative approach. It may be raised according to test evidence or an applicable code.

3.5.5 Effect of Corrosion

The fatigue resistance data given here refer to non-corrosive environments. Normal protection against atmospheric corrosion is assumed. A corrosive environment or unprotected exposure to atmospheric conditions may reduce the fatigue class. The position of the corresponding constant amplitude fatigue limit (CAFL or knee point) of the SN curve (traditionally the fatigue limit) may also be reduced considerably. The effect depends on the spectrum of fatigue actions **and** on the time of exposure.

For steel, except stainless steel, in marine environment not more than 70 % of the fatigue resistance values in terms of stress range shall be applied and no fatigue limit or knee point of the S-N curve shall be considered. In fracture mechanics crack propagation calculations the constant $\mathbf{C_0}$ in the Paris power law shall be multiplied by a factor of 3.0. A threshold $\mathbf{\Delta K}$ value shall not be considered.

No further specific recommendations are given for corrosion fatigue assessment. If no service experience is available, monitoring of the structure in service is recommended.

3.6 Fatigue Resistance Assessed on the Basis of Crack Propagation Analysis

The resistance of a material against cyclic crack propagation is characterized by the material parameters of the "Paris" power law of crack propagation

$$\frac{da}{dN} = C_0 \cdot \Delta K^m \quad if \quad \Delta K < K_{th} \quad else \quad \frac{da}{dN} = 0 \tag{3.8}$$

where the material parameters are

C_0 Constant of the power law
m Exponent of the power law
ΔK Range of cyclic stress intensity factor
ΔK_{th} Threshold value of stress intensity, under which no crack propagation is assumed
R **K_{min}/K_{max}**, taking all stresses including residual stresses into account (see Sect. 3.5.1)

In the absence of specified or measured material parameters, the values given below are recommended. They are characteristic values.

For elevated temperatures other than room temperature or for metallic materials other than steel, the crack propagation parameters vary with the modulus of elasticity **E** and may be determined accordingly.

$$C = C_{0,\,steel} \cdot \left(\frac{E_{steel}}{E}\right)^m \tag{3.9}$$

$$\Delta K_{th} = \Delta K_{th,\,steel} \cdot \left(\frac{E}{E_{steel}}\right) \tag{3.10}$$

3.6.1 Steel

See Table 3.15

Table 3.15 Parameters of the Paris power law and threshold data for steel

Units	Paris power law parameters	Threshold values ΔK_{th}			
		R ≥ 0.5	0 ≤ R≤0.5	R < 0	Surface crack depth < 1 mm
K [$N \cdot mm^{-3/2}$] da/dN [mm/cycle]	$C_0 = 5.21 \cdot 10^{-13}$ m = 3.0	63	170– 214 · R	170	≤63
K [$MPa\sqrt{m}$] da/dN [m/cycle]	$C_0 = 1.65 \cdot 10^{-11}$ m = 3.0	2.0	5.4– 6.8 · R	5.4	≤2.0

3.6.2 Aluminium

See Table 3.16

Table 3.16 Parameters of the Paris power law and threshold data for aluminium

Units	Paris power law parameters	Threshold values ΔK_{th}			
		$R \geq 0.5$	$0 \leq R \leq 0.5$	$R < 0$	Surface crack depth < 1 mm
K [$N \cdot mm^{-3/2}$] da/dN [mm/cycle]	$C_0 = 1.41 \cdot 10^{-11}$ $m = 3.0$	21	56.7– 72.3 · R	56.7	≤21
K [$MPa\sqrt{m}$] da/dN [m/cycle]	$C_0 = 4.46 \cdot 10^{-10}$ $m = 3.0$	0.7	1.8– 2.3 · R	1.8	≤0.7

3.6.3 Correlation of Fracture Mechanics to Other Verification Methods

The biggest portion of service life of welded joints is spent in crack propagation. So, estimates of fatigue life or the fatigue class FAT can be made by fracture mechanics calculations using appropriate parameters. The calculations should be verified at known structural details. A possible example of a set of parameters could be:

$a_i = 0.1$ mm	Initial crack size parameter (fitted value)
$a_i{:}c_i = 1$	Initial aspect ratio (at butt welds ground flush $a_i{:}c_i = 0.1$)
$a_f = \min(t/2;\ 12.5\ \text{mm})$	Final crack size parameter (t is wall thickness)
$r = t/25$	Toe radius for most cases
$\theta = 45°$	Weld angle for most cases, 30° for butt welds
$m = 3.0$	Exponent of the Paris-Erdogan power law

At cruciform joints or butt welds with partial penetration, the one half of the root gap shall be taken as the initial crack size parameter. Since the existence of a high stress concentration at the root gaps and a rapid growth in "c"-direction, a through-going crack or at least an initial aspect ratio $a_i{:}c_i = 0.1$ may be assumed and a two-dimensional analysis may be adequate.

At butt welds ground flush, the point of a possible crack initiation may be located in the weld metal. Thus the constant for weld metal shall be taken, and $a_i{:}c_i = 0.1$ is recommended. For material parameters see Table 3.17.

Misalignment shall be considered either in determination of the stress distribution by finite element analysis or by modification of the results of fracture mechanics calculations. See chapter 3.8.2.

Table 3.17 Constants Co of the power law for correlation (units in N and mm)

	Weld metal (root cracks)	Weld toes (base metal)
Steel	$5.21 \cdot 10^{-13}$	$3.00 \cdot 10^{-13}$
Aluminium	$1.41 \cdot 10^{-10}$	$0.81 \cdot 10^{-10}$

3.7 Fatigue Resistance Determination by Testing

3.7.1 General Considerations

Fatigue tests may be used to establish a fatigue resistance curve for a component or a structural detail, or the resistance of a material against (non critical) cyclic crack propagation.

It is recommended that test results are obtained at constant stress ratios **R**. The S-N data should be presented in a graph showing log(endurance in cycles) as the abscissa and log(range of fatigue actions) as the ordinate. For crack propagation data, the log(stress intensity factor range) should be the abscissa and the log(crack propagation rate) the ordinate.

Experimental fatigue data are scattered, with the extent of scatter tending to be greatest in the low stress/low crack propagation regime (e.g. see Fig. 3.12). For statistical evaluation, a Gaussian log-normal distribution should be assumed. If possible, at least 10 specimens should be tested.

Many methods of statistical evaluation are available. However, the most common approach for analysing fatigue data is to fit S-N or crack propagation curves by regression analysis, taking **log(N)** or **log(da/dN)** as the dependent variable.

Test results should be analysed to produce **characteristic** values (subscript **k**). These are values that represent 95 % survival probability (i.e. 5 % failure probability) calculated from the mean on the basis of a two-sided confidence of 75 %. More details on the use of the confidence level and formulae are given below.

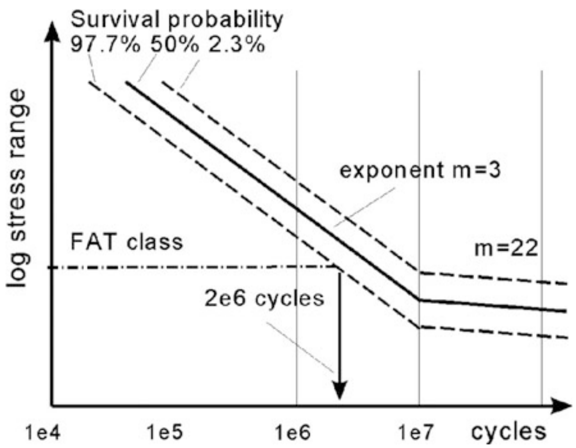

Fig. 3.12 Scatter band in S-N curve

At higher test cycles than about two or ten million cycles, the staircase method is recommended for testing and evaluation [70]. For a combined evaluation of failed and run-out specimens, maximum likelihood method is recommmended [71].

3.7.2 Evaluation of Test Data

Different methods for fatigue testing exist. For the derivation of S-N curves, testing at two stress range levels (**Δσ**) to give fatigue lives within the range of 5×10^4 to 10^6 cycles is preferred. For obtaining fracture mechanics crack propagation parameters, the range of stress intensity factor (**ΔK**) should be varied between the threshold and the critical level for fracture.

For the evaluation of test data originating from a test series, the characteristic values are calculated by the following procedure:

(a) Calculate $\log_{10}$ of all data: Stress range **Δσ** and number of cycles **N**, or stress intensity factor range **ΔK** and crack propagation rate **da/dN**.

(b) Calculate exponents **m** and constant **logC** (or $\mathbf{logC_0}$ respectively) of the formulae:

$$\text{for S - N curve} \quad \log N = \log C - m \cdot \log\Delta\sigma \tag{3.11}$$

$$\text{for crack propagation} \quad \log\left(\frac{da}{dN}\right) = \log C_0 + m \cdot \log\Delta K \tag{3.12}$$

by linear regression taking stress or stress intensity factor range as the independent variable, i.e. **logN = f(log Δσ)** or **log(da/dN) = f(log ΔK).**

The number and the spread of the data pairs should be critically assessed. If the number of pairs of test data **n < 10**, or if the data are not sufficiently evenly distributed to determine **m** accurately, a fixed value of **m** should be taken, as derived from other tests under comparable conditions, e.g. **m = 3** for steel and aluminium welded joints at stiff and thick-walled components. In all cases, the standard deviation of the exponent **m** shall be determined for a subsequent check if the pre-fixed exponent, e.g. **m = 3**, is still reasonable. For other conditions other slopes might be also adequate.

Values $\mathbf{x_i}$ equal to **logC** or $\mathbf{logC_0}$ are calculated from the $\mathbf{(N, \Delta\sigma)_i}$ or $\mathbf{(da/dN, \Delta K)_i}$ test results using the above equations.

(c) Calculate mean $\mathbf{x_m}$ and the standard deviation **Stdv** of **logC** (or $\mathbf{logC_0}$ respectively) using **m** obtained in b).

$$x_m = \frac{\sum x_i}{n} \qquad Stdv = \sqrt{\frac{\sum (x_m - x_i)^2}{n-1}} \tag{3.13}$$

d) Calculate the characteristic values $\mathbf{x_k}$ by the formulae
The values of **k** are given in Table 3.18.

Table 3.18 Values of **k** for the calculation of characteristic values

n	6	8	10	15	20	30	50	100
k	2.32	2.23	2.17	2.07	2.01	1.95	1.88	1.81

Note: In several areas of applications, the codes refer to mean minus two standard deviations, which corresponds to a survival probability of 97.7 %. Referring to survival probability of 95 % at two-sided confidence level of the mean of 75 % (one-sided 87.5 %, sometimes also 95 %) and considering the usual scatter of fatigue tests as shown in Fig. 3.12, the difference in terms of stress is less than 2 % and thus may be neglected. The method proposed above is equal to about mean minus two standard deviations at about 20 specimens.

$$\text{S} - \text{N data}: \quad x_k = x_m - k \cdot Stdv \tag{3.14}$$

$$\text{Crack propagation rate}: \quad x_k = x_m + k \cdot Stdv \tag{3.15}$$

$$\text{Values of } \mathbf{k}: \quad k = 1.645 \cdot \left(1 + \frac{1}{\sqrt{n}}\right) \tag{3.16}$$

For more details and information, see Appendix 6.4 and Refs. [68–72, 75].

In the case of S-N data, proper account should be taken of the fact that residual stresses are usually low in small-scale specimens. The results should be corrected to allow for the greater effects of residual stresses in real components and structures. Examples of ways to achieve this are by testing at high **R** values, e.g. **R = 0.5**, or by testing at **R = 0** and lowering the fatigue strength at 2 million cycles (FAT) by 20 %.

3.7.3 Evaluation of Data Collections

Usually data collections do not originate from a single statistical population. These heterogeneous populations of data require a special consideration in order to avoid problems arising from the wide scatter.

The evaluation procedure should consist of the following steps:

1. Calculate the constant **log C** of the S-N Wöhler curve for each data point (see Sect. 3.7.2.) using anticipated knowledge of the slope exponent from comparable test series, e.g. slope **m = 3.00** for steel or aluminium.
2. Plot all values **log C** in a Gaussian probability chart, showing the values of **log C** on the abscissa and the cumulative survival probability on the ordinate.
3. Check the probability plot for heterogeneity of the population. If it is heterogeneous, separate the portion of the population which is of interest (see illustration on Figs. 3.13 and 3.14).
4. Evaluate the interesting portion of population according to Sect. 3.7.2., which is the portion of the lowest values of **log C**.

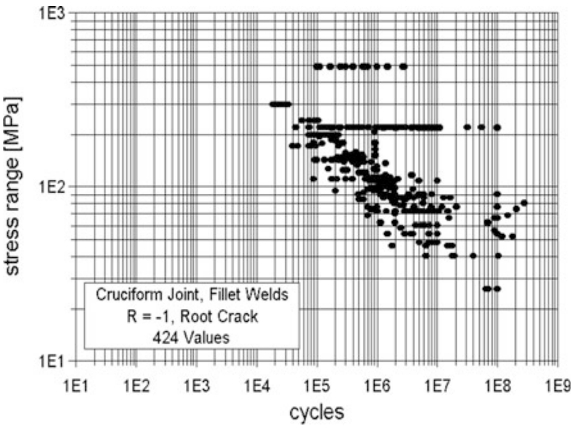

Fig. 3.13 Example of scatter in data collections

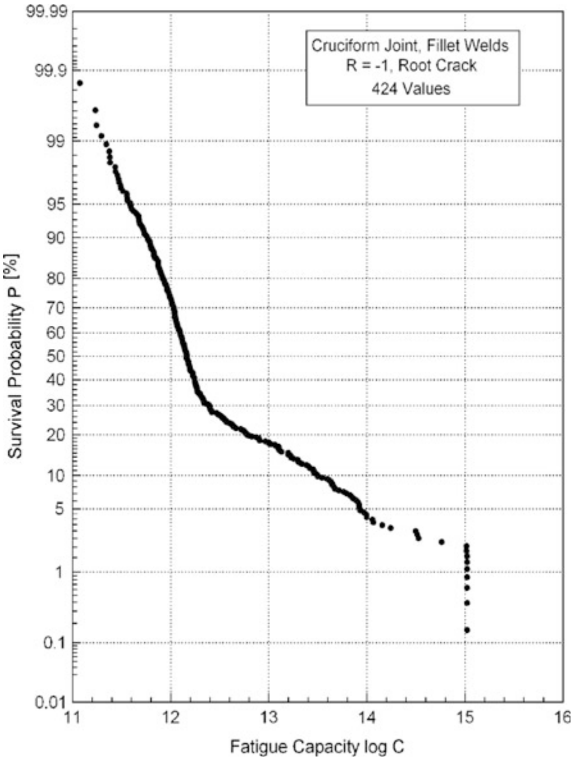

Fig. 3.14 Example of a heterogeneous population

3.8 Fatigue Resistance of Joints with Weld Imperfections

3.8.1 General

3.8.1.1 Types of Imperfections

The types of imperfections covered in this document are listed below. Other imperfections, not yet covered, may be assessed by assuming similar imperfections with comparable notch effect. Definitions are given in Ref. [48–50].

Imperfect shape
All types of misalignment including centre-line mismatch (linear misalignment) and angular misalignment (angular distortion, roofing, peaking).

Undercut

Volumetric discontinuities
Gas pores and cavities of any shape.
Solid inclusions, such as isolated slag, slag lines, flux, oxides and metallic inclusions.

Planar discontinuities
All types of cracks or crack-like imperfections, such as lack of fusion or lack of penetration (Note that for certain structural details intentional lack of penetration is already covered, e.g. partial penetration butt welds or fillet welded cruciform joints.
If a volumetric discontinuity is surface breaking or near the surface, or if there is any doubt about the type of an embedded discontinuity, it shall be assessed like a planar discontinuity.

3.8.1.2 Effects and Assessment of Imperfections

Three effects of geometrical imperfections can be distinguished, as summarized in Table 3.19.

Increase of general stress level
This is the effect of all types of misalignment due to secondary bending. The additional stress magnification factor can be calculated by appropriate formulae. The fatigue resistance of the structural detail under consideration is to be lowered by division by this factor.

Local notch effect
Here, interaction with other notches present in the welded joint is decisive. Two cases are to be distinguished:

Additive notch effect
If the location of the notch due to the weld imperfection coincides with a structural discontinuity associated with the geometry of the weld shape (e.g. weld

Table 3.19 Categorization and assessment procedure for weld imperfections

Effect of imperfection		Type of imperfection	Assessment
Increase of general stress level		Misalignment	Formulae for stress magnification factors
Local notch effect	additive	Weld shape imperfections, undercut	Tables given
	competitive	Porosity and inclusions not near the surface	Tables given
Crack-like imperfection		Cracks, lack of fusion and penetration, all types of imperfections other than given here	Fracture mechanics

toe), then the fatigue resistance of the welded joint is decreased by the additive notch effect. This may be the case at weld shape imperfections.

Competitive notch effect

If the location of the notch due to the weld imperfection does not coincide with a structural geometry associated with the shape geometry of the weld, the notches are in competition. Both notches are assessed separately. The notch giving the lowest fatigue resistance is governing.

Crack-like imperfections

Planar discontinuities, such as cracks or crack-like imperfections, which require only a short period for crack initiation, are assessed using fracture mechanics on the basis that their fatigue lives consist entirely of crack propagation.

After inspection and detection of a weld imperfection, the first step of the assessment procedure is to determine the type and the effect of the imperfection as given here.

If a weld imperfection cannot be clearly identified as a type or an effect of the types listed here, it is recommended that it is assumed to be crack-like [54, 57].

3.8.2 Misalignment

Misalignment in axially loaded joints leads to an increase of stress in the welded joint due to the occurrence of secondary shell bending stresses [55, 56]. The resulting stress is calculated by stress analysis or by using the formulae for the stress magnification factor $\mathbf{k_m}$ given in Table (3.20) and in Appendix 6.3.

Secondary shell bending stresses do not occur in continuous welds longitudinally loaded or in joints loaded in pure bending, and so misalignment will not reduce the fatigue resistance. However, misalignment in components, e.g. beams, subject to overall bending may cause secondary bending stresses in parts of the component, where the through-thickness stress gradient is small, e.g. in the flange of a beam, where the stress is effectively axial. Such cases should be assessed.

Table 3.20 Consideration of stress magnification factors due to misalignment

Type of k_m analysis	Nominal stress approach	Structural hot spot, effective notch and fracture mechanics appoach	
Type of welded joint	k_m already covered in FAT class	k_m already covered in SN curves	Default value of effective k_m to be considered in stress
Butt joint made in shop in flat position	1.15	1.05	1.10*
Other butt joints	1.30	1.05	1.25*
Cruciform joints	1.45	1.05	1.40*
Fillet welds on one plate surface	1.25	1.05	1.20**
Fillet welds on both plate surfaces	1.25	1.05	1.10***

* but not more than $(1 + 2.5 \cdot e_{max}/t)$, where e_{max} = permissible misalignment and t = wall thickness of loaded plate
** but not more than $(1 + 0.2 \cdot t_{ref}/t)$, where t_{ref} = reference wall thickness of fatigue resistance curves
*** but not more than $(1 + 0.1 \cdot t_{ref}/t)$, where t_{ref} = reference wall thickness of fatigue resistance curves

Some allowance for misalignment is already included in the tables of classified structural details (3.2). In particular, the data for transverse butt welds are directly applicable for misalignment which results in an increase of stress up to 30 %, while for the cruciform joints the increase can be up to 45 %. In the case of the structural hot spot stress and the effective notch stress assessment methods, a small but inevitable amount of misalignment corresponding to a stress magnification factor of $\mathbf{k_m = 1.05}$ is already included in the fatigue resistance S-N curves (Table 3.20).

Additional requirements apply for the joints listed in Table 3.20. The effect of a larger misalignment has to be additionally considered in the local stress (structural hot spot stress or effective notch stress). The misalignment effect may be present even in the vicinity of supporting structures. A corresponding stress increase must be taken into account also in crack propagation analyses. In all those cases where the stress magnification factor is calculated directly, use is made of an effective stress magnification factor $\mathbf{k_{m,eff}}$.

$$k_{m,\,eff} = \frac{k_{m,\,calculated}}{k_{m,\,\mathrm{alreadycovered}}} \tag{3.17}$$

For joints containing both linear and angular misalignment, both stress magnification factors should be applied using the formula:

$$k_m = 1 + (k_{m,\,axial} - 1) + (k_{m,\,angular} - 1) \tag{3.18}$$

Since misalignment reduces the fatigue resistance, either the calculated applied stress is multiplied by $\mathbf{k_{m,eff}}$ or the allowable stress range obtained from the relevant resistance S-N curve is divided by $\mathbf{k_{m,eff}}$.

Table 3.20 tabulates the factors $\mathbf{k_m}$ which are already covered in the different verification methods. Actual or specified fabrication tolerances may be assessed by the formulae given in Sect. 6.3.

3.8.3 Undercut

The basis for the assessment of undercut is the ratio **u/t**, i.e. depth of undercut to plate thickness. Though undercut is an additive notch, it is already considered to a limited extent in the tables of fatigue resistance of classified structural details (Sect. 3.2).

Undercut does not reduce the fatigue resistance of welds which are only loaded in the longitudinal direction, i.e. parallel to the undercut.

3.8.3.1 Steel

See Table 3.21

Table 3.21 Acceptance levels for weld toe undercut in steel

Fatigue class	Allowable undercut u/t	
	Butt welds	Fillet welds
100	0.025	Not applicable
90	0.05	Not applicable
80	0.075	0.05
71	0.10	0.075
63	0.10	0.10
56 and lower	0.10	0.10

Notes
[a]Undercut deeper than 1 mm shall be assessed as a crack-like imperfection
[b]The table is only applicable for plate thicknesses from 10–20 mm

3.8.3.2 Aluminium

See Table 3.22

Table 3.22 Acceptance levels for weld toe undercut in aluminium

Fatigue class	Allowable undercut u/t	
	Butt welds	Fillet welds
50	0.025	Not applicable
45	0.05	Not applicable
40	0.075	0.05
36	0.10	0.075
32	0.10	0.10
28 and lower	0.10	0.10

Notes
[a]Undercut deeper than 1 mm shall be assessed as a crack-like imperfection
[b]The table is only applicable for plate thicknesses from 10–20 mm

3.8.4 Porosity and Inclusions

Embedded volumetric discontinuities, such as porosity and inclusions, are considered as competitive weld imperfections which can provide alternative sites for fatigue crack initiation to those covered by the fatigue resistance tables of classified structural details (Sect. 3.2).

Before assessing the imperfections with respect to fatigue, it should be verified that the conditions apply for competitive notches, i.e. that the anticipated sites of crack initiation in the fatigue resistance tables do not coincide with the porosity or inclusions to be assessed and that there is no interaction between them.

It is important to ensure that there is no interaction between multiple weld imperfections, be they of the same or different type. Combined porosity or inclusions shall be treated as a single large imperfection. The defect interaction criteria given in Sect. 3.8.5 for the assessment of cracks also apply for adjacent inclusions. Worm holes shall be assessed as slag inclusions.

If there is any doubt about the coalescence of porosity or inclusions in the wall thickness direction or about the distance from the surface, the imperfections shall be assessed as cracks. It must be verified by NDT that the porosity or inclusions are embedded and volumetric. If there is any doubt, they are to be treated as cracks.

The parameter for assessing porosity is the maximum percentage of projected area of porosity in the radiograph; for inclusions, it is the maximum length. Directly adjacent inclusions are regarded as a single one.

3.8.4.1 Steel

See Table 3.23

Table 3.23 Acceptance levels for porosity and inclusions in welds in steel

Fatigue class	Max. length of an inclusion in mm		Limits of porosity in % of area * **
	As-welded	Stress relieved +	
100	1.5	7.5	3
90	2.5	19	3
80	4	58	3
71	10	no limit	5
63	35	no limit	5
56 and lower	no limit	no limit	5

* Area of radiograph used is length of weld affected by porosity multiplied by width of weld
** Maximum pore diameter or width of an inclusion less than 1/4 plate thickness or 6 mm
+ Stress relieved by post weld heat treatment

Table 3.24 Acceptance levels for porosity and inclusions in welds in aluminium

Fatigue class	Max. length of an inclusion in mm **	Limits of porosity in % of area * **
	As-welded	
40 and higher	1.5	0 +)
36	2.5	3
32	4	3
28	10	5
25	35	5
15 and lower	no limit	5

* Area of radiograph used is length of weld affected by porosity multiplied by width of weld
** Maximum pore diameter or width of an inclusion less than ¼ plate thickness or 6 mm
+ Single pores up to 1.5 mm allowed

3.8.4.2 Aluminium

Tungsten inclusions have no effect on fatigue behaviour and therefore do not need to be assessed (Table 3.24).

3.8.5 Crack-like Imperfections

3.8.5.1 General Procedure

Planar discontinuities, cracks or crack-like defects are identified by non-destructive testing and inspection. NDT indications are idealized as elliptical cracks (Fig. 3.15) for which the stress intensity factor is calculated according to Sect. 2.2.5.

For **embedded cracks**, the shape is idealized by a circumscribing ellipse, which is measured by its two half-axes **a** and **c**. The crack parameter **a** (crack depth) is the half-axis of the ellipse in the direction of the crack growth to be assessed. The remaining perpendicular half-axis is the half length of the crack **c**. The wall thickness parameter **t** is the distance from the centre of the ellipse to the nearest surface (Fig. 3.16). If **a/t > 0.75**, the defect should be re-categorized as a surface crack.

Surface cracks are described in terms of a circumscribing half-ellipse. The thickness parameter is wall thickness **t**. If **a/t > 0.75**, the defect is regarded as being fully penetrating and is to be re-categorized as a centre crack or an edge crack, whichever is applicable.

For details of dimensions of cracks and re-categorization see Appendix 6.2.

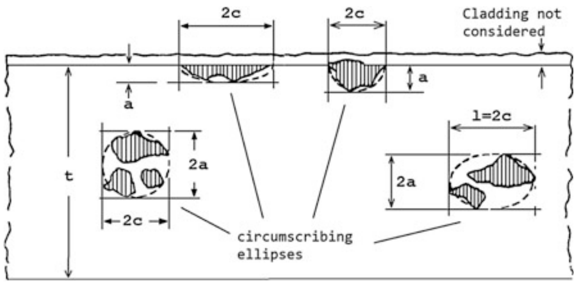

Fig. 3.15 Transformation of NDT indications into elliptic or semi-elliptic cracks

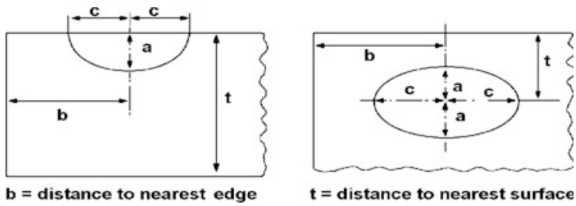

Fig. 3.16 Crack dimensions for assessment

3.8.5.2 Simplified Procedure

The simplified procedure makes use of the fatigue resistance at $2 \cdot 10^6$ cycles (analogous to FAT classes for the classified structural details) for ranges of crack types, sizes and shapes, of which the data are presented in Tables 3.25. These were obtained by integration of the crack propagation law for steel, given in Sect. 3.6.1, between the limits of an initial crack size $\mathbf{a_i}$ and a final crack size of 50 % of the wall thickness. In addition, use was made of the correction functions and the local weld geometry correction given in Sect. 6.2.4. (See Tables 6.1 and 6.3, also 6.14).

In assessing a defect by the simplified procedure, the stress range $\boldsymbol{\Delta\sigma_i}$ corresponding to the initial crack size parameter $\mathbf{a_i}$ and the stress range $\boldsymbol{\Delta\sigma_c}$ for the critical crack size parameter $\mathbf{a_c}$ are identified. The stress range $\boldsymbol{\Delta\sigma}$ or the FAT class corresponding to a crack propagation from $\mathbf{a_i}$ to $\mathbf{a_c}$ in $2 \cdot 10^6$ cycles is then calculated by:

$$\Delta\sigma = \sqrt[3]{\Delta\sigma_i^3 - \Delta\sigma_c^3} \tag{3.19}$$

The tables may be used for aluminium by dividing the resistance stress ranges at $2 \cdot 10^6$ cycles (FAT classes) for steel by **3**.

The tables have been calculated using Ref. [40, 42] with a constant of Co = 5.21e-13 [N; mm] and an exponent of m = 3.0 in order to cover the worst case under normal operation and environmental conditions. Corrosion is not considered. A possible misalignment has to be considered explicitly according to Table 3.20.

Note: The different definition of **t** for surface and embedded cracks in Table 3.25 shall be considered according to Fig. 3.16.

Table 3.25 Stress ranges at $2 \cdot 10^6$ cycles (FAT classes in N/mm^2) of welds containing cracks for the simplified procedure (following 3 pages)

Long crack at fillet weld toe, L/t = 2.5, a:c = 0.1														
a\ t	5	6	8	10	12	14	16	20	25	30	35	40	50	100
25	0	0	0	0	0	0	0	0	0	0	0	8	12	22
20	0	0	0	0	0	0	0	0	0	7	11	13	17	26
16	0	0	0	0	0	0	0	0	9	12	15	17	21	29
12	0	0	0	0	0	0	0	10	15	18	21	23	26	34
10	0	0	0	0	0	0	10	15	19	22	24	26	29	36
8	0	0	0	0	8	12	15	19	23	26	28	30	33	39
6	0	0	0	12	16	19	22	26	29	32	34	35	38	42
5	0	0	11	16	20	23	26	29	33	35	37	38	40	44
4	0	10	17	22	26	28	31	34	37	39	41	42	44	46
3	13	18	24	29	32	35	37	40	42	44	45	46	47	48
2	25	29	35	38	41	43	45	47	49	50	51	51	52	51
1	44	47	51	53	55	56	57	58	58	58	58	58	57	55
0.5	61	62	64	65	65	66	66	65	65	64	64	63	62	58
0.2	77	77	77	76	75	74	74	72	71	69	68	67	66	60
0.1	85	85	83	81	80	79	78	76	74	72	71	69	67	61
Short crack at fillet weld toe, L/t = 2.5, a:c = 0.5														
a\ t	5	6	8	10	12	14	16	20	25	30	35	40	50	100
25	0	0	0	0	0	0	0	0	0	0	0	17	22	31
20	0	0	0	0	0	0	0	0	0	15	20	23	27	35
16	0	0	0	0	0	0	0	0	17	22	26	28	31	37
12	0	0	0	0	0	0	0	20	26	29	32	34	36	41
10	0	0	0	0	0	0	19	26	30	33	35	37	39	43
8	0	0	0	0	17	23	27	31	35	37	39	40	42	45
6	0	0	0	23	28	32	34	38	41	42	44	45	46	48
5	0	0	22	29	33	36	38	41	44	45	46	47	48	50
4	0	19	30	35	39	41	43	45	47	48	49	50	51	52
3	26	32	38	42	45	47	48	50	51	52	53	53	54	54
2	40	44	48	51	53	54	55	56	57	57	58	58	58	56
1	58	60	62	63	64	65	65	65	66	65	64	64	63	58
0.5	72	73	74	74	74	74	73	72	71	69	68	67	65	60
0.2	86	86	84	82	81	80	78	76	74	72	71	70	68	61
0.1	93	91	88	86	84	82	81	78	76	74	72	71	69	62

(continued)

Table 3.25 (continued)

Long crack at butt weld toe, L/t = 1, a:c = 0.1														
a\ t	5	6	8	10	12	14	16	20	25	30	35	40	50	100
25		0	0	0	0	0	0	0	0	0	0	8	12	22
20	0	0	0	0	0	0	0	0	0	7	11	13	17	26
16	0	0	0	0	0	0	0	0	9	12	15	17	21	29
12	0	0	0	0	0	0	0	10	15	18	21	23	26	33
10	0	0	0	0	0	0	10	15	19	22	24	26	29	36
8	0	0	0	0	8	12	15	19	23	26	28	30	33	39
6	0	0	0	12	16	19	22	26	29	32	34	35	38	42
5	0	0	11	16	20	23	26	29	33	35	37	38	40	44
4	0	10	17	22	26	28	31	34	37	39	41	42	44	46
3	13	18	24	29	32	35	37	40	42	44	45	46	47	49
2	25	29	35	38	41	43	45	47	49	50	51	51	52	52
1	44	47	51	53	55	56	57	58	59	59	59	59	58	56
0.5	61	63	65	66	66	66	66	66	65	65	64	64	63	58
0.2	77	78	77	77	76	75	75	73	72	70	69	68	67	61
0.1	86	85	84	83	81	80	79	77	75	73	72	71	68	62
Short crack at butt weld toe, L/t = 1, a:c = 0.5														
a\ t	5	6	8	10	12	14	16	20	25	30	35	40	50	100
25	0	0	0	0	0	0	0	0	0	0	0	16	22	31
20	0	0	0	0	0	0	0	0	0	15	20	23	27	34
16	0	0	0	0	0	0	0	0	17	22	25	28	31	37
12	0	0	0	0	0	0	0	20	26	29	31	33	36	41
10	0	0	0	0	0	0	19	26	30	33	35	37	39	43
8	0	0	0	0	17	23	26	31	35	37	39	40	42	45
6	0	0	0	23	28	31	34	37	40	42	43	44	46	48
5	0	0	22	29	33	36	38	41	43	45	46	47	48	50
4	0	19	30	35	38	41	43	45	47	48	49	50	51	52
3	26	31	38	42	45	47	48	50	51	52	53	53	54	54
2	40	43	48	51	53	54	55	56	57	57	58	58	58	56
1	58	60	62	63	64	65	65	65	66	66	65	64	63	59
0.5	72	73	74	74	75	74	74	73	71	70	69	68	66	61
0.2	86	86	85	83	82	81	79	77	75	74	72	71	69	62
0.1	94	92	89	87	85	84	82	80	77	75	74	72	70	63

(continued)

Table 3.25 (continued)

Long surface crack at weld ground flush to surface, a:c = 0.1														
a\ t	5	6	8	10	12	14	16	20	25	30	35	40	50	100
25.0	0	0	0	0	0	0	0	0	0	0	0	8	13	23
20.0	0	0	0	0	0	0	0	0	0	7	11	13	17	26
16.0	0	0	0	0	0	0	0	0	9	12	15	17	21	30
12.0	0	0	0	0	0	0	0	10	15	18	21	23	26	34
10.0	0	0	0	0	0	0	10	15	19	22	24	26	29	37
8.0	0	0	0	0	8	12	15	20	23	26	29	30	33	41
6.0	0	0	0	12	16	19	22	26	29	32	34	36	38	45
5.0	0	0	11	16	20	23	26	30	33	36	38	39	42	48
4.0	0	10	17	22	26	28	31	34	38	40	42	43	46	52
3.0	13	18	25	29	32	35	37	40	43	45	47	49	51	56
2.0	25	29	35	39	42	44	46	49	51	53	55	56	58	63
1.0	44	47	52	55	58	59	61	63	66	67	68	69	71	74
0.5	63	65	69	72	74	75	77	78	80	81	82	83	84	86
0.2	87	89	91	93	95	96	96	98	99	99	100	101	101	103
0.1	105	106	109	110	111	112	112	113	114	115	115	115	116	117
Short surface crack at weld ground flush to surface, a:c = 0.5														
a\ t	5	6	8	10	12	14	16	20	25	30	35	40	50	100
25	0	0	0	0	0	0	0	0	0	0	0	17	23	95
20	0	0	0	0	0	0	0	0	0	15	20	24	29	39
16	0	0	0	0	0	0	0	0	17	23	27	30	34	43
12	0	0	0	0	0	0	0	21	27	31	35	37	40	48
10	0	0	0	0	0	0	20	27	32	36	39	41	44	51
8	0	0	0	0	17	24	28	34	38	42	44	46	49	55
6	0	0	0	23	29	34	37	41	45	48	50	52	54	59
5	0	0	22	30	35	39	42	46	50	52	54	55	58	62
4	0	20	31	38	42	45	48	52	55	57	58	60	62	66
3	27	33	41	47	50	53	55	58	61	63	64	65	67	71
2	43	48	54	58	61	63	65	67	69	71	72	73	74	77
1	66	69	73	76	78	79	80	82	84	85	86	86	87	90
0.5	86	88	91	93	94	95	96	98	99	99	100	100	101	103
0.2	111	112	114	115	116	117	117	118	119	119	120	120	121	122
0.1	129	130	132	133	133	134	134	135	136	136	136	137	137	138

(continued)

Table 3.25 (continued)

Long embedded crack, t = distance to nearest surface, a:c = 0.1															
a\ t	3	4	5	6	8	10	12	14	16	20	25	30	35	40	50
25	0	0	0	0	0	0	0	0	0	0	0	0	0	4	7
20	0	0	0	0	0	0	0	0	0	0	0	3	5	7	11
16	0	0	0	0	0	0	0	0	0	0	4	6	9	11	14
12	0	0	0	0	0	0	0	0	0	5	8	11	14	16	19
10	0	0	0	0	0	0	0	0	4	8	12	15	17	19	23
8	0	0	0	0	0	0	3	6	8	12	16	19	22	24	27
6	0	0	0	0	0	5	9	12	14	18	22	25	27	29	32
5	0	0	0	0	5	9	12	15	18	22	26	28	31	32	35
4	0	0	0	4	9	14	17	20	23	26	30	33	35	37	39
3	0	0	6	10	16	20	24	27	29	32	36	38	40	42	45
2	4	10	15	19	25	30	33	36	38	41	44	46	48	50	52
1	22	29	33	37	42	46	49	51	53	56	59	61	63	64	67
0.5	42	47	52	55	60	63	66	68	69	72	75	77	79	80	82
0.2	68	73	77	80	84	87	90	92	93	96	98	100	101	103	105
0.1	90	94	98	101	105	107	110	111	113	115	117	119	120	122	124
Short embedded crack, t = distance to nearest surface, a:c = 0.5															
a\ t	3	4	5	6	8	10	12	14	16	20	25	30	35	40	50
25	0	0	0	0	0	0	0	0	0	0	0	0	0	5	10
20	0	0	0	0	0	0	0	0	0	0	0	4	7	10	14
16	0	0	0	0	0	0	0	0	0	0	5	9	12	15	19
12	0	0	0	0	0	0	0	0	0	7	12	15	19	21	26
10	0	0	0	0	0	0	0	0	6	11	16	20	23	26	30
8	0	0	0	0	0	0	5	9	12	17	21	25	28	31	35
6	0	0	0	0	0	8	12	16	19	24	29	32	35	38	42
5	0	0	0	0	7	12	17	21	24	29	33	37	40	42	46
4	0	0	0	6	13	19	23	27	30	35	39	43	45	48	51
3	0	0	9	14	21	27	31	35	38	42	47	50	53	55	58
2	6	15	21	26	33	39	43	46	49	54	58	61	63	65	68
1	29	37	44	48	55	60	64	67	69	73	76	79	81	82	85
0.5	54	62	67	72	78	82	85	87	89	92	95	97	99	100	102
0.2	89	95	99	103	107	111	113	115	116	119	121	123	124	125	127
0.1	115	121	124	127	131	133	135	137	138	140	142	144	145	146	148

Chapter 4
Fatigue Assessment

4.1 General Principles

In a fatigue assessment, the fatigue actions and the fatigue resistance are related by means of an appropriate assessment procedure. It must be ensured that all three elements (actions, resistance and assessment procedure) correspond. Three procedures may be distinguished:

(a) Procedures based on S-N curves, such as

- Nominal stress approach
- Structural hot spot stress approach
- Effective notch stress approach

(b) Procedures based on fatigue crack propagation considerations
(c) Direct experimental approach by the fatigue testing of components or entire structures.

4.2 Combination of Normal and Shear Stress

If normal and shear stresses occur simultaneously, their combined effect shall be considered. Three cases may be distinguished:

(a) If the nominal shear stress range is less than 15 % of the normal stress range or if the fatigue damage sum due to the shear stress range is lower than 10 % of that due to the normal stress range, the effect of shear stress may be neglected.
(b) If the normal and shear stresses vary simultaneously in-phase, or if the plane of maximum principal stress does not change significantly (<20°) during cycling, the maximum principal stress range should be used, otherwise the procedure as given in Sect. 4.3.1 is recommended.

A.F. Hobbacher, *Recommendations for Fatigue Design of Welded Joints and Components*, IIW Collection, DOI 10.1007/978-3-319-23757-2_4

(c) If the normal and shear stresses vary independently out-of-phase (i.e. non-proportional loading), the procedure given in Sect. 4.3.1 is recommended.

Fracture mechanics fatigue crack propagation calculations should be based on the maximum principal stress range.

4.3 Fatigue Assessment Using S-N Curves

The fatigue assessment is carried out using

The design stress or spectrum of fatigue actions in terms of stress ranges $\boldsymbol{\Delta\sigma_{i,S,d}}$, in which the stresses of the characteristic spectrum $\boldsymbol{\Delta\sigma_{i,S,k}}$ have been multiplied by the partial safety factor $\boldsymbol{\gamma_F}$ for fatigue actions.

and

The design resistance Wöhler S-N curve based on design resistance stresses $\boldsymbol{\Delta\sigma_{R,d}}$, in which the characteristic resistance stress range $\boldsymbol{\Delta\sigma_{R,k}}$ has been divided by the partial safety factor $\boldsymbol{\gamma_M}$ for fatigue resistance.

The characteristic resistance S-N curve is derived from an appropriate fatigue class FAT, which may be modified further according to stress ratio, wall thickness, post weld improvement etc., and to the requirements of the damage calculation procedure.

Two types of verification are distinguished, a verification in terms of cycles and a verification in terms of stress.

Verification in Terms of Cycles:

An action as a constant amplitude design stress $\Delta\sigma_{S,d}$ a stress spectrum or a constant amplitude equivalent stress representing the spectrum $\Delta\sigma_{eq,S,d}$ is given on the load side and a modified design fatigue resistance class FAT_d ($\Delta\sigma_{R,d}$) is given on the resistance side. From both, the number of life cycles may be calculated as:

$$N_{calc} = 2 \cdot 10^6 \cdot \left(\frac{\Delta\sigma_{R,d}}{\Delta\sigma_{S,d}}\right)^m \quad or\ resp. \quad N_{calc} = 2 \cdot 10^6 \cdot \left(\frac{\Delta\sigma_{R,d}}{\Delta\sigma_{eq,S,d}}\right)^m \qquad (4.1)$$

$$N_{calc} \geq N_{spec}$$

where

$\Delta\sigma_{S,d}$	design value of the constant amplitude stress range
$\Delta\sigma_{eq,S,d}$	design value of an equivalent stress range, derived from a given load spectrum, which characterizes the loading, and a cumulative damage calculation
$\Delta\sigma_{R,d}$	design value of the fatigue resistance at $2\cdot10^6$ cycles derived from the modified fatigue class FAT of the structural detail

N_{calc} calculated number of life cycles
N_{spec} specified number of life cycles

Verification in Terms of Stress:

For **constant amplitude loading**, the design resistance stress range $\boldsymbol{\Delta\sigma_{R,d}}$ shall be determined at the required or specified number of stress cycles N_{spec}. The following fatigue criterion should then be checked:

$$\Delta\sigma_{S,\,d} = \Delta\sigma_{S,\,k} \cdot \gamma_F \leq \Delta\sigma_{R,\,d} = \frac{\Delta\sigma_{R,\,k}}{\gamma_M} \tag{4.2}$$

For a **constant amplitude loading** which produces both normal and shear stresses, the maximum principal stress $\Delta\sigma_{comp,S,d}$ shall be used, provided its direction is within ±60° from the normal to the weld.

$$\Delta\sigma_{comp,S,d} = \frac{1}{2} \cdot \left(\Delta\sigma_{S,d} + \sqrt{\Delta\sigma_{S,d} + 4 \cdot \Delta\tau_{S,d}}\right) \tag{4.3}$$

Otherwise the following criterion must be met, where the comparison value CV depends on the material and type of loading. See Table 4.1.

$$\left(\frac{\Delta\sigma_{S,d}}{\Delta\sigma_{R,d}}\right)^2 + \left(\frac{\Delta\tau_{S,d}}{\Delta\tau_{R,d}}\right)^2 \leq CV \tag{4.4}$$

For **variable amplitude loading**, a cumulative damage calculation procedure should be applied. Usually a modified "Palmgren-Miner" rule, as described in

Table 4.1 Assessment procedures for combined normal and shear stress using S-N curves

Type of load	Normal and shear stress	Assessment procedure	Specified damage sum D or comparison value CV
Constant amplitude	Proportional	Assessment on the basis of the maximum principal stress or $\left(\frac{\Delta\sigma_{S,d}}{\Delta\sigma_{R,d}}\right)^2 + \left(\frac{\Delta\tau_{S,d}}{\Delta\tau_{R,d}}\right)^2 \leq CV$	CV = 1.0
	Un-correlated	$\left(\frac{\Delta\sigma_{S,d}}{\Delta\sigma_{R,d}}\right)^2 + \left(\frac{\Delta\tau_{S,d}}{\Delta\tau_{R,d}}\right)^2 \leq CV$	CV = 0.5[a]
Variable amplitude	Proportional	Assessment on the basis of maximum principal stress and Miner's rule, or $\left(\frac{\Delta\sigma_{eq,S,d}}{\Delta\sigma_{R,d}}\right)^2 + \left(\frac{\Delta\tau_{eq,S,d}}{\Delta\tau_{R,d}}\right)^2 \leq CV$	D = 0.5 CV = 1.0
	Un-correlated	$\left(\frac{\Delta\sigma_{eq,S,d}}{\Delta\sigma_{R,d}}\right)^2 + \left(\frac{\Delta\tau_{eq,S,d}}{\Delta\tau_{R,d}}\right)^2 \leq CV$	D = 0.5 CV = 0.5[a]

Note: For fluctuating mean stress, a Palmgren-Miner sum of D = 0.2 is recommended
[a]For semi-ductile aluminium alloys CV = 1.0 is recommended [65]

Sect. 4.3.1, is appropriate. Relevant data associated with their resistance S-N curves (Figs. 4.1 and 4.2), that are used to apply the rule, are given in Table 4.2. For load spectra which are sensitive to the position of the constant amplitude fatigue limit (CAFL) or knee point on the S-N curve, or in which the spectrum changes during the service life, an additional assessment using fracture mechanics, as described in Sect. 4.4 is recommended referring also to Sects. 2.2.5 and 3.6.

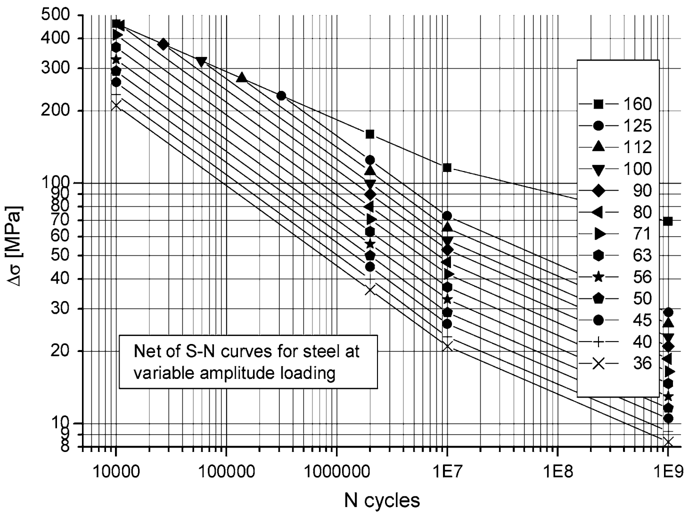

Fig. 4.1 Modified resistance S-N curves of steel for Palmgren-Miner summation

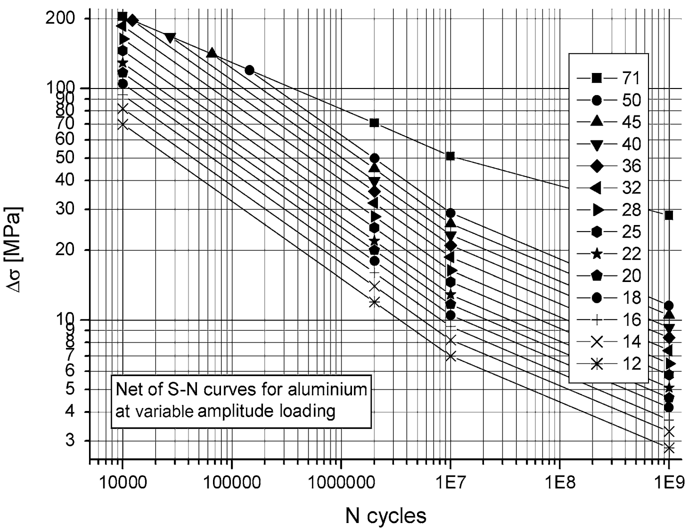

Fig. 4.2 Modified resistance S-N curves of aluminium for Palmgren-Miner summation

Table 4.2 FAT data, stress range at knee point of S-N curve, constants of S-N curves and constants for constant and variable amplitude loading (Palmgren-Miner summation)

Stress ranges		Values of constant C: $\mathbf{N = C/\Delta\sigma^m}$ or $\mathbf{N = C/\Delta\tau^m}$		
FAT class [MPa]	Stress range at knee point	For stress ranges above knee point	For stress ranges below knee point	
Welded structural details under normal stress:				
Δσ at **2E + 6 cycles**	**Δσ** at **1E + 7 cycles**	**m = 3**	Constant amplitude **m = 22**	Variable amplitude **m = 5**
125	73.1	3.906E + 12	1.014E + 48	2.091E + 16
112	65.5	2.810E + 12	9.064E + 46	1.207E + 16
100	58.5	2.000E + 12	7.541E + 45	6.581E + 15
90	52.7	1.458E + 12	7.583E + 44	4.046E + 15
80	46.8	1.024E + 12	5.564E + 43	2.245E + 15
71	41.5	7.158E + 11	3.954E + 42	1.236E + 15
63	36.9	5.001E + 11	2.983E + 41	6.800E + 14
56	32.8	3.512E + 11	2.235E + 40	3.773E + 14
50	29.3	2.500E + 11	1.867E + 39	2.141E + 14
45	26.3	1.823E + 11	1.734E + 38	1.264E + 14
40	23.4	1.280E + 11	1.327E + 37	7.016E + 13
36	21.1	9.331E + 10	1.362E + 36	4.143E + 13
32	18.7	6.554E + 10	9.561E + 34	2.299E + 13
28	16.4	4.390E + 10	5.328E + 33	1.179E + 13
25	14.6	3.125E + 10	4.128E + 32	6.691E + 12
22	12.9	2.130E + 10	2.710E + 31	3.531E + 12
20	11.7	1.600E + 10	3.163E + 30	2.192E + 12
18	10.5	1.166E + 10	2.925E + 29	1.295E + 12
16	9.4	8.192E + 09	2.563E + 28	7.184E + 11
14	8.2	5.488E + 09	1.270E + 27	3.685E + 11
12	7.0	3.456E + 09	3.910E + 25	1.705E + 11
Base material:				
Δσ at **2E + 6 cycles**	**Δσ** at **1E + 7 cycles**	**m = 5**	Constant amplitude **m = 22**	Variable amplitude **m = 9**
160	116.0	2.097E + 17	2.619E + 52	3.803E + 25
80	58.0	6.554E + 15	6.243E + 45	7.428E + 22
71	51.5	3.623E + 15	4.568E + 44	2.548E + 22
Shear stress:				
Δτ at **2E + 6 cycles**	**Δτ** at **1E + 8 cycles**	**m = 5**	Constant amplitude **m = 22**	Variable amplitude **m = 9**
100	45.7	1.993E + 16	3.297E + 44	8.695E + 22
80	36.6	3.277E + 15	2.492E + 42	1.179E + 22
36	16.5	1.209E + 14	6.090E + 34	9.065E + 18
28	12.8	3.442E + 13	2.284E + 32	9.223E + 17

In any field of application, for which there are no test data, or no service experience exists and the shape of the stress spectrum is not close to constant amplitude, the assessment procedure as detailed in Sect. 4.3.1 is recommended.

Verification in Terms of Stress at 2 million Cycles:

In the 2 million cycles equivalent procedure, the equally damaging stress range at 2 million cycles $\boldsymbol{\Delta\sigma_{S,d,E2}}$ is determined. It can be directly compared with the factored and modified fatigue class FAT.

$$\Delta\sigma_{\mathrm{S,d,E2}} \leq \mathrm{FAT}/\gamma_{\mathrm{M}} \tag{4.5}$$

The 2 million cycles equivalent $\boldsymbol{\Delta\sigma_{S,d,E2}}$ for constant amplitude fatigue action is calculated by

$$\Delta\sigma_{S,d,E2} = \sqrt[m]{\frac{n \cdot \Delta\sigma_{S,d}^{m}}{2 \cdot 10^{6}}} \tag{4.6}$$

where **n** is the specified number of cycles corresponding to the total anticipated load history of the joint and $\boldsymbol{\Delta\sigma_{S,d}}$ is the design stress range of the fatigue action.

4.3.1 Linear Damage Calculation by the "Palmgren-Miner" Rule

First, the required number of cycles shall be specified, and the design resistance S-N curve shall be determined. If a fatigue limit is considered and if the maximum design stress range $\boldsymbol{\Delta\sigma_{max,S,d}}$ in the load spectrum is lower than the assumed design fatigue limit $\boldsymbol{\Delta\sigma_{L,R,d}}$ for the design fatigue resistance S-N curve, the life of the welded joint can be assumed to be infinite and no further damage calculation is necessary. However, this procedure is not recommended for aluminium or for steels required to survive for very high numbers of load cycles (see Sect. 3.2) and [64, 66].

For other situations, the assumed constant amplitude fatigue limit (CAFL) or knee point is ignored. The S-N curve must be extrapolated beyond it at the shallower slope of $\mathbf{m_2 = 2 \cdot m_1\text{-}1}$ [62] as shown in Figs. 4.1 and 4.2. For fatigue verification, it has to be shown that [60, 61]:

$$D_{calc} = \sum \frac{n_i}{N_i} \leq D_{spec} = 0.5\ldots1.0 \tag{4.7}$$

where

D_{calc}	calculated damage sum (note restrictions in Sects. 4.2 and 4.3)
D_{spec}	specified damage sum as in Table 4.1
i	index for block number in load spectrum of required design life
n_i	number of cycles of design load stress range $\boldsymbol{\Delta\sigma_{i,S,d}}$ in load spectrum block **i**
Ni	number of cycles to failure at design stress range $\boldsymbol{\Delta\sigma_{i,S,d}}$ obtained from the modified design fatigue resistance S-N curve.

The order of sequence of the blocks has no effect on the results of this calculation provided, that the size of the spectrum allows for about 20 repetitions in summing.

It is accepted that the stresses below the assumed constant amplitude fatigue limit or below the knee point must be included in cumulative damage calculation relating to welded joints. There are currently different opinions about how this should be achieved. The method presented here (Figs. 4.1 and 4.2) appears in a number of codes. However, recent research indicates that assuming a specified damage sum or fatigue damage ratio of $D_{spec} = 1$ can be non-conservative. Here, this question is partially solved by recommending a value of $D_{spec} = 0.5$.

Note: It has been observed that for spectra with high mean stress fluctuations, the damage sum may be even lower, possibly down to $D_{spec} = 0.2$.

In some cases an equivalent constant amplitude stress range $\boldsymbol{\Delta\sigma_{eq,S,d}}$ may need to be determined and compared directly with the constant amplitude resistance S-N curve. $\boldsymbol{\Delta\sigma_{eq,S,d}}$ is calculated for $\boldsymbol{\Delta\sigma_{eq,S,d} > \Delta\sigma_{L,d}}$ as follows:

$$\Delta\sigma_{eq,S,d} = \sqrt[m_1]{\frac{1}{D_{spec}} \cdot \frac{\sum\left(n_i \cdot \Delta\sigma_{i,S,d}^{m_1}\right) + \Delta\sigma_{L,d}^{(m_1-m_2)} \cdot \sum\left(n_j \cdot \Delta\sigma_{j,S,d}^{m_2}\right)}{\sum n_i + \sum n_j}} \tag{4.8a}$$

For $\boldsymbol{\Delta\sigma_{eq,S,d} < \Delta\sigma_{L,d}}$:

$$\Delta\sigma_{eq,S,d} = \sqrt[m_2]{\frac{1}{D_{spec}} \cdot \frac{\Delta\sigma_{L,d}^{(m_2-m_1)} \cdot \sum\left(n_i \cdot \Delta\sigma_{i,S,d}^{m_1}\right) + \sum\left(n_j \cdot \Delta\sigma_{j,S,d}^{m_2}\right)}{\sum n_i + \sum n_j}} \tag{4.8b}$$

where:

D_{spec}	specified Miner sum ($D_{spec} = 1$, if values from Table 4.1 are used)
$\Delta\sigma_{eq,S,d}$	design value of equivalent stress range (loads) for $(\Sigma n_i + \Sigma n_j)$ cycles
m_1	slope above the knee point of the SN curve
m_2	slope below the knee point of the SN curve
$\Delta\sigma_{i,S,d}$	design values of stress ranges (loads) above the knee point
$\Delta\sigma_{j,S,d}$	design values of stress ranges (loads) below the knee point
$\Delta\sigma_{L,d}$	design value of stress range (resistance) at the knee point of S-N curve (Table 4.2)
n_i	number of cycles at applied stress range $\Delta\sigma_i$
n_j	number of cycles at applied stress range $\Delta\sigma_j$

For calculation of equivalent shear stress $\Delta\tau_{eq,S,d}$, the same formula applies expressed in terms of the corresponding shear stress ranges. If $\Delta\sigma_{eq,S,d}$ or $\Delta\tau_{eq,S,d}$ are below the knee points $\Delta\sigma_{L,d}$ or $\Delta\tau_{L,d}$, the corresponding constant amplitude fatigue lives are obtained from the S-N curves for the relevant FAT class extrapolated beyond the knee point at slope $\mathbf{m_2}$ (Eq. 4.8).

If all stress ranges are all above or all below the knee point, the formula simplifies to:

$$\textit{all above}: \quad \Delta\sigma_{eq,S,d} = \sqrt[m_1]{\frac{1}{D_{spec}} \cdot \frac{\sum (n_j \cdot \Delta\sigma_{i,S,d}^{m_i})}{\sum n_i}} \tag{4.9a}$$

$$\textit{all below}: \quad \Delta\sigma_{eq,S,d} = \sqrt[m_2]{\frac{1}{D_{spec}} \cdot \frac{\sum \left(n_j \cdot \Delta\sigma_{j,S,d}^{m_2}\right)}{\sum n_j}} \tag{4.9b}$$

The effects of combination of normal and shear stresses shall be assessed on the basis of the following criterion:

$$\left(\frac{\Delta\sigma_{eq,S,d}}{\Delta\sigma_{R,d}}\right)^2 + \left(\frac{\Delta\tau_{eq,S,d}}{\Delta\tau_{R,d}}\right)^2 \leq CV \tag{4.10}$$

where $\mathbf{\Delta\sigma_{R,d}}$ and $\mathbf{\Delta\tau_{R,d}}$ are the design resistance normal and shear stress ranges derived from the specified number of cycles and the appropriate FAT class. CV is a comparison value, which is given in Table 4.1.

In cases where the stresses are acting in different directions with respect to the weld, they are assessed by different methods, e.g. nominal stress, structural hot-spot stress or effective notch stress method, the verification by the above given formulae must be performed with the fatigue resistance data for the corresponding method.

In the **2 million cycles equivalent** procedure, the same applied as for formula (4.8) with the difference that the equivalence is for 2 million cycles, where n_i and n_j refer to the **total anticipated load history** of the joint. Assuming the most damaging blocks or $\Delta\sigma_{eq,S,d}$ being above the knee point of the S-N curve, then the 2 million cycles equivalent stress range $\Delta\sigma_{S,d,E2}$ for constant amplitude fatigue action is calculated by

$$\Delta\sigma_{S,d,E2} = \sqrt[m_1]{\frac{1}{D_{spec}} \cdot \frac{\sum (n_i \cdot \Delta\sigma_{i,S,d}^{m_1}) + \Delta\sigma_{L,d}^{(m_1-m_2)} \cdot \sum (n_j \cdot \Delta\sigma_{j,S,d}^{m_2})}{2 \cdot 10^6}} \tag{4.11}$$

In cases where the most damaging blocks or $\Delta\sigma_{eq,S,d}$ are below the knee point of the S-N curve, then calculate

$$\Delta\sigma_{S,d,E2} = \sqrt[m_2]{\frac{1}{D_{spec}} \cdot \frac{\Delta\sigma_{L,d}^{(m_2-m_1)} \cdot \sum (n_i \cdot \Delta\sigma_{i,S,d}^{m_1}) + \sum (n_j \cdot \Delta\sigma_{j,S,d}^{m_2})}{2 \cdot 10^6}} \tag{4.12}$$

The assessment procedures for an interaction of fluctuating normal and shear stress are given in Table 4.1. If Table 4.1 is used for the 2 million cycles equivalent procedure, all fatigue action data are 2 million cycles equivalents. The fatigue resistance data are modified and factored fatigue class values FAT_{mod}/γ_M.

Note: The verification procedures for multi-axial and non-proportional loading are in development. The procedures given in Table 4.1 describe a conservative approach. In cases of special interest, the user may consult the relevant literature [67].

For the grid of fatigue resistance S-N curves with the initial slope of **m = 3** predominantly used in Sect. 3.2, stepping down one class corresponds to a division of the stress range by **1.12**. So, different levels of safety $\boldsymbol{\gamma_M}$ of an applied S-N curve may be considered (see Sect. 6.4.3).

4.3.2 Nonlinear Damage Calculation

A nonlinear fracture mechanics damage calculation according to Sect. 4.4 is recommended in cases, where

(a) The Palmgren-Miner summation is sensitive to the exact location of the knee point of the fatigue resistance S-N curve,
(b) The spectrum of fatigue actions (loads) varies in service or is changed, and so the sequence of loads becomes significant or
(c) The resistance S-N curve of a pre-damaged component has to be estimated.

Where the parameters for a fracture mechanics fatigue assessment are not known and only the resistance S-N curve is known, the S-N curve can be used to derive dimensionless fracture mechanics parameters, which allow a damage calculation [63]. The procedure is based on the "Paris" power law of crack propagation

$$\frac{da}{dN} = C_0 \cdot \Delta K^m \quad if \quad \Delta K > \Delta K_{th} \tag{4.13}$$

$$\text{but} \quad \frac{da}{dN} = 0 \qquad if \quad \Delta K \leq \Delta K_{th} \tag{4.14}$$

where

a dimensionless crack parameter
N Number of cycles
ΔK Stress intensity factor range
$\boldsymbol{\Delta K_{th}}$ Threshold stress intensity factor range below which no crack propagation is assumed
$\boldsymbol{C_0}$, **m** material constants

The characteristic stress intensity factor range $\mathbf{\Delta K_{S,k}}$ of the fatigue action is calculated with the stresses in the spectrum $\mathbf{\Delta\sigma_{i,S,k}}$ and the crack parameter **a.**

$$\Delta K_{S,\,k} = \Delta\sigma_{S,\,k} \cdot \sqrt{a} \tag{4.15}$$

The characteristic resistance parameters can be derived from the characteristic constant amplitude fatigue resistance S-N curve: The threshold value corresponds to the fatigue limit, $\mathbf{\Delta K_{th,k} = \Delta\sigma_{L,R,k} \cdot \sqrt{a}}$, **m** equals the slope of the S-N curve, and the constant $\mathbf{C_{0,k}}$ can be calculated from a data point ($\mathbf{\Delta\sigma_{S\text{-}N}}$ and $\mathbf{N_{S\text{-}N}}$) on the S-N curve, preferably from the fatigue class at $2 \cdot 10^6$ cycles.

$$C_{0,\,k} = \frac{2}{(m-2) \cdot N_{S-N} \cdot \Delta\sigma_{S-N}^{m}} \tag{4.16}$$

The fatigue assessment is carried out according to Sect. 4.4, using an initial crack parameter $\mathbf{a_i = 1}$ and a final one $\mathbf{a_f = \infty}$ or a large number e.g. $\mathbf{a_f = 10^9}$. The restrictions on life cycles given in Sect. 4.3 are to be considered. The actual fatigue class $\mathbf{FAT_{act}}$ of a pre-damaged component thus becomes $\mathbf{FAT_{act.} = FAT/\sqrt{a}}$.

4.4 Fatigue Assessment by Crack Propagation Calculation

The fatigue action represented by the design spectrum of stress intensity factor ranges

$$\Delta K_{S,\,d} = \Delta K_{S,\,k} \cdot \gamma_F \tag{4.17}$$

is verified by the material resistance design parameters against crack propagation

$$C_{0,\,d} = C_{0,\,k} \cdot \gamma_M^m \tag{4.18}$$

$$\Delta K_{th,\,d} = \frac{K_{th,\,k}}{\gamma_M} \tag{4.19}$$

using the "Paris" power law

$$\frac{da}{dN} = C_0 \cdot \Delta K^m \quad if \quad \Delta K > \Delta K_{th} \quad else \quad \frac{da}{dN} = 0 \tag{4.20}$$

where

a Crack size
N Number of cycles
ΔK Stress intensity factor range

ΔK_{th} Threshold value of stress intensity factor range below which no crack propagation is assumed
C_0, m material constants

For applied stress intensity factors, which are high compared with the fracture toughness of the material, **K_{mat}**, an acceleration of crack propagation will occur. In these cases, the following extension of the "Paris" power law of crack propagation is recommended. In the absence of an accurate value of the fracture toughness, a conservative estimate should be made.

$$\frac{da}{dN} = \frac{C_0 \cdot \Delta K^m}{(1-R) \cdot \frac{\Delta K}{K_{mat}}} \tag{4.21}$$

where
K_{mat} Fracture toughness of the material
R Stress ratio

The fatigue life **N** is determined by integration starting from an initial crack parameter **a_i** to a final one **a_f** [51–53]. The calculated number of life cycles **N** must be greater or equal to the required number of life cycles.

The same formulae apply for a crack growth calculation in a **c**-direction, if that was required by the selected procedure.

In general, the integration has to be carried out numerically. The increment for one cycle is **Δa** as given in Eq. 4.17. It is recommended that a continuous spectrum be subdivided into an adequate number of stress range blocks, e.g. 8 or 10 blocks, and that the integration be performed block-wise by summing the increments of **a** and the number of cycles of the blocks. The entire size of the spectrum in terms of cycles should be adjusted by multiplying the block cycles by an appropriate factor in order to ensure at least 20 loops over the whole spectrum in the integration procedure. If the sequence of loading is not known, the highest stresses in spectrum should be processed first.

$$\begin{aligned} \Delta a &= C_{0,d} \cdot \Delta K_{a,d}^m \cdot 1\ cycle \quad if \quad \Delta K_{a,d} > \Delta K_{th,d} \quad else \quad \Delta a = 0 \\ \Delta c &= C_{0,d} \cdot \Delta K_{c,d}^m \cdot 1\ cycle \quad if \quad \Delta K_{c,d} > \Delta K_{th,d} \quad else \quad \Delta c = 0 \end{aligned} \tag{4.22}$$

When using weight functions, the integration of the power law of crack propagation has to be performed over the implicite integral of the weight function.

$$N = \int_{x=a_i}^{x=a_f} \frac{dx}{C_0 \cdot \Delta K^m} = \int_{x=a_i}^{x=a_f} \frac{dx}{C_0 \cdot \left[\int_{x=0}^{x=a} \Delta\sigma(x) \cdot h(x,a) \cdot dx\right]^m} \tag{4.23}$$

4.5 Fatigue Assessment on the Basis of Service Testing

4.5.1 General

An experimental fatigue assessment of components or structures may be required for different reasons:

(a) Existence of a new design with no or insufficient knowledge or experience of its fatigue behaviour.
(b) Verification of a component or structure for a specified survival probability under a special fatigue action (stress) history.
(c) Optimization of design and/or fabrication with respect to weight, safety and economy after initial design. For example, the selected dimensions may be justified on the basis of higher fatigue resistance data than those presented here. Support for this might require component testing.
A preliminary design may be done by assuming an about 50 % higher fatigue resistance than given by the FAT classes. Later the design has to be verified by component test. In production, an adequate quality assurance system has to be established to make sure that the quality in test and in production are always equal.

In component testing, the statistical nature of fatigue must be considered. It might also be necessary to take into account differences in fabrication quality between the tested component and the actual structure. The system of quality assurance should be documented. The verification or assessment might also depend on the safety strategy considered (see Sect. 5.2), with some distinction between safe-life, fail-safe and damage tolerant strategies.

Ideally, the fatigue tests should be performed under loading conditions that represent the service fatigue action history (see Sect. 3.7), factored if necessary by the partial safety factors $\boldsymbol{\gamma_F}$ and $\boldsymbol{\gamma_M}$ (i.e., the stress levels of the action history have to be multiplied by $\boldsymbol{\gamma_F\ \gamma_M}$ for testing) (Table 4.3).

The **all failed** approach is the normal way of testing a small sample of which each specimen represents the same weld details. The test data may be suitable for producing a S-N curve, in which case their statistical analysis considers only the data of the failed specimens disregarding the results from the non-failed ones. However, there are techniques for including those as well, if necessary (e.g. [75]).

The **first to fail** approach is usually used to save time when a large number of identical specimens are tested. The results could be used to establish a safe fatigue life for the component, but only at the level of the test.

The **p to fail** approach is used in similar way to the “first to fail” one. A common situation would be one, in which the test specimen contains many potential sites of fatigue cracking, and when repair of cracks allows to continue the test. Each time when a detail fails, the test is stopped and the failed detail is repaired. At the end, possibly all details have failed and thus the “all failed” approach could be applied.

Table 4.3 Testing approaches

No	Testing procedure	Approach
1	All specimens from the samples are tested to failure	All failed
2	Testing is stopped at failure of first specimen from the sample	First to fail
3	Testing is stopped when **p** specimens of the **n** samples have failed	**p** to fail

If only **p** specimens out of the **n** possible ones failed, the "p to fail" approach may be used.

This section considers the **all failed** and **first to fail** approaches. Other approaches and details of statistical analysis are considered in Appendix 6.4.

The following test result data should be documented according to the selected approach:

- The mean of the log of number of cycles to failure of all **n** failed samples or details.
- The number of cycles to failure of the first failed detail within **n** tested details.
- The number of cycles to failure of the first **p** failed details within **n** tested details.

The tests should be performed according to well established and appropriate procedures or standards [68].

In order to relate the results of the fatigue test to service operation, an estimate of the standard deviation of **log N** is required, possibly taking into account the fact that this can vary along the S-N curve, see Fig. 3.1.

If the number of test results **n < 10**, or if the procedure of first failure or **p** failures in **n** specimens approach is used, the standard deviation in terms of log cycles can be conservatively estimated as follows:

0.18 for geometrically simple structures at fatigue endurances between 10^4 and 10^5 cycles

0.25 for complex structures at fatigue endurances up to 10^6 cycles

No estimate can be given for fatigue endurances approaching the endurance limit. Here, special verification procedures are recommended, see Ref. [69]

4.5.2 Acceptance Criteria

The required or usable fatigue life of the component or structure should be less than the minimum probable fatigue life estimated on the basis of the tests, such that

$$N_d < \frac{N_T}{F} \tag{4.24}$$

Table 4.4 F-factors for failure of all test specimens

Stdv.\n	2	4	6	8	10
0.18	3.93	2.64	2.45	2.36	2.30
0.250	6.86	3.90	3.52	3.32	3.18

Table 4.5 F-factors for the first test specimen to fail

Stdv.\n	2	4	6	8	10
0.18	2.72	2.07	1.83	1.69	1.55
0.25	4.07	2.77	2.34	2.09	1.85

where

$\mathbf{N_T}$ The log mean fatigue life in cycles of the test specimens, or the life of the first test specimen to fail, whichever is applicable

F Factor dependent of the number of test results available as defined in Tables 4.4 and 4.5 as appropriate. The **F**-factors refer to a survival probability as decribed in Sect. 3.7

$\mathbf{N_d}$ Number of cycles, up to which the component or structure may be used in service

If all components or test specimens are tested to failure, values of **F** from Table 4.4 shall be used.

If the tests are carried out until failure of the first test specimen, values of **F** from Table 4.5 shall be used.

The factor **F** may be further modified according to safety requirements as given in Sect. 5.3.

4.5.3 Safe Life Assessment

Safe life assessment considers each structural element and detail as independent. Each element should fulfill the acceptance criteria defined in Sect. 4.5.2.

The partial safety factors γ_F applied to fatigue actions (loads) and γ_M applied to fatigue resistance may be selected from Table 5.1.

4.5.4 Fail Safe Assessment

Fatigue life assessment of fail safe structures depends largely on the design and service operation parameters of the structure. The effectiveness of statically over-determined (hyperstatic) behaviour or redundancy of structural components, the possibility of detection of failures in individual structural parts and the possibility of repair determine the level of safety required in the individual structural parts. Consequently, no general recommendation can be given.

The factor **F** given in Sect. 4.5.2 can be used for general guidance and to establish agreement.

The partial safety factors γ_F applied to fatigue actions (loads) and γ_M applied to fatigue resistance may be selected from Table 5.1.

4.5.5 Damage Tolerant Assessment

The verification that a structure is damage tolerant requires the demonstration that the structure can sustain fatigue cracking without failure until such time as the cracking is detected. When fatigue testing is employed as a part of the verification procedure, the failure criterion of the tests should be chosen to reflect the influence of the type of loading and the operation conditions of the actual structure.

The criteria for factoring the observed lives obtained in the tests depend of the application. It is recommended to establish agreement on the choice of the factor **F** between the relevant parties.

The partial safety factors γ_F applied to fatigue actions (loads) and γ_M applied to fatigue resistance may be selected from Table 5.1.

Chapter 5
Safety Considerations

5.1 Basic Principles

A component has to be designed for an adequate survival probability. The required survival probability depends on the

- Uncertainties and scatter in the fatigue assessment data
- Safety strategy
- Consequences of failure.

Uncertainties in the fatigue assessment data may also origin from the **fatigue actions**, such as

- Determination of loads and load history
- Determination of stresses or stress intensity factors from the model used for analysis
- Dynamic response problems.

These uncertainties can be covered by an appropriate partial safety factor for the fatigue actions γ_F, which is **not considered here**. However, it is emphasized that assumptions made at the design stage should be conservative and ideally checked during early stages of service operation.

Uncertainties in a fatigue assessment arising from the **fatigue resistance** data and damage calculation methods include:

- Scatter in fatigue resistance data,
- Scatter of verification results from damage calculations.

The last two sources of uncertainty are considered here. For normal applications, they are already covered in the fatigue resistance data given here. For special applications, the data may be modified by the selection of an adequate partial safety factor γ_M.

A.F. Hobbacher, *Recommendations for Fatigue Design of Welded Joints and Components*, IIW Collection, DOI 10.1007/978-3-319-23757-2_5

5.2 Fatigue Design Strategies

Different service operation conditions require different fatigue design strategies. The definition of a fatigue design strategy refers predominantly to the method of fatigue analysis, inspection and monitoring in service.

5.2.1 *Infinite Life Design*

This strategy is based on keeping all fatigue actions under an assumed resistance fatigue limit or threshold value. If regular in-service monitoring is **not** specified, the survival probability must be high. This strategy is most suited to components that experience very high numbers of cycles, which are uniform or preferably close to constant amplitude.

The strategy often relies on the assumption that there is always a fatigue limit below which infinite life can be expected. However, there are increasing doubts that this is the case for welded components. It is recommended that due consideration should be given to the adoption of am S-N curve that does not become horizontal at the CAFL or 'knee' point, but continues at a very shallow slope, as indicated in Sect. 3.2.

5.2.2 *Safe Life Design*

This design strategy is used in situations where regular inspection in service is not possible or the consequences of failure are very high. Consequently a very high survival probability is required.

5.2.3 *Fail Safe Design*

This design strategy is based on the assumption that the component or structure can tolerate extensive fatigue cracking without failing, possibly because it is statically over-determined (hyper-static) or there is an adequate redundancy. Regular monitoring in service is not usually provided. It is relied on the redistribution of forces if cracking does occur, which can be readily detected and repaired. Welded joints in such structures can be designed for a normal survival probability.

5.2.4 *Damage Tolerant Design*

This design strategy is based on the assumption that fatigue cracks will form but they will be readily detectable in service before they become critical.

Fracture mechanics can be used to calculate suitably inspection intervals. However, apart from fatigue considerations it may also be necessary to ensure that the material is sufficiently tough to tolerate the largest fatigue crack that could be present before it has been detected. A normal probability of survival is adequate.

5.3 Partial Safety Factors

The requirement for a partial safety factor to be applied to the fatigue resistance data $\boldsymbol{\gamma_M}$ depends largely on such circumstances as

- Fatigue design strategy
- Consequences of failure
- Practical experience in fields of application.

Examples of possible values for partial safety factors are given in Table 5.1, but no general recommendations can be given. In most cases of the use of the conservative fatigue resistance data given in the present recommendations, $\boldsymbol{\gamma_M = 1}$ should be adequate for design or assessment of components or structures of normal fabrication quality, which will be regularly inspected in service.

The safety factors $\boldsymbol{\gamma_M = 1}$ are given in terms of stress. If safety factors are needed in terms of cycles, $\boldsymbol{\Gamma_M}$ may be calculated using the exponent **m** of the resistance S-N curve or Paris power law of crack propagation.It should be noted that the slope **m** of the S-N resistance curves may vary over the range of application (e.g. see Fig. 3.1).

$$\Gamma_{M,cycles} = \gamma_M^m \tag{5.1}$$

where $\Gamma_{M,\,cycles}$ refers to a partial safety factor in terms of cycles and γ_M refers to stress. No general recommendations on partial safety factors can be given. For special fields of application, safety factors on load actions $\boldsymbol{\gamma_F}$ and on fatigue resistance $\boldsymbol{\gamma_M}$ may be established. Table 5.1 shows a possible example for $\boldsymbol{\gamma_M}$ which may be adjusted according to the special requirements of the individual application.

Table 5.1 Possible examples of partial safety factors γ_M for fatigue resistance

Partial safety factor $\boldsymbol{\gamma_M}$ → Consequence of failure	Fail safe and damage tolerant strategy	Safe life and infinite life strategy
Loss of secondary structural parts	1.0	1.15
Loss of the entire structure	1.15	1.30
Loss of human life	1.30	1.40

5.4 Quality Assurance

Weld quality assurance is based on adequate organization of work flow in design, fabrication, destructive and non-destructive inspection of materials and welds, and the individual acceptance levels for the different types of weld imperfections. Acceptable levels for different types of weld imperfections related specifically to fatigue resistance may be found in Sect. 3.8 or in other fatigue based weld quality codes [e.g. 53].

Since more general weld quality acceptance criteria are needed for practical shop fabrication, the standards ISO 5817 for steel and ISO 10042 for aluminium are widely used. However, it should be noted that these are based more on traditional perceptions of what constitutes good workmanship, than on objective criteria related specially to the influence of the imperfection on the strength, including fatigue strength of the welded joint. Consequently they can be irrelevant, over-conservative and even potentially unsafe from the fatigue viewpoint.

Nevertheless, there is a growing tendency to relate them to strength requirements. For example, ISO 5817:2006 quality level **D** might be specified for statically loaded structures and **B** for fatigue or special requirements, even though these levels are not completely consistent in terms of their effect on fatigue properties. Besides regulations and quality codes, the general standards of good workmanship should to be maintained. For conservative reasons, an ISO 5817:2006 level **B** or even **B+** may be specified or modified in conjunction with Sect. 3.8 or other weld quality codes with an adequate consideration to fatigue [e.g. see Ref. 53].

It is recommended to have a documentation or a drawing on which the required fatigue class for each weld is written. If an imperfection needs an assessment, it can be done on a basis of fatigue performance. A direct relation to quality groups of ISO 5817 and fatigue properties is given in Ref. [76], see also Appendix 6.4.

5.5 Repair of Components

The most common cause of damage in welded structures and components is fatigue. Before the start of any repair of such damage, it is vitally important to establish the reasons for its occurrence since these will influence decisions to be made about the need for repair and for the repair method [77–80]. Possible reasons for fatigue damage include:

- Under-estimation of service loading, number of cycles and shape of load spectrum
- Unexpected sources of fatigue loading
- Inadequate stress analysis
- Inadequate structural design, especially of weld details
- Unsuitable material e.g. regarding toughness, corrosion resistance or weldability

- Poor workmanship (e.g. parts missing or not properly positioned, unsatisfactory application of thermal cutting, significant weld imperfections such as poor penetration, severe undercut, severe misalignment, unauthorized welding of fabrication aids)
- Unexpected dynamic response leading to vibrations not considered in design
- Environmental influences detrimental to fatigue e.g. corrosion or elevated temperature
- Faulty operation, e.g. overload
- Accident, e.g. collision

In most cases of damage, design, loads and imperfections are the governing parameters of the failure, material properties are often secondary.

The actions to be taken should be based on the results of the investigations. Possible actions are:

- No repair
- Delayed repair
- Immediate repair
- More frequent or continuous crack monitoring, in-service inspection or vibration monitoring
- Change in operating conditions

A large variety of repair methods exist. They may generally include the following aspects:

- Removal of crack
- Modification of detail design
- Modification of service loading
- Selection of adequate material and repair welding procedure
- Application of a weld toe improvements technique (see Sect. 5.2)
- Quality control of the repair weld

6 Appendices

The appendices are intended to give special guidance, background information and additional explanations. They are not normative.

6.1 Loading History

6.1.1 Markov Transition Matrix

A Markov transition matrix is a method for recording the numbers of half-cycles of each particular stress range in a fatigue loading stress-time history and the number of 'transitions' from one extreme level (peak or trough) to another. Its general form is illustrated in Fig. 6.1. The actual spectrum is broken down into a number of equally spaced stress levels $\mathbf{a_1, a_2, a_3\ldots\ a_n}$ 32 stress levels are sufficient. The two axes define the starting and the finishing level of each half-cycle, and each individual cell $\mathbf{a_{i,j}}$ of the matrix defines the number of transitions from a level **i** to a level **j** stress. Falling stress half-ranges (from the peak in the stress-time history) appear in the cells below the diagonal, while rising stress half-cycles (from troughs in the stress-time history) appear in those above it, as indicated in Fig. 6.1.

The data for the transition matrix can be obtained by measurement or by time simulation computations. A time stress-time signal for fatigue tests or crack propagation simulations or a cumulative frequency diagram (stress spectrum) for a damage calculation can be generated from the transition matrix by a Markov random draw (Table 6.1).

The original version of this chapter was revised. Belated corrections have been updated. An erratum to this chapter is available at DOI 10.1007/978-3-319-23757-2_8

The original version of this chapter was revised. An erratum to this chapter can be found at DOI 10.1007/978-3-319-23757-2_7

A.F. Hobbacher, *Recommendations for Fatigue Design of Welded Joints and Components*, IIW Collection, DOI 10.1007/978-3-319-23757-2_6

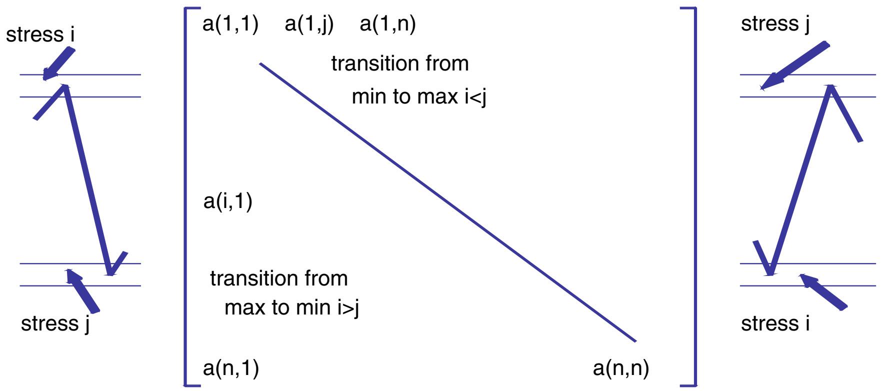

Fig. 6.1 Principle of the transition matrix

Table 6.1 Illustration of a transition matrix

1	2	3	4	5	6	7	8	9	10	11	12	13	14	→	30	31	32
2	x		#					#									
3		x	#					#									
4			x					#									
5	—	—	4	x	—	—	—	**20**	20 transitions from level 5 trough to level 9 peak								
6			#		x												
7			#			x											
8			#				x				**Rising ranges**						
9			#					x									
10	—	—	**45**						x								
11	45 transitions from level 4 peak to level 10 trough									x							
12											x						
13												x					
14								**Falling ranges**					x				
↓														x			
30															x		
31																x	
32																	x

6.1.2 'Rainflow' or 'Reservoir' Counting Method

The algorithm of reservoir counting method is well explained by using the analogy of the flow of water from a reservoir, the boundary of which is the stress-time

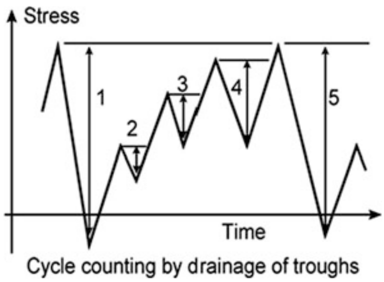

Fig. 6.2 Illustration of reservoir counting

history, as illustrated in Fig. 6.2. Water is drained from the troughs in the stress-time history and the stress range is the largest drop before emptying that part of the reservoir.

Rainflow counting is similar but in this case, the stress-time history is visualized as a pagoda roof and stress cycles are defined in terms of the distances travelled by water flowing down the roof [58, 59]. The same results are obtained from each method.

6.2 Fracture Mechanics

6.2.1 *Rapid Calculation of Stress Intensity Factors*

A simplified method may be used to determine $\mathbf{M_k}$-factors [31]. Here, the $\mathbf{M_k}$-factors are derived from the non-linear total stress distribution $\boldsymbol{\sigma_{nl}}\mathbf{(x)}$ along the anticipated crack path **x** assuming no crack being present. Hence, the function of the stress concentration factor $\mathbf{k_{t,nl}(x)}$ can be calculated [33]. The integration for a certain crack length **a** yields:

$$M_k = \frac{2}{\pi} \cdot \int\limits_{x=0}^{x=a} \frac{k_t, nl^{(x)}}{\sqrt{a^2 - x^2}} dx \qquad (6.1)$$

For different crack lengths **a**, a function $\mathbf{M_k(a)}$ can be established, which is preferably presented in the form:

$$M_k(a) = const/a^{\exp} \qquad M_k(a) \geq 1 \qquad (6.2)$$

6.2.2 *Dimensions of Cracks*

See Table 6.2

Table 6.2 Dimensions for assessment of crack-like imperfections (example)

Idealizations and dimensions of crack-like imperfection for fracture mechanics assessment procedure (t = wall thickness).

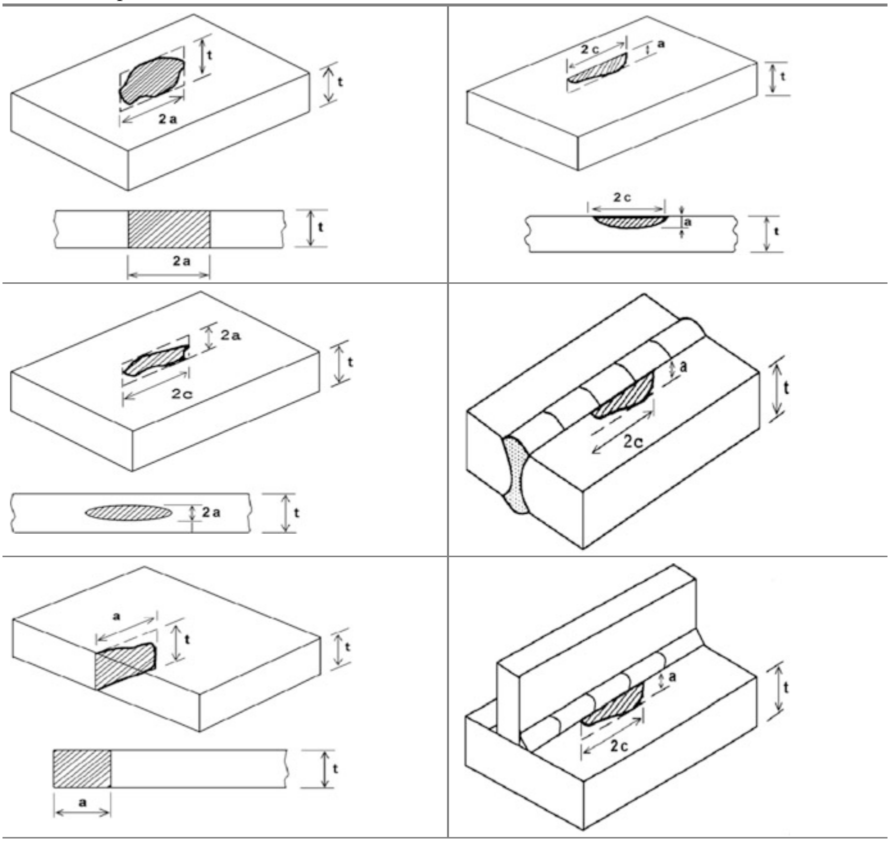

6.2.3 *Interaction of Cracks*

Adjacent cracks may interact and behave like a single large one. The interaction between adjacent cracks should be checked according to an interaction criterion. There are different interaction criteria, and in consequence no strict recommendation can be given. It is recommended to proceed according to an accepted codes and compilations, e.g. [53].

6.2.4 *Formulae for Stress Intensity Factors*

Stress intensity factor formulae may be taken from literature, see references [25–32]. The formulae given below address most of the cases relevant to welded joints.

6.2.4.1 Standard Solutions

See Table 6.3

Table 6.3 Stress intensity factors at welds

<table>
<tr><td colspan="2">Surface cracks under membrane stress</td></tr>
<tr><td>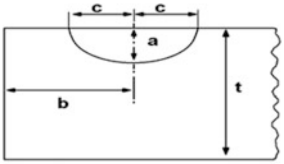
b = distance to nearest edge</td><td>The formula for the stress intensity factor K_1 is valid for $a/c < 1$,
for more details see Ref. [26]</td></tr>
<tr><td colspan="2">$K_1 = \sigma\sqrt{(\pi \cdot a / Q)} \cdot F_s$
$Q = 1 + 1.464\,(a/c)^{1.65}$
$F_s = \left[M_1 + M_2 \cdot (a/t)^2 + M_3 \cdot (a/t)^4\right] \cdot g \cdot f \cdot f_w$
$M_1 = 1.13 - 0.09\,(a/c)$
$M_2 = -0.54 + 0.89/(0.2 + a/c)$
$M_3 = 0.5 - 1/(0.65 + a/c) + 14(1 - a/c)^{24}$
$f_w = [\sec(\pi \cdot c\,\sqrt{(a/t)}/(2 \cdot b))]^{1/2}$
g and f are dependent to direction
"a"−direction : $g = 1 \quad f = 1$
"c"−direction : $g = 1 + \left[0.1 + 0.35\,(a/t)^2\right]$
$f = \sqrt{(a/c)}$</td></tr>
<tr><td colspan="2">Embedded cracks under membrane stress</td></tr>
<tr><td>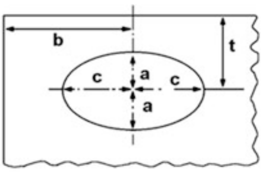
t = distance to nearest surface</td><td>The formula for the stress intensity factor K_1 is valid for $a/c < 1$,
for more details see Ref. [27], where D is the diameter in mm and P is the internal pressure in N/mm^2.</td></tr>
</table>

(continued)

Table 6.3 (continued)

K_1, Q, F_s, f_w as given before for surface cracks, but:

$$M_1 = 1$$

$$M_2 = 0.05/\left(0.11 + (a/c)^{3/2}\right)$$

$$M_3 = 0.29/\left(0.23 + (a/c)^{3/2}\right)$$

g and f are dependent to direction

"a" – direction: $g = 1 \quad f = 1$

"c" – direction: $g = 1 - (a/t)^4/(1 + 4a/c) \quad f = \sqrt{(a/c)}$

Surface cracks under shell bending and membrane stress

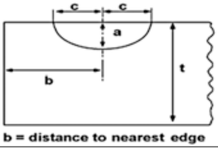	The formula for the stress intensity factor K_1 is valid for a/c < 1, for more details see Ref. [26].

$$K_1 = (\sigma_{mem} + H \cdot \sigma_{ben})\sqrt{(\pi \cdot a / Q)} \cdot F_s$$

$$Q = 1 + 1.464(a/c)^{1.65}$$

$$F_s = \left[M_1 + M_2 \cdot (a/t)^2 + M_3 \cdot (a/t)^4\right] \cdot g \cdot f \cdot f_w$$

$$M_1 = 1.13 - 0.09\,(a/c)$$

$$M_2 = -0.54 + 0.89/(0.2 + a/c)$$

$$M_3 = 0.5 - 1/(0.65 + a/c) + 14(1 - a/c)^{24}$$

$$f_w = [\sec(\pi \cdot c\sqrt{(a/t)}/(2 \cdot b))]^{1/2}$$

g and f are dependent to direction

"a" – direction: $g = 1 \quad f = 1$

"c" – direction: $g = 1 + \left[0.1 + 0.35(a/t)^2\right] \quad f = \sqrt{(a/c)}$

The function H is given by the formulae:

"a" – direction: $H = 1 + G_1(a/t) + G_2(a/t)^2$

where $G_1 = -1.22 - 0.12 \cdot (a/c)$

$G_2 = 0.55 - 1.05 \cdot (a/c)^{0.75} + 0.47(a/c)^{1.5}$

"c" – direction: $H = 1 - 0.34(a/t) - 0.11(a/c)(a/t)$

Surface cracks under internal pressure

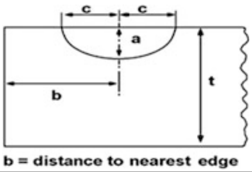	The formula for the stress intensity factor K_1 is valid for a/c < 1, for more details see Ref. [27], where D is the diameter in mm and P is the internal pressure in N/mm^2.

(continued)

Table 6.3 (continued)

$K_1 = \sigma \sqrt{(\pi \cdot a / Q)} \cdot F_s$

$S = p \cdot D_{inner} / (2t)$

$Q = 1 + 1.464(a/c)^{1.65}$

$F_s = 0.97 \cdot \left[M_1 + M_2 \cdot (a/t)^2 + M_3 \cdot (a/t)^4\right] \cdot C \cdot g \cdot f \cdot f_w$

$M_1 = 1.13 - 0.09\,(a/c)$

$M_2 = -0.54 + 0.89/(0.2 + a/c)$

$M_3 = 0.5 - 1/(0.65 + a/c) + 14(1 - a/c)^{24}$

$f_w = [\sec(\pi \cdot c \sqrt{(a/t)}/(2 \cdot b))]^{1/2}$

$C = \left[\left(D_{out}^2 + D_{in}^2\right) / \left(D_{out}^2 - D_{in}^2\right) + 1 - 0.5 \cdot \sqrt{a/t}\,\right] \cdot 2t/D_{in}$

g and f are dependent to direction

"a" – direction : $g = 1$ $f = 1$

"c" – direction : $g = 1 + \left[0.1 + 0.35(a/t)^2\right]$ $f = \sqrt{(a/c)}$

Through the wall cracks under internal pressure

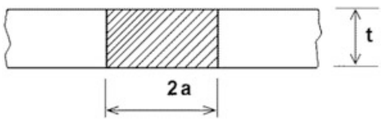

In sphere and longitudinal cracks in cylinder loaded by internal pressure. M_k covers increase of stress concentration factor due to bulging effect of shell. For details see Ref. [27, 30]

$K = \sigma_{mem} \cdot \sqrt{(\pi \cdot a)} \cdot M_k$

where $M_k = 1.0$ for $x < 0.8$

and

$M_k = \sqrt{(0.95 + 0.65 \cdot x - 0.035 \cdot x^{1.6})}$ for $x > 0.8$

and $x < 50$

with $x = a / \sqrt{(r \cdot t)}$

a half distance between crack tips of through the wall crack

r radius of curvature perpendicular to the crack plane

t wall thickness

Root gap in a fillet welded cruciform joint

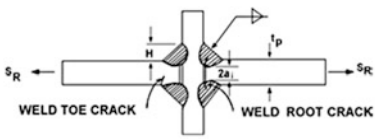

The formula for the stress intensity factor K is valid for H/t from 0.2 to 1.2 and for a/w from 0.0 to 0.7. For more details see Ref. [29].

$$K = \frac{\sigma \cdot (A_1 + A_2 \cdot a/W) \cdot \sqrt{\pi \cdot a \cdot \sec(\pi \cdot a/(2 \cdot W))}}{1 + 2 \cdot H/t}$$

where $w = H + t/2$

σ = nominal stress range in the longitudinal plates

and with $x = H/t$

$A_1 = 0.528 + 3.287 \cdot x - 4.361 \cdot x^2 + 3.696 \cdot x^3 - 1.875 \cdot x^4 + 0.415 \cdot x^5$

$A_2 = 0.218 + 2.717 \cdot x - 10.171 \cdot x^2 + 13.122 \cdot x^3 - 7.755 \cdot x^4 + 1.783 \cdot x^5$

Parametric formulae for Mk functions have been established for a variety of types of welded joints [31, 32] (Table 6.4).

Table 6.4 Formulae for $\mathbf{M_k}$ values for different welded joints

Transverse non-loadcarrying attachment

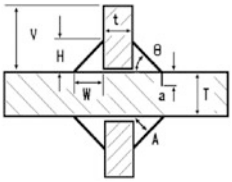

Dim.	**min**	**max**
H/T	0.2	1
W/T	0.2	1
θ	15°	60°
A/T	0.175	0.72
t/T	0.125	2

$$M_k = C \cdot \left(\frac{a}{T}\right)^k \qquad M_k = \ \geq 1$$

$$C = 0.8068 - 0.1554 \cdot \left(\frac{H}{T}\right) + 0.0429\left(\frac{H}{T}\right)^2 + 0.0794\left(\frac{W}{T}\right) \qquad (1)$$

$$k = -0.1993 - 0.1839\left(\frac{H}{T}\right) + 0.0495\left(\frac{H}{T}\right)^2 + 0.0815\left(\frac{H}{T}\right)$$

Cruciform joint K-butt weld

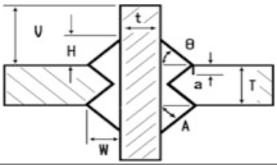

Dim.	**min**	**max**
H/T	0.2	1
W/T	0.2	1
θ	15°	60°
A/T	0.175	1.3
t/T	0.5	20

$$M_k = C \cdot \left(\frac{a}{T}\right)^k \qquad M_k \geq 1$$

$$C = 0.7061 - 0.4091\left(\frac{H}{T}\right) + 0.1596\left(\frac{H}{T}\right)^2 + 0.3739\left(\frac{W}{T}\right) - 0.1329\left(\frac{W}{T}\right)^2 \qquad (2)$$

$$k = -0.2434 - 0.3939\left(\frac{H}{T}\right) + 0.1536\left(\frac{H}{T}\right)^2 + 0.3004\left(\frac{W}{T}\right) - 0.0995\left(\frac{W}{T}\right)^2$$

Cruciform joint fillet welds

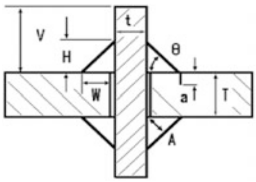

Dim.	**min**	**max**
H/T	0.2	1
W/T	0.2	1
θ	15°	60°
A/T	0.175	0.8
t/T	0.5	10

$$M_k = C \cdot \left(\frac{a}{T}\right)^k \qquad M_k \geq 1$$

If 0.2 < H/T < 0.5 and 0.2 < W/T <0.5 and a/T < 0.07 then:

$$C = 2.0175 - 0.8056\left(\frac{H}{T}\right) - 1.2856\left(\frac{W}{T}\right) \qquad (3)$$

$$k = -0.3586 - 0.4062\left(\frac{H}{T}\right) + 0.3004\left(\frac{W}{T}\right)$$

If 0.2 < H/T < 0.5 and 0.2 < W/T <0.5 and a/T > 0.07 then:

$$C = 0.2916 - 0.0620\left(\frac{H}{T}\right) + 0.69421\left(\frac{W}{T}\right) \qquad (4)$$

$$k = -1.1146 - 0.213224062\left(\frac{H}{T}\right) + 1.4319\left(\frac{W}{T}\right)$$

If 0.5 < H/T < 1.5 and 0.5 < W/T <1.5

(continued)

Table 6.4 (continued)

$$C = 0.9055 - 0.4369\left(\frac{H}{T}\right) + 0.1753\left(\frac{H}{T}\right)^2 + 0.0665\left(\frac{W}{T}\right)^2$$

$$k = -0.2307 - 0.5470\left(\frac{H}{T}\right) + 0.2167\left(\frac{H}{T}\right)^2 + 0.2223\left(\frac{W}{T}\right) \quad (5)$$

Lap joint

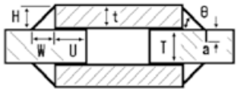

Dim.	**min**	**max**
H/T	0.25	1
W/T	0.25	2
U/T	0	1.5
θ	15°	60°
A/T	0.175	0.8
t/T	0.5	10

$$M_k = C \cdot \left(\frac{a}{T}\right)^k \qquad M_k \geq 1 \ (6)$$

$$C = 1.0210 - 0.3772 \cdot \left(\frac{H}{T}\right) + 0.1844 \cdot \left(\frac{H}{T}\right)^2 + 0.0187 \cdot \left(\frac{W}{T}\right)^2 - 0.1856 \cdot \left(\frac{U}{T}\right) + 0.1362 \cdot \left(\frac{U}{T}\right)^2$$

$$k = -0.4535 - 0.1121 \cdot \left(\frac{H}{T}\right) + 0.3409 \cdot \left(\frac{W}{T}\right) - 0.0824 \cdot \left(\frac{W}{T}\right)^2 + 0.0877 \cdot \left(\frac{U}{T}\right) - 0.0417 \cdot \left(\frac{U}{T}\right)^2$$

Longitudinal non-loadcarrying attachment

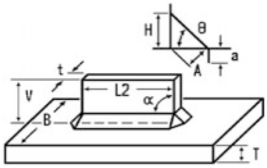

Dim. min max

Dim.	**min**	**max**
L/T	5	40
B/T	2.5	40
θ/45°	0.670	1.33
t/T	0.25	2
A = 0.7	t	

$$M_k = C \cdot \left(\frac{a}{T}\right)^k \qquad M_k = \ \geq 1 \ (7)$$

$$C = 0.9089 - 0.2357 \cdot \left(\frac{t}{T}\right) + 0.0249\left(\frac{L}{T}\right) - 0.00038\left(\frac{L}{T}\right)^2 + 0.0186\left(\frac{B}{T}\right) - 0.1414\left(\frac{\Theta}{45°}\right)$$

$$k = -0.02285 + 0.0167\left(\frac{t}{T}\right) - 0.3863\left(\frac{\Theta}{45°}\right) + 0.1230\left(\frac{\Theta}{45°}\right)^2$$

An example of a 3-dimensional M_k-solution was published by Bowness and Lee [35–37] (Fig. 6.3):

The fitted formulae are valid for membrane stress and a weld toe angle of 45° and:

$$0.005 < a/t < 1.0$$
$$0.1 < a/c < 1.0$$
$$0.5 < L/t < 2.75 \ \text{ if } L/t > 2.75 \text{ then } L/t = 2.75$$

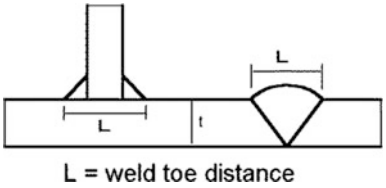

Fig. 6.3 Relevant dimensions for different joint types

Membrane stress:
Deepest point

$$g1 = -1.0343 * (a/c)^2 - 0.15657 * (a/c) + 1.3409$$
$$g2 = 1.3218 * (a/c)^{-0.61153}$$
$$g3 = -0.87238 * (a/c) + 1.2788$$
$$g4 = -0.46190 * (a/c)^3 + 0.6709 * (a/c)^2 - 0.37571 * (a/c) + 4.6511$$
$$f1 = 0.43358 \cdot (a/t)^{\left(g1 + (g2 \cdot (a/t))^{g3}\right)} + 0.93163 \cdot \exp\left((a/t)^{-0.050966}\right)$$
$$f2 = -0.21521 * (1 - (a/t))^{176.4199} + 2.8141 * (a/t)^{(-0.1074 * (a/t))}$$
$$g5 = -0.015647 * (L/t)^3 + 0.09089 * (L/t)^2 - 0.17180 * (L/t) - 0.24587$$
$$g6 = -0.20136 * (L/t)^2 + 0.93311 * (L/t) - 0.41496$$
$$g7 = 0.20188 * (L/t)^2 - 0.97857 * (L/t) + 0.068225$$
$$g8 = -0.027338 * (L/t)^2 + 0.12551 * (L/t) - 11.218$$
$$f3 = 0.33994 * (a/t)^{g5} + 1.9493 * (a/t)^0.23003 + (g6 * (a/t)^2 + g7 * (a/t) + g8)$$
$$Mka = f1 + f2 + f3$$
$$\text{if } Mka < 1 \text{ then } Mka = 1$$

surface point

$$g1 = 0.0078157 * (c/a)^2 - 0.070664 * (c/a) + 1.8508$$
$$g2 = -0.000054546 * (L/t)^2 + 0.00013651 * (L/t) - 0.00047844$$
$$g3 = 0.00049192 * (L/t)^2 - 0.0013595 * (L/t) + 0.011400$$
$$g4 = 0.0071654 * (L/t)^2 - 0.033399 * (L/t) - 0.25064$$
$$g5 = -0.018640 * (c/a)^2 + 0.24311 * (c/a) - 1.7644$$
$$g6 = -0.0016713 * (L/t)^2 + 0.0090620 * (L/t) - 0.016479$$
$$g7 = -0.0031615 * (L/t)^2 - 0.010944 * (L/t) + 0.13967$$
$$g8 = -0.045206 * (L/t)^3 + 0.32380 * (L/t)^2 - 0.68935 * (L/t) + 1.4954$$
$$f1 = g1 \cdot (a/t)^{\left(g2 \cdot (c/a)^2 + g3 \cdot (c/a) + g4\right)} + g5 \cdot (1 - (a/t))^{\left(g6 \cdot (c/a)^2 + g7 \cdot (c/a) + g8\right)} + g9$$

$g9 = -0.25473 * (a/c)^2 + 0.40928 * (a/c) + 0.0021892$

$g10 = 37.423 * (a/c)^2 - 15.741 * (a/c) + 64.903$

$f2 = \left(-0.28639 \cdot (a/c)^2 + 0.35411 \cdot (a/c) + 1.643\right) \cdot (a/t)^{g9} + 0.27449 \cdot (1 - (a/t))^{g10}$

$g11 = -0.10553 * (L/t)^3 + 0.59894 * (L/t)^2 - 1.0942 * (L/t) - 1.2650$

$g12 = 0.043891 * (L/t)^3 - 0.24898 * (L/t)^2 + 0.44732 * (L/t) + 0.60136$

$g13 = -0.011411 * (a/c)^2 + 0.004369 * (a/c) + 0.51732$

$f3 = g11 \cdot (a/t)^{0.75429} + g12 \cdot \exp((a/t)^{g13})$

$Mkc = f1 * f2 * f3$

if $Mkc < 1$ then $Mkc = 1$

Bending stress:
Deepest point

$g1 = -0.014992 * (a/c)^2 - 0.02401 * (a/c) - 0.23851$

$g2 = 0.61775 * (a/c)^{(-1.0278)}$

$g3 = 0.00013242 * (a/c) - 1.4744$

$g4 = - 0.28783 * (a/c)^3 + 0.58706 * (a/c)^2 - 0.37198 * (a/c) - 0.89887$

$fx = (g1 + (g2 \cdot (a/t)^{g3})$

if $fx > 10$ then $fx = 10$

else $f1 = 0.065916 \cdot (a/t)^{fx} + 0.52086 \cdot \exp((a/t)^{-0.10364}) + g4$

$g5 = -17.195 * (a/t)^2 + 12.468 * (a/t) - 0.51662$

$f2 = -0.021995 \cdot (1 - a/t)^{2.8086} + 0.021403 \cdot (a/t)^{g5}$

$g6 = -0.059798 * (L/t)^3 + 0.38091 * (L/t)^2 - 0.8022020 * (L/t) + 0.31906$

$g7 = -0.358 * (L/t)^2 + 1.3975 * (L/t) - 1.7535$

$g8 = 0.31288 * (L/t)^2 - 1.3599 * (L/t) + 1.6611$

$g9 = -0.001470 * (L/t)^2 - 0.0025074 * (L/t) - 0.0089846$

$f3 = 0.23344 \cdot (a/t)^{g6} - 0.14827 \cdot (a/t)^{-0.20077} + (g7 \cdot (a/t)^2 + g8 \cdot (a/t) + g9)$

$Mka = f1 + f2 + f3$

if $Mka < 1$ then $Mka = 1$

Surface point

$$g1 = 0.0023232 \cdot (c/a)^2 - 0.000371 \cdot (c/a) + 4.5985$$
$$g2 = -0.000044010 * (L/t)^2 + 0.00014425 * (L/t) + 0.00086706$$
$$g3 = 0.00039951 * (L/t)^2 - 0.0013715 * (L/t) + 0.014251$$
$$g4 = 0.0046169 * (L/t)^2 - 0.017917 * (L/t) - 0.16335$$
$$g5 = -0.018524 * (c/a)^2 + 0.27810 * (c/a) - 5.4253$$
$$g6 = -0.00037981 * (L/t)^2 + 0.0025078 * (L/t) + 0.00014693$$
$$g7 = -0.0038508 * (L/t)^2 + 0.023212 * (L/t) - 0.026862$$
$$g8 = -0.011911 * (L/t)^3 + 0.082625 * (L/t)^2 - 0.16086 * (L/t) + 1.2302$$
$$g9 = 0.27798 * (a/t)^3 - 1.2144 * (a/t)^2 - 2.4680 * (a/t) + 0.099981$$
$$g10 = -0.25922 * (a/c)^2 + 0.39566 * (a/c) + 0.011759$$
$$fy = (g2 * (c/a)^2 + g3 * (c/a) + g4)$$
$$\text{if } fy > 10 \text{ then } f1 = 0$$
$$\text{else } f1 = g1 \cdot (a/t)^{fy} + g5 \cdot (1 - (a/t))^{\left(g6 \cdot (c/a)^2 + g7 \cdot (c/a) + g8\right)} + g9$$
$$g11 = 6.5964 * (a/c)^2 + 55.787 * (a/c) + 37.053$$
$$f2 = (-0.35006 * (a/c)^2 + 0.40768 * (a/c) + 1.7053) * (a/t)^{g}10 + 0.24988 * (1 - (a/t))^{g11}$$
$$g12 = -0.14895 * (L/t)^3 + 0.815 * (L/t)^2 - 1.4795 * (L/t) - 0.89808$$
$$g13 = 0.055459 * (L/t)^3 - 0.30180 * (L/t)^2 + 0.54154 * (L/t) + 0.53433$$
$$g14 = -0.01343 * (a/c)^3 + 0.0066702 * (a/c) - 0.75939$$
$$f3 = g12 \cdot (a/t)^{0.94761} + g13 \cdot \exp (a/t)^{g14}$$
$$Mkc = f1 + f2 + f3$$
$$\text{if } Mkc < 1 \text{ then } Mkc = 1$$

More detailed formulae containing the effect of the weld angle may be found in Ref. [37].

6.2.4.2 Weight Function for a Surface Crack

Here, an example of a 3-dimensional weight function for a given distribution of stress [40] is given:

$$K_a = \int_0^a \sigma(x) \cdot M_a(x,a) \cdot dx \qquad K_c = \int_0^a \sigma(x) \cdot M_c(x,a) \cdot dx$$

The weight functions for the stress intensity factors at the deepest point (a) and the surface (c) are:

$$M_a(x,a) = \frac{2}{\sqrt{2\pi(a-x)}} \cdot \left[1 + M_{1,a}\left(1-\frac{x}{a}\right)^{\frac{1}{2}} + M_{2,a}\left(1-\frac{x}{a}\right) + M_{3,a}\left(1-\frac{x}{a}\right)^{\frac{3}{2}}\right]$$

$$M_c(x,a) = \frac{2}{\sqrt{\pi \cdot x)}} \cdot \left[1 + M_{1,c}\left(\frac{x}{a}\right)^{\frac{1}{2}} + M_{2,c}\left(\frac{x}{a}\right) + M_{3,c}\left(\frac{x}{a}\right)^{\frac{3}{2}}\right]$$

The coefficients for the functions are:

$$\mathrm{A0} = 0.456128 - 0.114206 * (\mathrm{a/c}) - 0.046523 * (\mathrm{a/c})^2$$

$$\mathrm{A1} = 3.022 - 10.8679 * (\mathrm{a/c}) + 14.94 * (\mathrm{a/c})^2 - 6.8537 * (\mathrm{a/c})^3$$

$$\mathrm{A2} = -2.28655 + 7.88771 * (\mathrm{a/c}) - 11.0675 * (\mathrm{a/c})^2 + 5.16354 * (\mathrm{a/c})^3$$

$$\mathrm{B0} = 1.1019 - 0.019863 * (\mathrm{a/c}) - 0.043588 * (\mathrm{a/c})^2$$

$$\mathrm{B1} = 4.32489 - 14.9372 * (\mathrm{a/c}) + 19.4389 * (\mathrm{a/c})^2 - 8.52318 * (\mathrm{a/c})^3$$

$$\mathrm{B2} = -3.03329 + 9.96083 * (\mathrm{a/c}) - 12.582 * (\mathrm{a/c})^2 + 5.3462 * (\mathrm{a/c})^3$$

$$\alpha = 1.14326 + 0.0175996 * (\mathrm{a/t}) + 0.501001 * (\mathrm{a/t})^2$$

$$\beta = 0.45832 - 0.102985 * (\mathrm{a/t}) - 0.398175 * (\mathrm{a/t})^2$$

$$\gamma = 0.97677 - 0.131975 * (\mathrm{a/t}) + 0.484875 * (\mathrm{a/t})^2$$

$$\delta = 0.448863 - 0.173295 * (\mathrm{a/t}) - 0.267775 * (\mathrm{a/t})^2$$

$$\mathrm{Q} = 1 + 1.464 * (\mathrm{a/c})^{1.65}$$

$$\mathrm{Y0} = \mathrm{B0} + \mathrm{B1} * (\mathrm{a/t})^2 + \mathrm{B2} * (\mathrm{a/t})^4$$

$$\mathrm{Y1} = \mathrm{A0} + \mathrm{A1} * (\mathrm{a/t})^2 + \mathrm{A2} * (\mathrm{a/t})^4$$

$$\mathrm{M1a} = 3.1415 \cdot (4 \cdot \mathrm{Y0} - 6 \cdot \mathrm{Y1})/\sqrt{2 \cdot \mathrm{Q}} - 24/5$$

$$\mathrm{M2a} = 3$$

$$\mathrm{M3a} = 2 \cdot (3.1415 \cdot \mathrm{Y0}/\sqrt{2 \cdot \mathrm{Q}} - \mathrm{M1a} - 4)$$

$$\mathrm{F1} = \alpha * (\mathrm{a/c})^{\beta}$$

$$\mathrm{F2} = \gamma * (\mathrm{a/c})^{\delta}$$

$$\mathrm{M1c} = 3.1415 \cdot (30 \cdot \mathrm{F2} - 18 \cdot \mathrm{F1})/\sqrt{4 \cdot \mathrm{Q}} - 8$$

$$\mathrm{M2c} = 3.1415 \cdot (60 \cdot \mathrm{F1} - 90 \cdot \mathrm{F2})/\sqrt{4 \cdot \mathrm{Q}} - 15$$

$$\mathrm{M3c} = -1 * (1 + \mathrm{M1c} + \mathrm{M2c})$$

The formulae are valid for $0 < \mathrm{a/t} < 0.8$ and for $0.2 < \mathrm{a/c} < 1$.

6.2.5 Stress Distribution at a Weld Toe

Several parametric formulae exist, which may be useful for the weight function approach. An example is given here [42]. The formulae are valid for

$$\frac{\pi}{6} \leq \alpha \leq \frac{\pi}{3} \qquad \textit{and} \qquad \frac{1}{50} \leq \frac{\rho}{t} \leq \frac{1}{15}$$

For membrane stress, the stress distribution is

$$\sigma_m(x) = \frac{k_{t,0}^m \cdot \sigma_0}{2\sqrt{2}} \cdot \left[\left(\frac{x}{\rho} + \frac{1}{2} \right)^{-\frac{1}{2}} + \frac{1}{2} \left(\frac{x}{\rho} + \frac{1}{2} \right)^{-\frac{3}{2}} \right] \cdot \frac{1}{G_m}$$

$$\textit{where} \quad k_{t,0}^m = 1 + 0.388 \cdot \alpha^{0.37} \cdot \left(\frac{\rho}{t} \right)^{-0.454}; \quad E_m = 1.05 \cdot \alpha^{0.18} \cdot \left(\frac{\rho}{t} \right)^{q}$$

$$q = -0.12 \cdot \alpha^{-0.62}; \quad T_m = \frac{x}{t} - 0.3 \cdot \frac{\rho}{t}$$

$$G_m = 0.06 + \frac{0.94 \cdot \exp(-E_m \cdot T_m)}{1 + E_m^3 \cdot T_m^{0.8} \cdot \exp\left(-E_m \cdot T_m^{1.1}\right)} \quad \textit{if} \quad \frac{x}{\rho} > 0.3 \quad \textit{else} \quad G_m = 1$$

For bending stress:
Where

$$\sigma_b(x) = \frac{k_{t,0}^b \cdot \sigma_0}{2\sqrt{2}} \cdot \left[\left(\frac{x}{\rho} + \frac{1}{2} \right)^{-\frac{1}{2}} + \frac{1}{2} \left(\frac{x}{\rho} + \frac{1}{2} \right)^{-\frac{3}{2}} \right] \cdot \frac{1}{G_b}$$

$$\textit{where} \quad k_{t,0}^b = 1 + 0.512 \cdot \alpha^{0.573} \cdot \left(\frac{\rho}{t} \right)^{-0.469}; \quad E_b = 0.9 \cdot \left(\frac{\rho}{t} \right)^{-(0.0026 + 0.0825/\alpha)}$$

$$T_b = \frac{x}{t} - 0.4 \cdot \frac{\rho}{t}$$

$$G_b = 0.07 + \frac{0.93 \cdot \exp(-E_b \cdot T_{bm})}{1 + E_b^3 \cdot T_b^{0.6} \cdot \exp\left(-E_b \cdot T_b^{1.2}\right)} \quad \textit{if} \quad \frac{x}{\rho} > 0.4 \quad \textit{else} \quad G_b = 1$$

where

$\boldsymbol{\sigma_0}$	reference stress at the surface, structural stress at the toe
$\mathbf{k_{t,0}(x)}$	geometrical stress concentration factor at the surface, **m** indicates membrane, **b** indicates bending
x	coordinate from surface down
$\boldsymbol{\alpha}$	weld angle in radians
t	wall thickness
$\boldsymbol{\rho}$	weld toe radius
$\boldsymbol{\sigma_m(x)}$	stress distribution for membrane stress
$\boldsymbol{\sigma_b(x)}$	stress distribution for bending stress

6.3 Formulae for Misalignment

See Table 6.5

Table 6.5 Formulae for assessment of misalignment

No	Type of misalignment	
1	*Axial misalignment between flat plates*	
	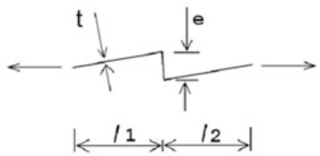	$k_m = 1 + \lambda \cdot \frac{e \cdot l_1}{t \cdot (l_1 + l_2)}$
	λ is dependent on restraint, **λ=6** for unrestrained joints. For remotely loaded joints assume $\mathbf{l_1 = l_2}$.	
2	*Axial misalignment between flat plates of differing thickness*	
	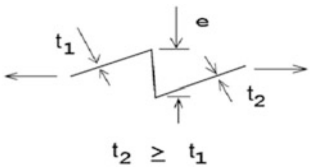	$k_m = 1 + \frac{6 \cdot e}{t_1} \cdot \frac{t_1^n}{t_1^n + t_2^n}$
	Relates to remotely loaded unrestraint joints. The use of **n=1.5** is supported by tests.	
3	*Axial misalignment at joints in cylindrical shells with thickness change*	
	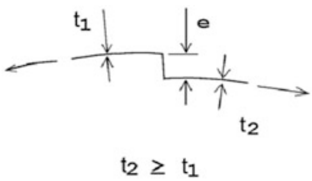	$k_m = 1 + \frac{6 \cdot e}{t_1 \cdot (1 - \nu^2)} \cdot \frac{t_1^n}{t_1^n + t_2^n}$
	n=1.5 in circumferential joints and joints in spheres. **n=0.6** for longitudinal joints.	
4	*Angular misalignment between flat plates*	
	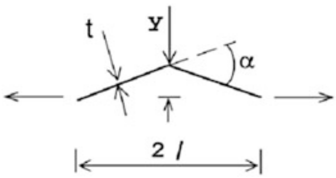	Assuming fixed ends: with $\beta = \frac{2 \cdot l}{t} \cdot \sqrt{\frac{3 \cdot \sigma_m}{E}}$ $k_m = 1 + \frac{3 \cdot y}{t} \cdot \frac{\tanh(\beta/2)}{\beta/2}$ alternat.: $k_m = 1 + \frac{3 \cdot \alpha \cdot l}{2 \cdot t} \cdot \frac{\tanh(\beta/2)}{\beta/2}$ Assuming pinned ends: $k_m = 1 + \frac{6 \cdot y}{t} \cdot \frac{\tanh(\beta)}{\beta}$ alternat.: $k_m = 1 + \frac{3 \cdot \alpha \cdot l}{t} \cdot \frac{\tanh(\beta)}{\beta}$
	The **tanh** correction allows for reduction of angular misalignment due to the straightening of the joint under tensile loading. It is always **≤1** and it is conservative to ignore it. σ_m is membrane stress range.	

(continued)

Table 6.5 (continued)

No	Type of misalignment	
5	*Angular misalignment at longitudinal joints in cylindrical shells*	
	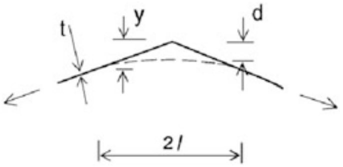	Assuming fixed ends: with $\beta = \frac{2 \cdot l}{t} \cdot \sqrt{\frac{3 \cdot (1 - \nu^2) \cdot \sigma_m}{E}}$ $k_m = 1 + \frac{3 \cdot d}{t \cdot (1 - \nu^2)} \cdot \frac{\tanh(\beta/2)}{\beta/2}$ assuming pinned ends: $k_m = 1 + \frac{6 \cdot d}{t \cdot (1 - \nu^2)} \cdot \frac{\tanh(\beta)}{\beta}$
	d is the deviation from the idealized geometry	
6	*Ovality in pressurized cylindrical pipes and shells*	
	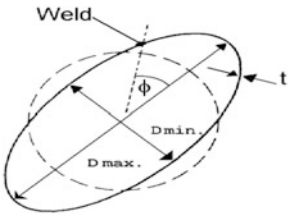	$k_m = 1 + \frac{1.5 \cdot (D_{\max} - D_{\min}) \cdot \cos\phi}{t \cdot \left[1 + \frac{0.5 \cdot p_{\max} \cdot (1 - \nu^2)}{E} \cdot \left(\frac{D}{t}\right)^3\right]}$
7	*Axial misalignment of cruciform joints (toe cracks)*	
	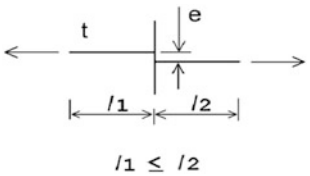	$k_m = 1 + \lambda \cdot \frac{e \cdot l_1}{t \cdot (l_1 + l_2)}$ **λ** is dependent on restraint
	λ varies from **λ=3** (fully restrained) to **λ=6** (unrestraint). For unrestrained remotely loaded joints assume: $\mathbf{l_1 = l_2}$ and **λ=6**	
8	*Angular misalignment of cruciform joints (toe cracks)*	
	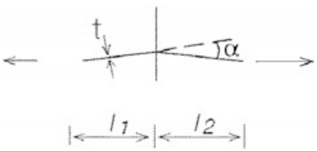	$k_m = 1 + \lambda \cdot \alpha \cdot \frac{l_1 \cdot l_2}{t \cdot (l_1 + l_2)}$ **λ** is dependent on restraint
	If the in-plane displacement of the transverse plate is restricted, **λ** varies from λ=0.02 to **λ=0.04**. If not, **λ** varies from **λ=3** to **λ=6**.	
9	*Axial misalignment in fillet welded cruciform joints (root cracks)*	
	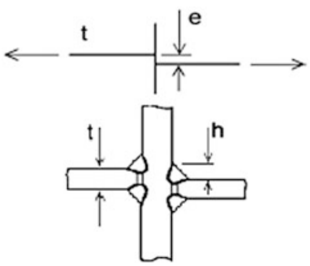	$k_m = 1 + \lambda \cdot \frac{e \cdot}{t + h}$
	$\mathbf{k_m}$ refers to the stress range in weld throat.	

6.4 Statistical Considerations on Safety

6.4.1 Statistical Evaluation of Fatigue Test Data

The methods for evaluation of fatigue test data as described in Sect. 3.7 consider different statistical effects, when evaluating a set of fatigue data. Ideally, all the following effects should be considered, e.g.

- Variance of data
- Probability distribution of the mean value by its confidence interval
- Probability distribution of the variance by its confidence interval
- Difference of the distribution of the whole set of data (population) and the distribution of the sample (Gaussian versus t-distribution)
- Deviation from the assumed Gaussian distribution which can be evaluated by a likelihood or χ^2 testing

For design, a safety margin is considered, which is applied to the mean values. The values used for design are the so called **characteristic** values (index **k**).

These characteristic values are, in principle, values at a **α = 95 %** survival probability (5 % probability of failure) calculated from the mean value $\mathbf{x_m}$ on the basis of two sided tolerance limits of the 75 % confidence level of the mean $\mathbf{x_m}$, for details see Sect. 3.7.

$$x_k = x_m - k \cdot Stdv \tag{6.3}$$

The factor $\mathbf{k_i}$ considers the first four (as described above) and corresponds to:

- the minimum value of the mean confidence interval
- the maximum value of the variance confidence interval

Taking into account that the probability distribution of the mean corresponds to a Student's law (t-distribution) and the probability distribution of the variance corresponds to a Chi-square law (χ^2), the general formula for $\mathbf{k_i}$ is given by:

$$k_1 = \frac{t_{(p,\, n-1)}}{\sqrt{n}} + \phi^{-1}_{(\alpha)} \cdot \sqrt{\frac{n-1}{\chi^2_{(\frac{1+\beta}{2},\, n-1)}}} \tag{6.4}$$

where

t value of the two sided t-distribution (Student's law) for p = β = 0.75, or of the one sided t-distribution for a probability of p = (1 + β)/2 = 0.875 at **n-1** degrees of freedom

n number of test results

φ distribution function of the Gaussian normal distribution probability of exceedence of α = 95 % (superscript **-1** indicates inverse function)

χ^2 Chi-square for a probability of (1 + β)/2 = 0.875 at **n-1** degrees of freedom

Table 6.6 **k**-values for the different methods

n	t	χ^2	k_1	k_2
2	2.51	0.028	11.61	3.41
3	1.61	0.27	5.41	2.57
4	1.44	0.69	4.15	2.36
5	1.36	1.21	3.6	2.25
10	1.24	4.47	2.73	2.04
15	1.21	8.21	2.46	1.96
20	1.20	12.17	2.32	1.91
25	1.19	16.26	2.24	1.88
30	1.18	20.45	2.17	1.86
40	1.18	29.07	2.09	1.83
50	1.17	37.84	2.04	1.81
100	1.16	83.02	1.91	1.76

If the variance is fixed from other tests or standard values, no confidence interval has to be considered and so the factor is given by (Table 6.6):

$$k_2 = \frac{t_{(0.875,\, n-1)}}{\sqrt{n}} + \phi^{-1}_{(0.95)} = \frac{t_{(0.875,\, n-1)}}{\sqrt{n}} + 1.645 \tag{6.5}$$

6.4.2 *Statistical Evaluation of Results from Component Testing*

Testing All Test Specimens to Failure

When all specimens are tested to failure, the procedure is to estimate the mean log N_T of the S-N curve and the associated standard deviation.

Starting from the formula in Sect. 4.5.2, there is

$$N_d = \left(\frac{N_T}{F}\right) \tag{6.6}$$

which defines the safety factor **F** by:

$$\log(N_T) - \log(F) > \log(N_d) \tag{6.7}$$

Taking the acceptance criterion $\mathbf{x_m - k \cdot Stdv > x_k}$ from Sect. 3.7 the factor **F** can be deduced:

$$\log(F) = k \cdot Stdv \tag{6.8}$$

With the formula for **k** the different values of **F** can be calculated, depending on the number of test results **n** and on the assumed standard deviation **Stdv** of **logN** for those results.

$$k = \frac{t_{(0.875,n-1)}}{\sqrt{n}} + \Phi^{-1}_{(0.95)} = \frac{t_{(0.875,n-1)}}{\sqrt{n}} + 1.645 \tag{6.9}$$

Testing All Test Specimens Simultaneously Until First Failure

When all test specimens are tested simultaneously until the first to fail, only one value of log N_T is obtained and the standard deviation cannot be derived from test results (Table 6.7).

Starting from the formula in Sect. 4.5.2, there is

$$N_d = \frac{N_T}{F} \tag{6.10}$$

which defines the safety factor **F** by:

$$\log(N_T) - \log(F) > \log(N_d) \tag{6.11}$$

When considering statistical evaluation, account must be taken of additional effects as illustrated in Fig. 6.4:

- Distribution of the 1/n-th extreme value
- Distribution of the sample between 1/n-th extreme and mean
- Safety margin for the characteristic value

Table 6.7 Values **k** testing until all failed

n	2	4	6	8	10	100
k	3.34	2.37	2.19	2.10	2.04	1.76

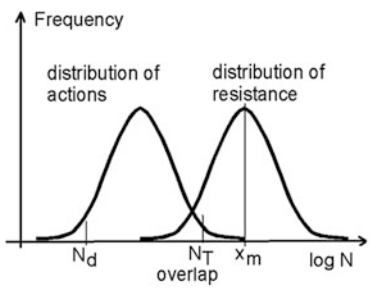

Fig. 6.4 Distribution of action and resistance

Table 6.8 Values **k** for testing until first failure

n	2	4	6	8	10
k	2.44	1.77	1.48	1.28	1.07

For more details see Ref. [73, 74].

where
N_T Life of first specimen to fail
x_m Mean of the sample
N_d Design value

log N_T is considered as the probable maximum (safe side) of the distribution of the minimum value of the log N distribution. The mean of the sample **x_m** is therefore given by:

$$x_k = x_m - k_a \cdot \alpha \cdot Stdv + k_b \cdot Stdv \tag{6.12}$$

with
Stdv standard deviation of the sample
α from table of variance order statistics
k_a, k_b from table of expected values of normal order statistics

Taking the acceptance criterion **$x_m - k_1$ Stdv > x_k** from Sect. 3.7, the factor **F** can be deduced:

$$\log(F) = (k_a \cdot \alpha - k_b + k_1) \cdot Stdv \tag{6.13}$$

The different values of **F** can be calculated, depending on number of test results **n** and the assumed standard deviation **Stdv** of the test specimens in terms of **log N** (Table 6.8).

Testing All Specimens Simultaneously Until p Failures Amongst n Specimens

Values of k may be taken from the relevant literature or from Ref. [75].

6.4.3 Statistical Considerations for Partial Safety Factors

No general recommendations on partial safety factors are given. For special fields of application, safety factors on load actions γ_F and on fatigue resistance γ_M may be established. Table 6.9 shows a possible example for γ_M which may be adjusted according to the special requirements of the individual application.

Table 6.9 Possible examples of partial safety factors γ_M for fatigue resistance

Partial safety factor γ_M → consequence of failure	Fail safe and damage tolerant strategy	Safe life and infinite life strategy
Loss of secondary structural parts	1.0	1.15
Loss of the entire structure	1.15	1.30
Loss of human life	1.30	1.40

6.5 Fatigue Resistance of ISO 5817 Quality

The quality groups B, C and D as defined in ISO 5817 are not completely consistent in terms of fatigue properties of the welded joints. A correlation between the fatigue properties and the individual types of weld imperfections is given in Table 6.6. For more details, see Ref. [76] (Table 6.10).

Note: The dimensions of acceptable weld imperfections within a quality group are partially dependent of the wall thickness and partially absolute values. So a wall thickness of 10 mm was chosen for the table. Absolute dimensions are less harmful for thicker walls and thus conservative. The limitations of fatigue resistance due to bigger wall thicknesses still apply.

Table 6.10 Fatigue resistance of weld imperfections as defined by ISO 5817-2006 for steel

No ISO 5817 2006	No. ISO 6520-1 1998	Type of imperfection	Remarks	t mm	Maximum usable fatigue class FAT in assessment by nominal stress method for the different quality groups		
					D	C	B
1 Surface imperfections							
1.1	100	Crack	Fitness for purpose assessment by fracture mechanics recommended		Not allowed	Not allowed	Not allowed
1.2	104	End crater crack	Fitness for purpose assessment by fracture mechanics recommended		Not allowed	Not allowed	Not allowed
1.3	2017	Surface pore	Butt weld	>6	FAT 40	FAT 71	Not allowed
			Fillet weld (Root crack)		FAT 40	FAT 40	
1.4	2025	Open end crater cavity	Butt weld	>6	FAT 40	FAT 71	Not allowed
			Fillet weld (Root crack)		FAT 40	FAT 40	
1.5	401	Lack of fusion	Fitness for purpose assessment by fracture mechanics recommended		Not allowed	Not allowed	Not allowed
		Micro lack of fusion	Fitness for purpose assessment by fracture mechanics recommended. Butt weld	>6	FAT 63	FAT 80	Not allowed
			Fillet weld (Root crack)		FAT 40	FAT 40	
1.6	4021	Insufficient root penetration	Verification of net section!	>6	FAT 63	Not allowed	Not allowed
1.7	5011	Continuous undercut	Butt weld	>3	FAT 71	FAT 90	FAT 90
			Fillet weld (Toe crack)	>3	FAT 63	FAT 80	FAT 80
	5012	Non-continuous undercut	Butt weld	>3	FAT 71	FAT 90	FAT 90
			Fillet weld (Toe crack)	>3	FAT 63	FAT 80	FAT 80
1.8	5013	Root notch	Butt weld	>3	FAT 40	FAT 71	FAT 90
1.9	502	Excessive weld overfill	Butt weld	>3	FAT 80	FAT 80	FAT 90

(continued)

Table 6.10 (continued)

No ISO 5817 2006	No. ISO 6520-1 1998	Type of imperfection	Remarks	t mm	Maximum usable fatigue class FAT in assessment by nominal stress method for the different quality groups		
					D	C	B
1.10	503	Excessive convexity	Fillet weld	>3	FAT 63	FAT 71	FAT 80
1.11	504	Excessive root overfill		>6	FAT 80	FAT 80	FAT 90
1.12	505	Incorrect weld toe	Butt weld	>3	FAT 80	FAT 80	FAT 90
			Fillet weld (Toe crack)	>3	FAT 63	FAT 71	FAT 80
1.13	506	Overlap		>3	FAT 80	Not allowed	Not allowed
1.14	509	Sagging, incomplete filled groove		>3	FAT 40	FAT 71	FAT 90
	511	Root sagging		>3	FAT 40	FAT 71	FAT 90
1.15	510	Blowholes			Not allowed	Not allowed	Not allowed
1.16	512	Excessive asymmetry	Fillet weld (Toe crack)		FAT 80	FAT 80	FAT 80
1.17	515	Root concavity		>6	FAT 63	FAT 71	FAT 90
1.18	516	Root porosity	Butt weld	>6	FAT 71	Not allowed	Not allowed
			Fillet weld (Root crack)		FAT 40		
1.19	517	Insufficient weld start	Butt weld		FAT 71	Not allowed	Not allowed
			Fillet weld (Root crack)		FAT 40		
1.20	5213	Insufficient throat thickness	Root crack, verification of net section!	>6	FAT 40	FAT 40	Not allowed
1.21	5214	Excessive throat thickness	Root crack		FAT 40	FAT 40	FAT 40
1.22	601	Arc strikes	Butt weld		FAT 90	Not allowed	Not allowed
			Fillet weld (Toe crack)		FAT 63		

(continued)

Table 6.10 (continued)

No ISO 5817 2006	No. ISO 6520-1 1998	Type of imperfection	Remarks	t mm	Maximum usable fatigue class FAT in assessment by nominal stress method for the different quality groups		
					D	C	B
1.23	602	Sputter	Depending on surface quality. Butt weld		FAT 90	FAT 90	FAT 90
			Fillet weld (Toe crack)		FAT 63	FAT 63	FAT 63
2. *Inner imperfections*							
2.1	100	Crack	Fitness for purpose assessment by fracture mechanics recommended		Not allowed	Not allowed	Not allowed
2.2	1001	Micro-crack	Fitness for purpose assessment by fracture mechanics recommended	>6	FAT 63	Not allowed	Not allowed
			Fillet weld (Root crack)		FAT 40		
2.3	2011	Pore	Butt weld	>6	FAT 80	FAT 100	FAT 125
	2012	Porosity	Fillet weld (Root crack)		FAT 40	FAT 40	FAT 40
2.4	2013	Pore net clustered porosity	Without a special assessment, or at an additional limitation of projected area. Butt weld	>6	FAT 50 ≤5 % : FAT 71	FAT 63 ≤4 % : FAT 80	FAT 71 ≤3 %: FAT 90
			Fillet weld (Root crack)		FAT 40	FAT 40	FAT 40
2.5	2014	Pore line	Butt weld	>6	FAT 71	FAT 80	FAT 90
			Fillet weld (Root crack)		FAT 40	FAT 40	FAT 40
2.6	2015 2016	Wormhole	Butt weld	>6	FAT 71	FAT 80	FAT 90
			Fillet weld (Root crack)		FAT 40	FAT 40	FAT 40
2.7	202	Cavity	Butt weld	>6	FAT 71	Not allowed	Not allowed
			Fillet weld (Root crack)		FAT 40		

(continued)

Table 6.10 (continued)

No ISO 5817 2006	No. ISO 6520-1 1998	Type of imperfection	Remarks	t mm	Maximum usable fatigue class FAT in assessment by nominal stress method for the different quality groups		
					D	C	B
2.8	2024	End crater cavity	Butt weld	>6	FAT 71	Not allowed	Not allowed
			Fillet weld (Root crack)		FAT 40		
2.9	300 301 302 303	Solid inclusion Slag inclusion Flux inclusion Oxide inclusion	Butt weld (height of inclusion < 1/4-t) or at additional limitation of length L		FAT 56 L ≤ 10 mm: FAT 71	FAT 63 L ≤ 4 mm: FAT 80	FAT 80 L ≤ 2,5 mm: FAT 90
			Fillet weld (height of inclusion < 1/4- a), Root crack		FAT 36	FAT 40	FAT 40
2.10	304	Metallic inclusion except copper	Butt weld		FAT 100	FAT 100	FAT 125
			Fillet weld (Root crack)		FAT 40	FAT 40	FAT 40
2.11	3042	Copper inclusion	Butt weld		FAT 100	FAT 100	FAT 125
			Fillet weld (Root crack)		FAT 40	FAT 40	FAT 40
2.12	401 4011 4012 4013	Lack of penetration Flank LOP Interpass LOP Root LOP	Butt weld		FAT 40	Not allowed	Not allowed
			Fillet weld (Root crack)		FAT 36		
2.13	402	Lack of penetration (At longer imperfection verification of net section!)	Butt weld		FAT 40	Not allowed	Not allowed
			HV-Weld		FAT 36	Not allowed	Not allowed
			Fillet weld (Root crack)		FAT 36	Not allowed	Not allowed

(continued)

Table 6.10 (continued)

No ISO 5817 2006	No. ISO 6520-1 1998	Type of imperfection	Remarks	t mm	Maximum usable fatigue class FAT in assessment by nominal stress method for the different quality groups		
					D	C	B
3. *Imperfecions of weld geometry*							
3.1	507	Angular misalignment	calculative verification recommended, if necessary	>6	FAT 45	FAT 63	FAT 90
(3.2)[a]	508	Angular misalignment	calculative verification recommended, if necessary		FAT 36	FAT 56	FAT 90
3.2	617	Lack of fit at fillet welds	Without influence				
4. *Multiple imperfections*							
4.1	none	Multiple imperfections in arbitrary section	Engineering assessment of interaction[b]				
4.2	none	Multiple imperfection in longitudinal direction of weld	Engineering assessment of interaction[b]				

[a]This item is no longer part of ISO 5817:2006, but it was contained in ISO 5817:2003. Nevertheless, this item is relevant for fatigue

[b]Only general remarks can be given for engineering assessment. It may be done by verification of the net section using FAT 36, by the effective notch stress method or by fracture mechanics considerations

Erratum to: Recommendations for Fatigue Design of Welded Joints and Components

Erratum to:
A.F. Hobbacher, *Recommendations for Fatigue Design of Welded Joints and Components*, IIW Collections, DOI 10.1007/978-3-319-23757-2

In the original version of the book, the received belated corrections in Chaps. 1, 3, 6 have to be updated. The erratum book has been updated with the changes.

The updated original online version of this chapter can be found at
DOI 10.1007/978-3-319-23757-2_1.

DOI 10.1007/978-3-319-23757-2_3.

DOI 10.1007/978-3-319-23757-2_6

A.F. Hobbacher, *Recommendations for Fatigue Design of Welded Joints and Components*, IIW Collection, DOI 10.1007/978-3-319-23757-2_7

Erratum to: Recommendations for Fatigue Design of Welded Joints and Components

Erratum to:
A.F. Hobbacher, *Recommendations for Fatigue Design of Welded Joints and Components*, IIW Collections, https://doi.org/10.1007/978-3-319-23757-2

In the original version of the book, the belated corrections from author to modify the sentence in Sect. 3.7.3 of Chapter 3 and to update the equations in Tables 6.3 and 6.4 of Chapter 6 have been incorporated. An erratum chapters and the book have been updated with the changes.

The updated version of these chapters can be found at
https://doi.org/10.1007/978-3-319-23757-2_3
https://doi.org/10.1007/978-3-319-23757-2_6

A.F. Hobbacher, *Recommendations for Fatigue Design of Welded Joints and Components*, IIW Collection, https://doi.org/10.1007/978-3-319-23757-2_8

References

General

1. ISO 2394 General principles on reliability for structures. Second edition 1986-10-14
2. Niemi E (1995) Recommendations concerning stress determination for fatigue analysis of welded components. IIW doc. XIII-1458-92/XV-797-92 Abington Publishing, Cambridge
3. Gurney TR (1978) Fatigue of welded structures. Cambridge University Press, Cambridge
4. Maddox SJ (1991) Fatigue strength of welded structures. Abington Publishing, Abington
5. Radaj D (1990) Design and analysis of fatigue resistent welded structures. Abington Publishing, Cambridge
6. Hobbacher A et al (1982) Design recommendations for cyclic loaded welded steel structures IIW doc. XIII-998-81/XV-494-81. Weld World 20:153–165
7. Radaj D, Sonsino CM, Fricke W (2006) Fatigue assessment of welded joints by local approaches, 2nd ed. Woodhead Publishing, Cambridge, UK
8. Gurney TR (2006) Cumulative damage of welded joints. Woodhead Publishing Ltd., Cambridge, UK. ISBN-13:978-1-85573-938-3

Structural Hot Spot Stress Procedure:

9. Huther M, Henry J Recommendations for hot spot stress definition in welded joints. IIW doc. XIII-1416-91
10. Huther M, Parmentier G, Henry J Hot spot stress in cyclic fatigue for linear welded joints. IIW doc. XIII-1466-92/XV-796-92
11. Niemi E, Fricke W, Maddox SJ (2006) Fatigue analysis of welded components—designer's guide to structural hot-spot stress approach. IIW doc. XIII-1819-00/XV-1090-01, update June 2003. Woodhead Publishing, Cambridge, UK
12. Dong P, Hong JK (2002) Assessment of ASME's FSRF rules for vessel and piping welds using a new structural stress method (Master S-N Curve Approach). IIW doc. XIII-1929-02/XV-1182-02. Weld World 48:28–36
13. Doerk O, Fricke W, Weissenborn Ch Comparison of different calculation methods for structural stresses at weld joints. IIW doc. XIII-1919-02/XV-1124-02
14. Zhao X-L, Packer JA (2000) Recommended fatigue design procedure for welded hollow section joints. IIW doc. XIII-1772-99 / XV-1021-99. Abington Publishing, Abington, Cambridge

A.F. Hobbacher, *Recommendations for Fatigue Design of Welded Joints and Components*, IIW Collection, DOI 10.1007/978-3-319-23757-2

15. Haibach E (1968) Die Schwingfestigkeit von Schweissverbindungen aus der Sicht einer örtlichen Beanspruchungsmessung (The fatigue strength of welded joints considered on the basis of a local stress measurement). LBF Report FB77, Fraunhofer-Inst. f Betriebsfestigkeit Darmstadt Germany
16. Xiao Z-G, Yamada K (2004) A method of determining geometric stress for fatigue strength evaluation of steel welded joints. Int J Fatigue 26:1277–1293 and IIWdoc. XIII-2022-04/ XV-1175-04

Effective Notch Stress Procedure

17. Petershagen H (1986) A comparison of approaches to the fatigue strength assessment of welded components IIW document XIII-1208-86
18. Petershagen H (1989) Experiences with the notch stress concept according to Radaj (transl.) 15. Vortragsveranstaltung des DVM Arbeitskreises Betriebsfestigkeit, Ingolstadt 18.-19.10
19. Olivier R, Köttgen VB, Seeger T (1989) Welded connections I: Fatigue assessment of welded connections based on local stresses (transl.) Forschungskuratorium Maschinenbau, Bericht No. 143, Frankfurt 1989 (143 pages)
20. Köttgen VB, Olivier R, Seeger T (1991) Fatigue analysis of welded connections based on local stresses IIW document XIII-1408-91
21. Morgenstern C, Sonsino CM, Hobbacher A (2004) Fatigue design of aluminium welded joints by local stress concept with the fictitious notch radius of $r_f = 1$ mm. IIW-Doc. No. XIII–2009–04
22. Fricke W (2006) Round robin study on stress analysis for the effective notch stress approach. IIW document XIII-2129-06/XV-1223-06
23. Fricke W (2008) Guideline for the fatigue assessment by notch stress analysis for welded structures. IIW document XIII-2240-08/XV-1289-08
24. Hobbacher. A. Database for the Effective Notch Stress Method at Steel. IIW Joint Working Group Doc. JWG-XIII-XV-197-08, International Institute of Welding (2008)

Fracture Mechanics

25. Murakami Y (1987) Stress intensity factors handbook. Pergamon Press, Oxford
26. Newman JC, Raju IS (1983) Stress intensity factor equations for cracks in three-dimensional finite bodies. ASTM STP 791:I-238–I-265.
27. Newman JC, Raju IS (1980) Stress intensity factors for internal surface cracks in cylindrical pressure vessels. J Press Vessel Technol 102:342–346
28. Newman JC, Raju IS (1981) An empirical stress intensity factor equation for the surface crack. Eng Fract Mech 15(1–2):185–192
29. Frank KH, Fisher JW (1979) Fatigue strength of fillet welded cruciform joints. J Struct Div Proc ASCE 105:1727–1740
30. Folias ES (1965) Axial crack in pressurized cylindrical shell. Int J Fract Mech 1(2):104
31. Hobbacher A (1993) Stress intensity factors of welded joints. Eng Fract Mech 46(2):173–182; (1994) 49(2):323
32. Maddox SJ, Andrews RM (1990) Stress intensity factors for weld toe cracks, in ‘Localized Damage Computer Aided Assessment and Control’. In: Aliabadi MH, Brebbia CA, Cartwright DJ (eds) Computational Mechanics Publications, Southamton. ISBN 1 853 12 070 7; co-published with Springer-Verlag, Heidelberg, ISBN 3 540 527 17 6
33. Albrecht P, Yamada K (1977) Rapid calculation of stress intensity factors. J Struct Div ASCE 103(ST2):377–389

34. Pang HLJ (1990) A review of stress intensity factors for semi-elliptical surface crack in a plate and fillet welded joint. The Welding Institute, Abington, Cambridge, UK, TWI Report 426/1990 IIW doc. XIII-1433-91
35. Bowness D, Lee MMK (1996) Stress intensity factor solutions for semi-elliptical weld-toe cracks in T-butt geometries. Fatigue Fract Eng Mater Struct 19(6):787–797
36. Bowness D, Lee MMK (2000) Prediction of weld toe magnification factors for semi-elliptical cracks in T-but joints. Int J Fatigue 22(5):389–396
37. Bowness D, Lee MMK (2002) Fracture mechanics assessment of fatigue cracks in offshore tubular structures. University of Swansea, Swansea, UK. ISBN 0 7176 23289
38. Nykänen T, Marquis G, Björk T Simplified assessment of weld quality for fatigue loaded cruciform joints. IIW document XIII-2177-07.
39. Fett T, Munz D (1997) Stress intensity factors and weight functions. Computational Mechanics Publications, Southampton
40. Shen G, Plumtree A, Glinka G (1991) Weight function for the surface point of semi elliptical surface crack in a finite thicknedd plate. Eng Fract Mech 40(1):167–176
41. Moftakhar AA, Glinka G (1992) Calculation of stress intensity factors by efficient integration of weight functions. Eng Fract Mech 43(5):749–756
42. Hall MS, Topp DA, Dover WD (1995) Parametric equations for stress intensity factors in weldments. Project Report TSC/MSH/0244, Technical Software Consultants Ltd., Milton Keynes, U.K. 1990 taken from: Mohanan CC (ed) Early Fatigue Crack Growth at Welds, Computational Mechanics Publications, Southampton UK 1995.
43. Fracture Mechanics Proof of strength for engineering components. VDMA-Verlag Frankfurt-M, Germany (2009)
44. Engesvik KM (1981) Analysis of uncertainties in the fatigue capacity of welded joints. Doctoral thesis, Division of Marine Structures, University of Trondheim, Norwegian Institute of Technology, Trondheim Norway

Fatigue Strength Modifications

45. Ørjasæter O (1995) Effect of plate thickness on fatigue of welded components. IIW doc. XIII-1582-95/XV-890-95
46. Haagensen PJ, Maddox SJ (2006) IIW Recommendations for weld toe improvement by grinding, TIG dressing and hammer peening for steel and aluminium structures. IIW doc. XIII-1815-00 (rev. 24 Feb. 2006). (See more references listed in document!)
47. Krebs J, Kassner M (2006) Influence of welding residual stresses on fatigue design of welded joints and components. IIW doc. XIII-2126-06/XV-1220-06

Weld Imperfections

48. ISO 6520:1982: Weld irregularities
49. ISO 5817:2006: Welding—fusion-welded joints in steel, nickel, titanium and their alloys—quality levels for imperfections
50. ISO 10042: Welding—arc-welded joints in aluminium and its alloys—quality levels for imperfections
51. IIW guidance on assessment of the fitness for purpose of welded structures. IIW doc. SST-1157-90 (1990)
52. Hobbacher A et al (1988) Recommendations for assessment of weld imperfections in respect of fatigue. IIW doc. XIII-1266-88/XV-659-88

53. BS 7910:2005: Guidance on methods for assessing the acceptability of flaws in metallic structures British Standard Institution, London
54. Ogle MH (1991) Weld quality specifications for steel and aluminium structures. IIW doc. XV-776-91. Weld World 29(11/12):341–362
55. Berge S, Myhre H (1977) Fatigue strength of misaligned cruciform and butt joints. IIW doc. XIII-863-77. Norw Marit Res 5(1)
56. Maddox SJ (1985) Fitness for purpose assessment of misalignment in transverse butt welds subject to fatigue loading. IIW doc. XIII-1180-85 (more references in the document)
57. Hobbacher A (2006) Problems of effect of weld imperfections on fatigue and their consideration in design codes. Int J Steel Struct 6:289–298

Stress Spectrum

58. Endo T et al (1974) Fatigue of metals subjected to varying stress - prediction of fatigue lives (transl.) Kyushu District Meeting of the JSME, Nov. 1967. also: Rain flow method—the proposal and the applications. Memoir Kyushu Institute of Technical Engineering
59. Standard Practice for Cycle Counting in Fatigue Analysis. ASTM E 1049-85

Damage Calculation

60. Palmgren A (1924) On life duration of ball bearings (transl.). VDI-Z 68:339–341
61. Miner AM (1945) Cumulative damage in fatigue. J Appl Mech 151–164
62. Haibach E (1970) Modified linear damage accumulation hypothesis considering the decline of the fatigue limit due to progressive damage (transl.) Laboratorium für Betriebsfestigkeit, Darmstadt, Germany, Techn. Mitt. TM 50/70
63. Hobbacher A (1977) Cumulative fatigue by fracture mechanics. Trans ASME Ser E J Appl Mech 44:769–771
64. Sonsino CM, Maddox SJ, Hobbacher A (2004) Fatigue life assessment of welded joints under variable amplitude loading—state of present knowledge and recommendations for fatigue design regulations. In: Proceedings of the annual IIW-assembly and international conference, July 15–16, 2004 Osaka/Japan, S. 87–102
65. Sonsino CM, Wiebesiek J (2007) Assessment of multiaxial spectrum loading of welded steel and aluminium joints by modified equivalent stress and Gough-Pollard algorithms. IIW doc. XIII-2158r1-07/XV-1250r1-07
66. Sonsino CM, Maddox SJ, Haagensen P (2005) A short study on the form of the S-N curves for weld details in the high-cycle-fatigue regime. IIW doc. XIII-2045-05
67. Bäckström M (2000) Multiaxial fatigue life assessment of welds based on nominal and hot spot stresses. Doctoral Thesis Lappeenranta Univ. of Technology Lappeenranta Finland 2003. VTT Publications 502/1235-0621, VTT Information Service, POB 2000, FIN-02044 VTT. ISBN 951-38-6233-X

Fatigue Testing

68. Lieurade HP, Huther M, Maddox SJ (2006) Recommendations on fatigue testing of welded joints IIW doc. XIII-2114-06 (ISO proposal)
69. Sonsino CM (2007) Fatigue testing under variable amplitude loading. Int J Fatigue 29:1080–1089

70. Dixon WJ, Mood AM (1948) A method for obtaining and analyzing sensitivity data. J Am Stat Assoc 43:108–126
71. Spindel JE, Haibach E (1979) The method of maximum likelihood applied to the statistical analysis of fatigue data including run-outs. Int J Fatigue 1(2):81–88
72. Sonsino CM, Bruder Th, Baumgartner JS-N (2010) Lines for welded thin joints—suggested slopes and FAT values for applying the notch stress concept with various reference radii. Weld Worls 54(11/12)

Quality and Safety Considerations

73. Huther M (1990) Uncertainties, confidence intervals and design criteria IIW doc. XIII-1371-90
74. Schneider CRA, Maddox SJ (2006) Best practise guide on statistical analysis of fatigue data obtained from specimens containing many welds. IIW doc. XIII-2138-06
75. Marquis G, Mikkola T (2000) Analysis of welded structures with failed and non-failed welds, based on maximum likelihood. IIW document XIII-1822-00
76. Hobbacher A, Kassner M (2012) On relation between fatigue properties of welded joints vs. quality criteria and groups in ISO 5817. IIW doc. XIII-2323r1-10. Weld World 11–12

Fatigue Failure and Repair

77. Anon (1973/1979) Fatigue fractures in welded constructions. Publication de la Soudure Autogène, vols. 1, II
78. Anon (1990) IIW Guidance on assessment of fitness-for-purpose of welded structures. IIW SST-1157-90
79. Petershagen H (1996) IIW Recommendations on the Repair of Fatigue-Loaded Welded Structures. IIW doc. XIII-1632-96
80. Miki C, Goto K, Itoh Y Database of repair cases for fatigue failure on the internet. IIW doc. XIII-1830-00. http://www.wg5.cv.titech.ac.jp